



2333-17

Workshop on Science Applications of GNSS in Developing Countries (11-27 April), followed by the: Seminar on Development and Use of the Ionospheric NeQuick Model (30 April-1 May)

11 April - 1 May, 2012

GNSS Remote Sensing: Troposphere Profiling through Radio Occultation

NOTARPIETRO Riccardo
*Politecnico di Torino
Corso Duca degli Abruzzi 24
10129 Torino
ITALY*

**Workshop on Science Applications of GNSS in Developing
Countries**

11-27 April, 2012



The Abdus Salam
International Centre for Theoretical Physics

GNSS REMOTE SENSING: TROPOSPHERE PROFILING THROUGH RADIO OCCULTATION



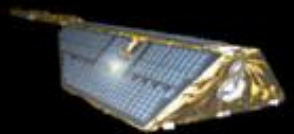
RICCARDO NOTARPIETRO
POLITECNICO di TORINO

riccardo.notarpietro@polito.it +39.011.5644623

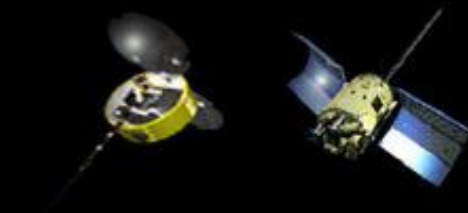
REMOTE SENSING GROUP



POLITECNICO
DI TORINO

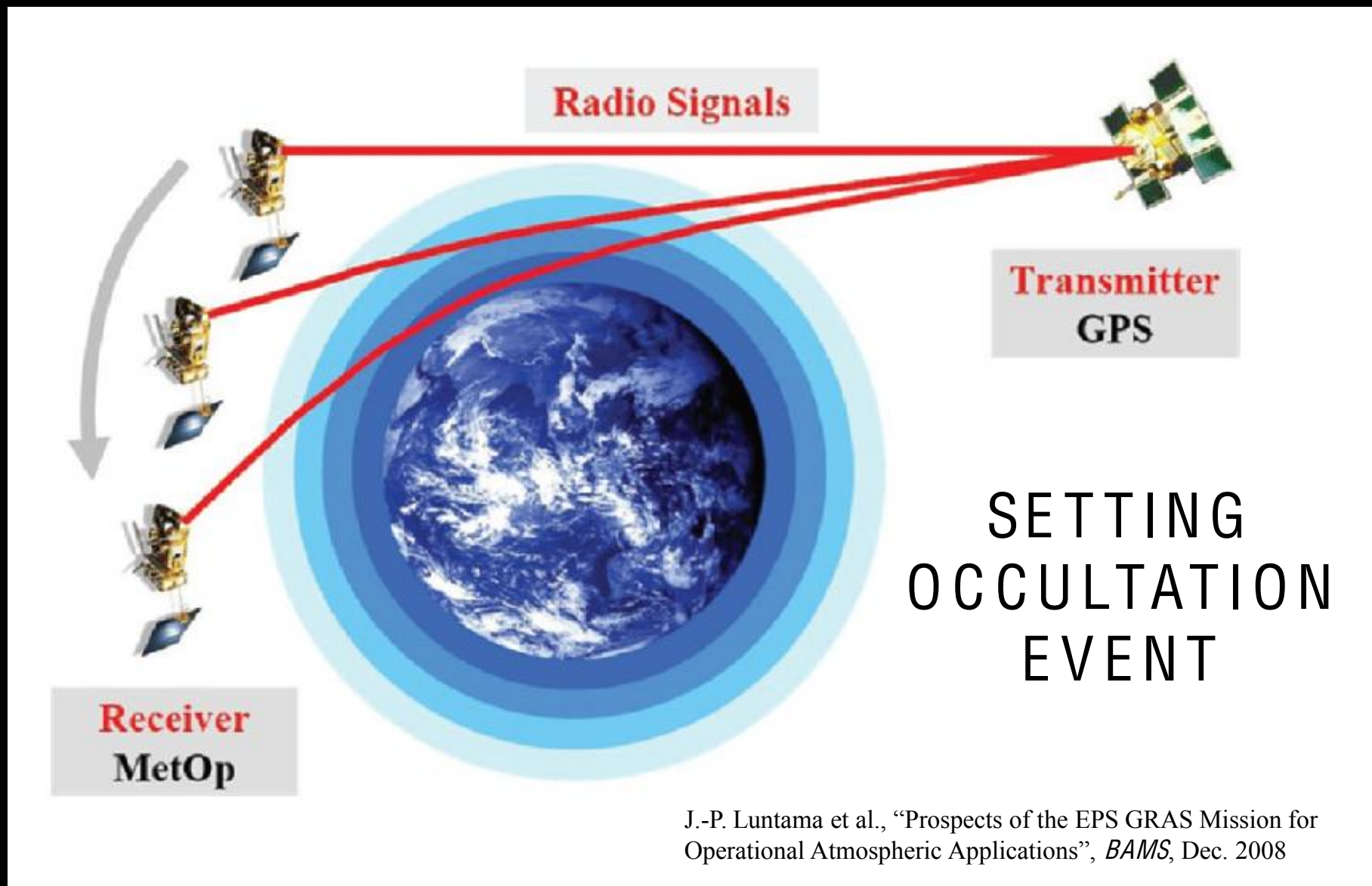


Sun and „satellite“ sets

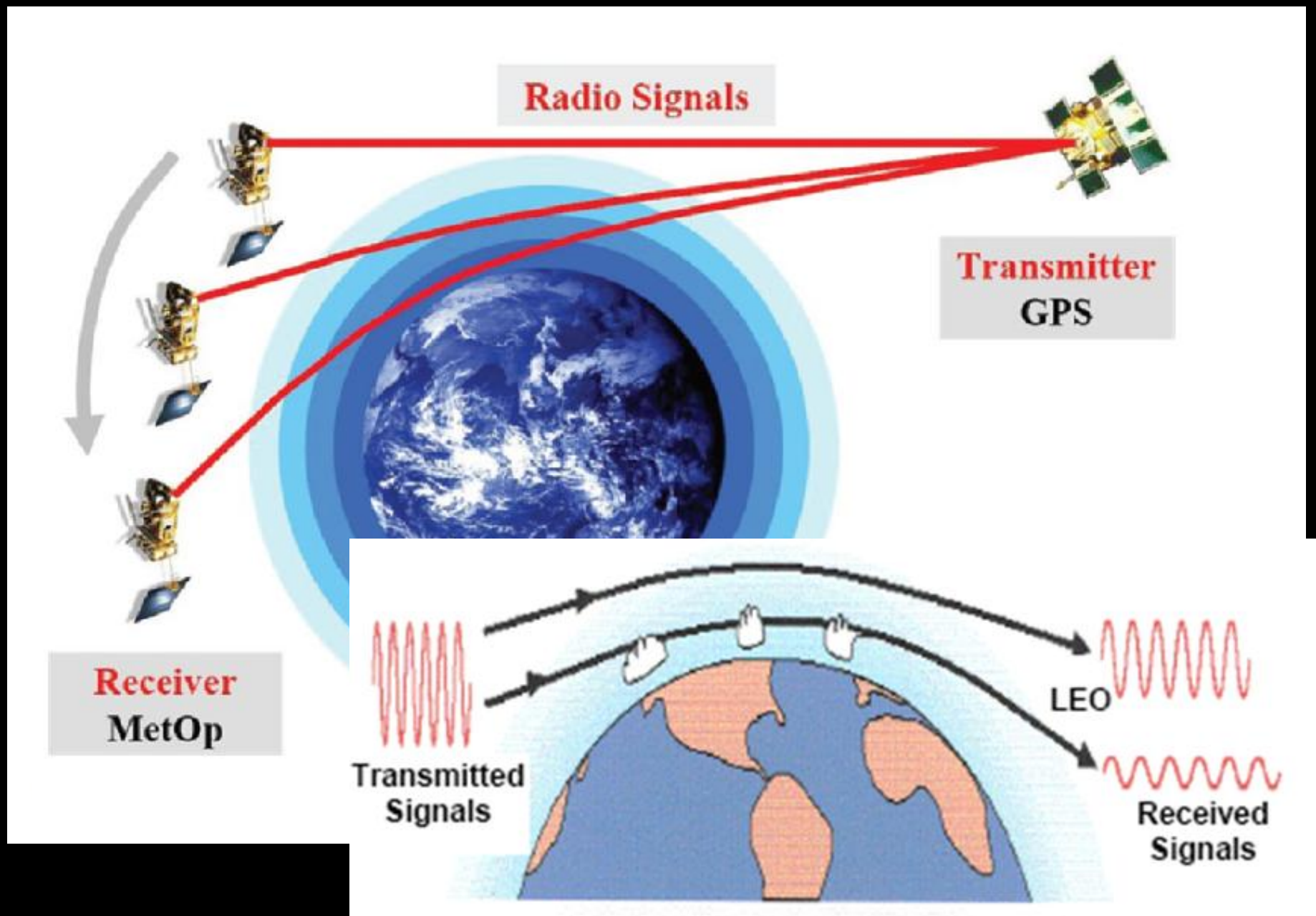


J. Wickert, presented at OPAC-2 Workshop, Graz, 2004

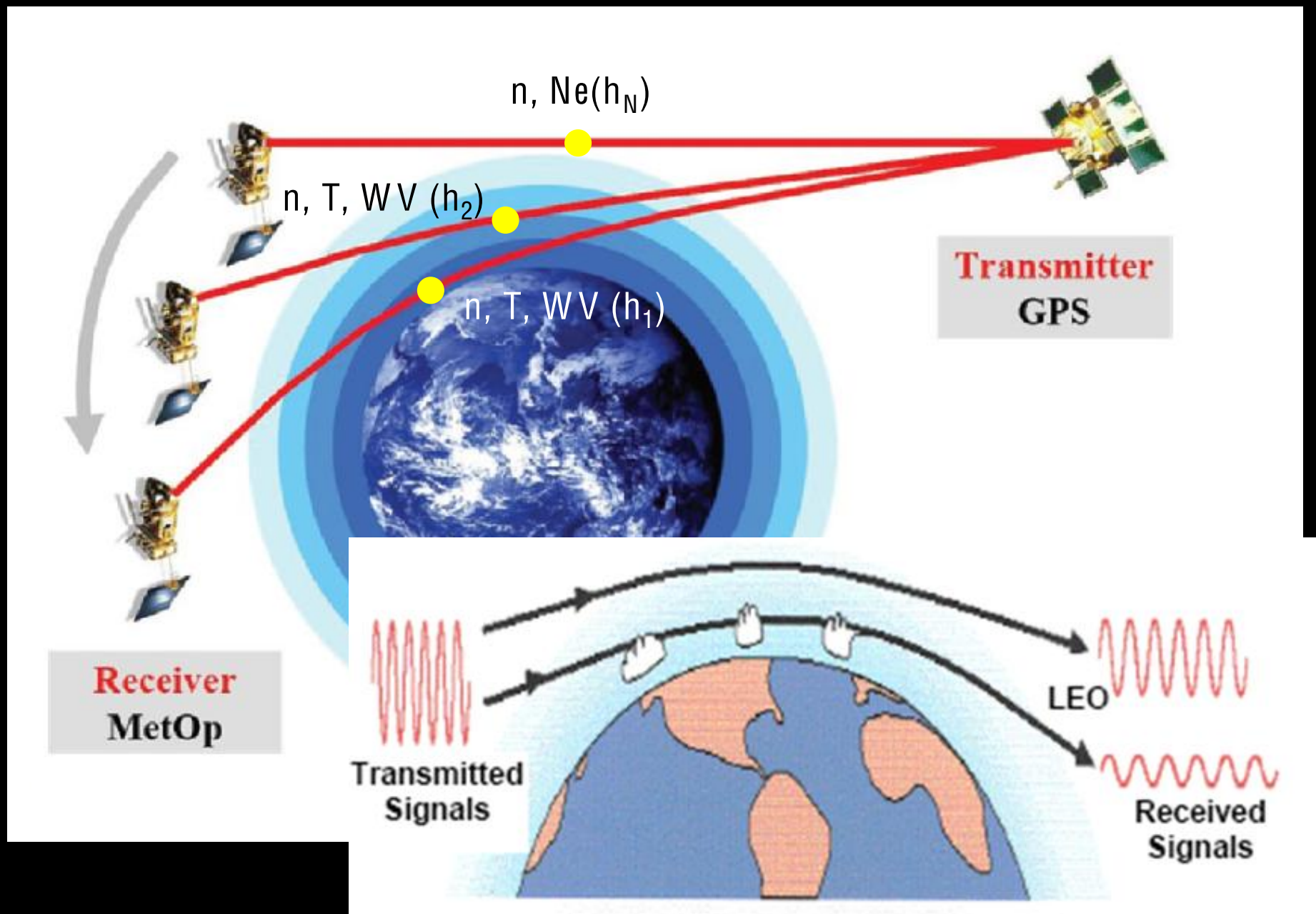
GNSS RADIO OCCULTATION PRINCIPLE

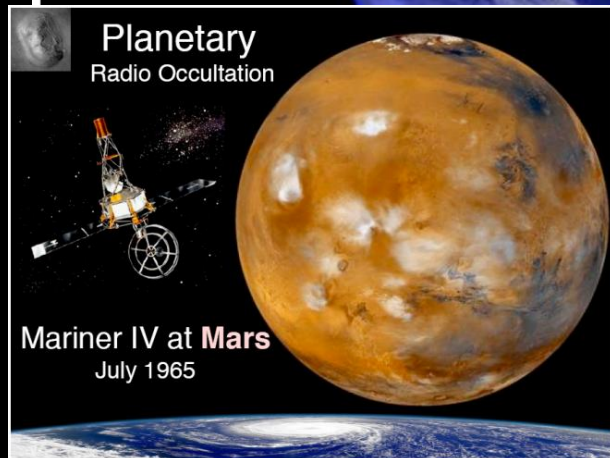
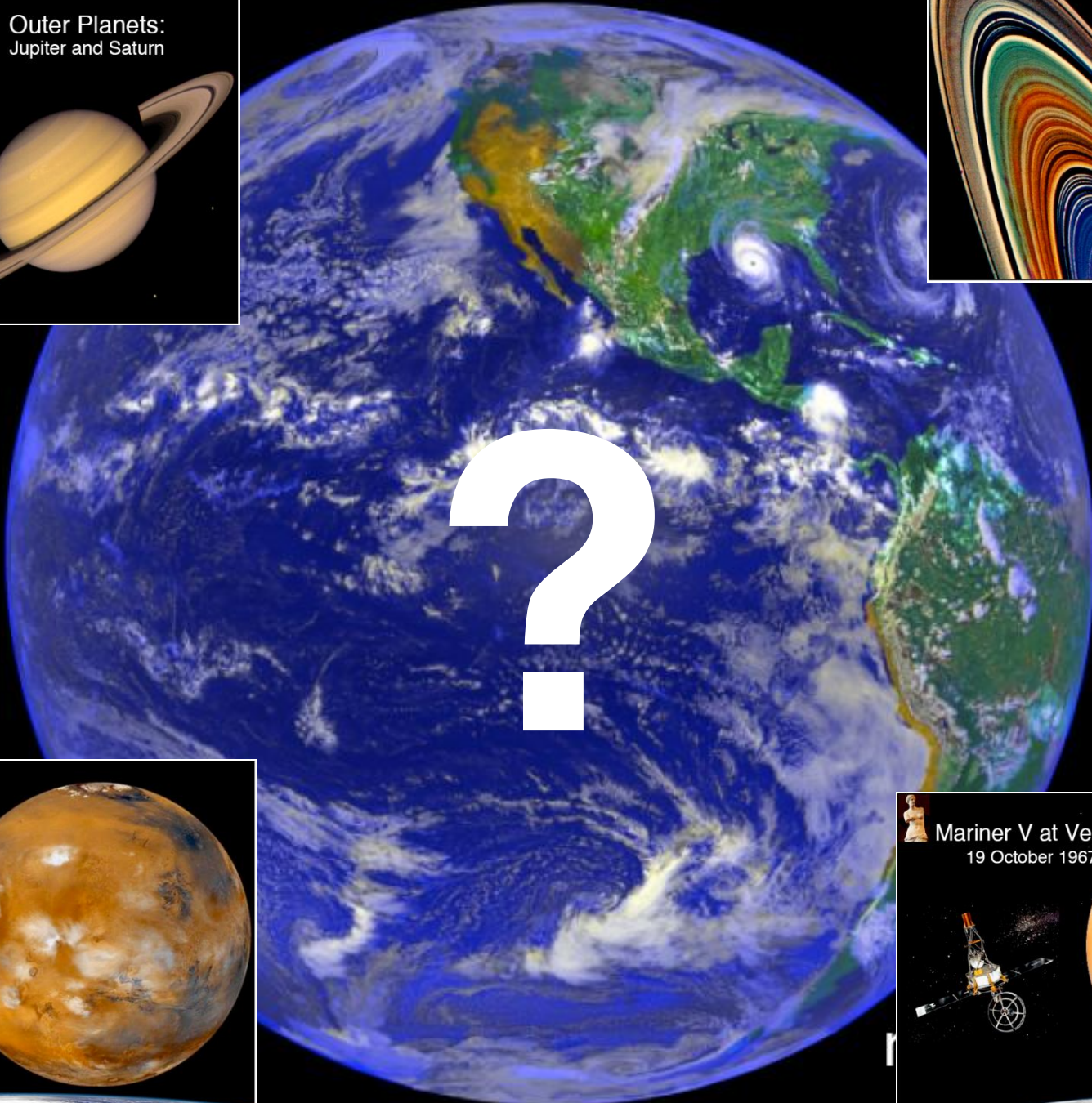
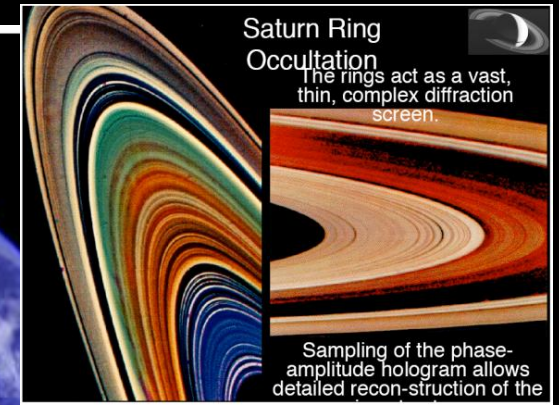
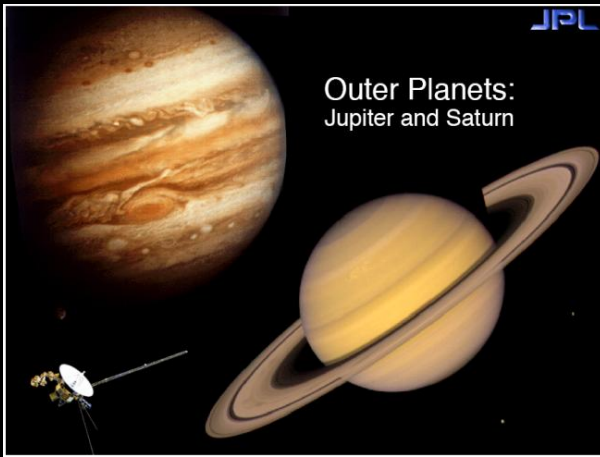


GNSS RADIO OCCULTATION PRINCIPLE



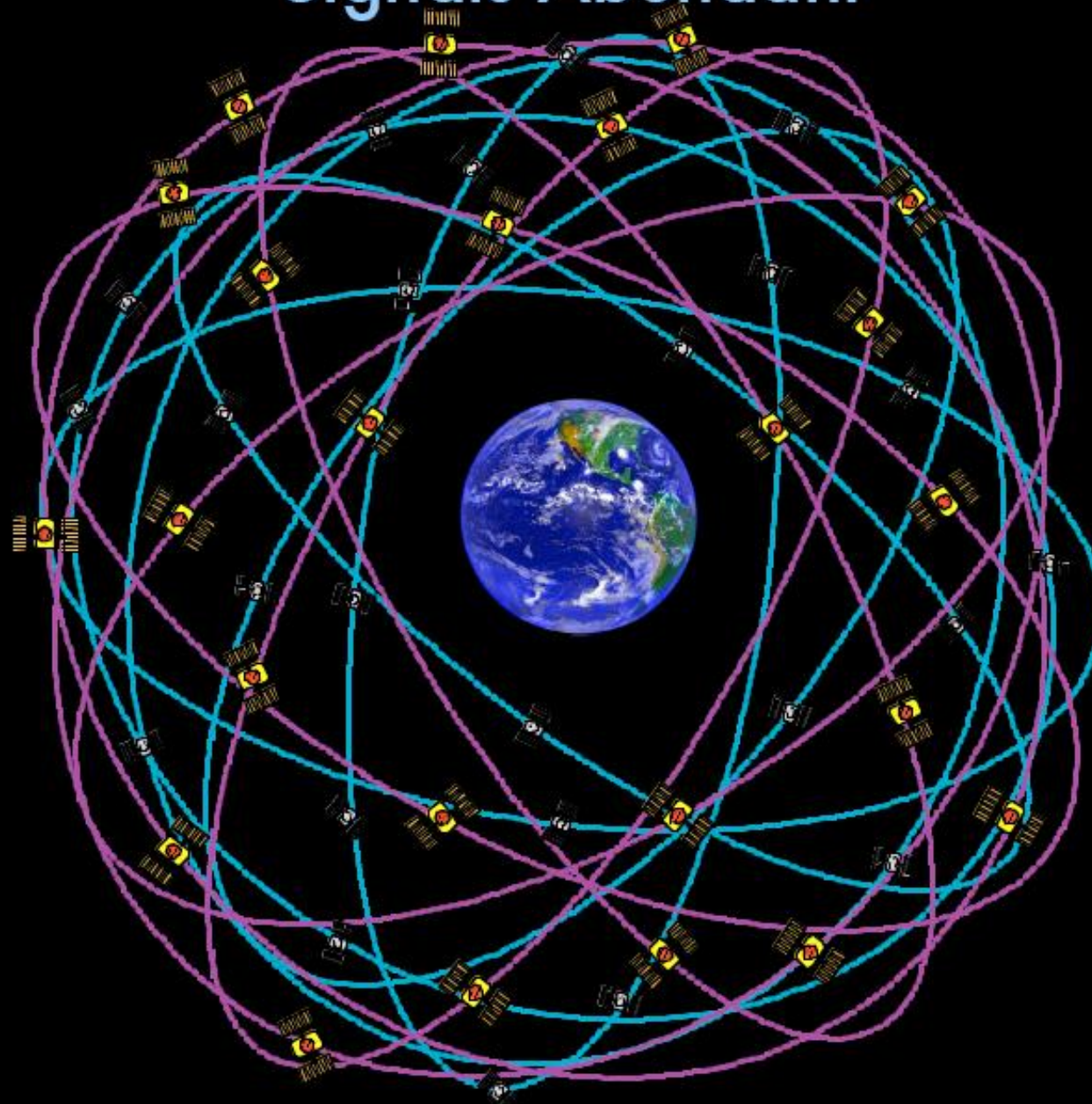
GNSS RADIO OCCULTATION PRINCIPLE





Signals Abundant

JPL

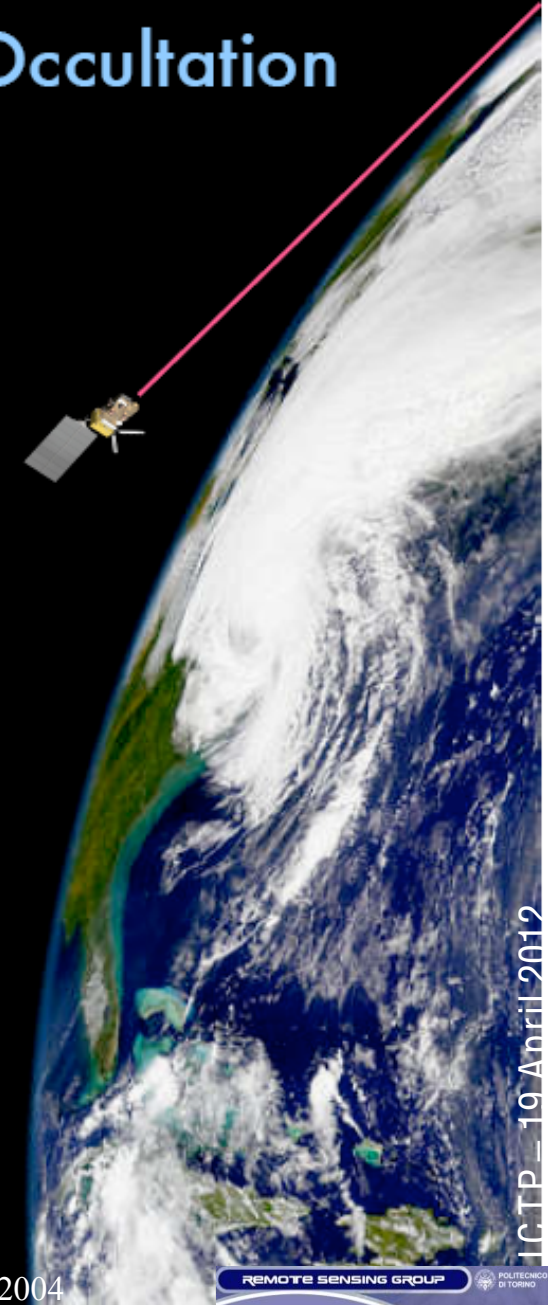


GPS
Glonass
Galileo

60-90
sources
in space

Unique Attractions of GPS Radio Occultation

1. High accuracy: Averaged profiles to < 0.1 K
2. Assured long-term stability
3. All-weather operation
4. Global 3D coverage: stratopause to surface
5. Vertical resolution: ~ 100 m in lower trop
6. Independent height & pressure/temp data
7. Compact, low-power, low-cost sensor



Unique Attractions of GPS Radio Occultation

TABLE 1. GRAS product accuracy requirements.

		Level 1 products	Level 2 products	
		Bending angle	Specific humidity	Temperature
Coverage		Global	Global	Global
Horizontal sampling		The average distance between individual soundings over a period of 12 h is less than 1,000 km		
Vertical range^a		Surface–80 km	Surface–100 hPa	Surface–1 hPa
Vertical sampling rate^b	0–5 km	2–5 Hz	0.4–2 km	0.3–3 km
	5–15 km	2–5 Hz	1–3 km	1–3 km
	15–35 km	2–5 Hz	—	1–3 km
	35–50 km	2–5 Hz	—	1–3 km
RMS accuracy^c	0–5 km	0.4%	0.25–1 g kg ^{-1e}	0.5–3 K
	5–15 km	0.4%	0.05–0.2 g kg ^{-1e}	0.5–3 K
	15–35 km	1 μrad or 0.4% ^d	—	0.5–3 K
	35–50 km	1 μrad or 0.4% ^d	—	0.5–5 K
Timeliness		2 h 15 min	3 h	3 h

^aLowest product level is determined by the lowest signal tracking height.

^bAfter noise filtering.

^cWith no systematic biases.

^dWhichever is greater.

^eEquivalent to a requirement of 5% in relative humidity.

J.-P. Luntama et al., “Prospects of the EPS GRAS Mission for Operational Atmospheric Applications”, *BAMS*, Dec. 2008

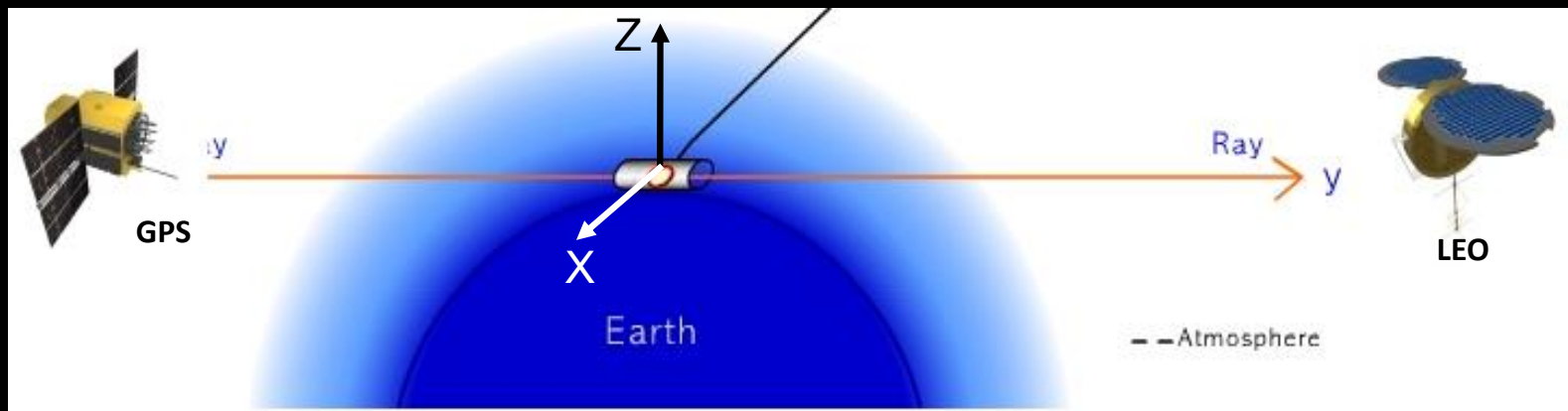
RO Measurement Resolution

Cross-track Resolution (driven by First Fresnel Zone dimension)

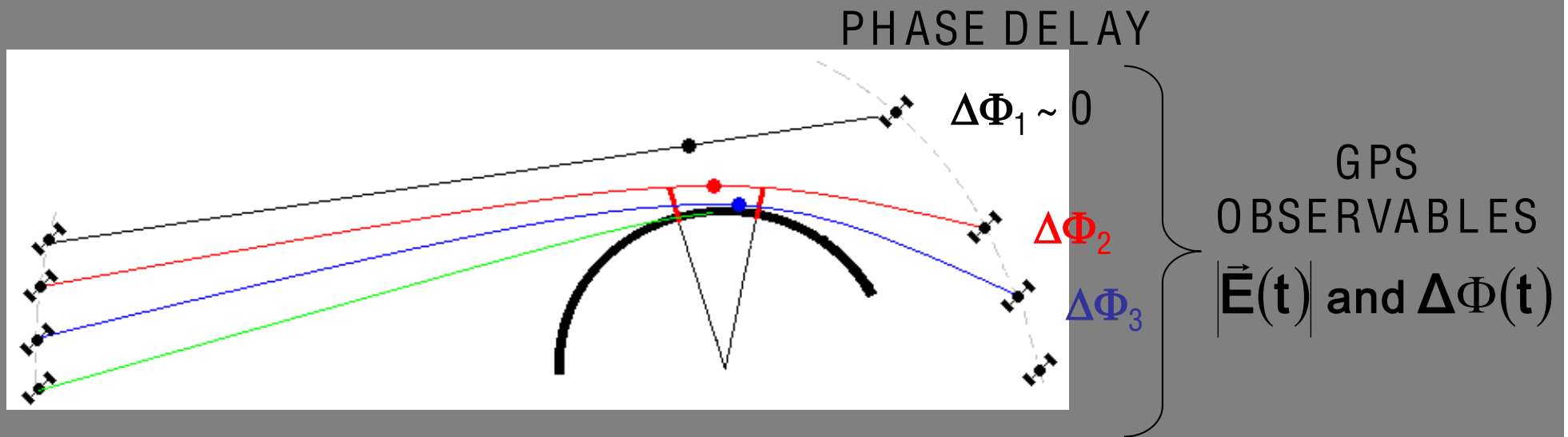
- $\Delta z \sim 2$ km in stratosphere
 ~ 0.5 km in the lower troposphere (using GO algorithms) or ~ 100 m using Radio Holographic inversion methods
- $\Delta x \sim 2$ km

Along-track Resolution

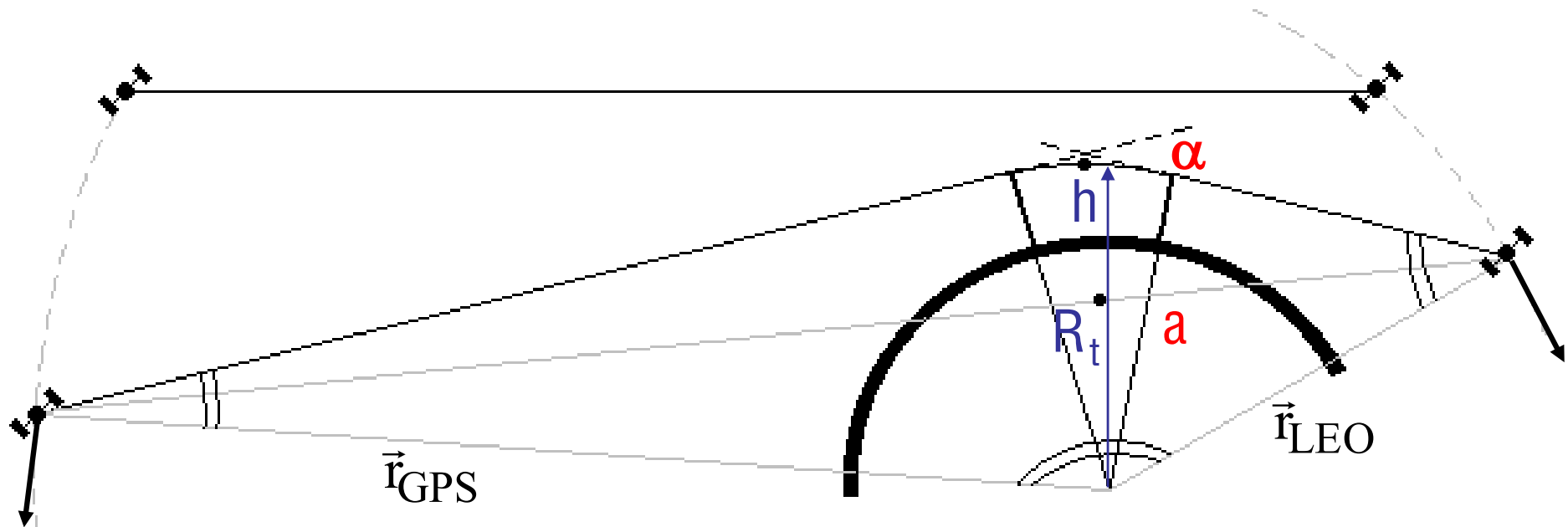
- $\Delta y \sim 600$ km in stratosphere
 ~ 200 km in in the lower troposphere



GPS RADIO OCCULTATION TECHNIQUE



GPS RADIO OCCULTATION TECHNIQUE



$$\vec{E}(t) \longrightarrow \alpha(a) = -2a \int_a^{\infty} \frac{1}{\sqrt{(R_t + h)^2 n^2(h) - a^2}} \frac{1}{n(h)} \frac{dn(h)}{dh} dh$$

Spherical symmetry hypothesis

- Geometric Optics
- Radio Holographic methods

ABEL

$$[n_{\text{retr}}(h) - 1] 10^6 = 77.6 \frac{p_d(h)}{T(h)} + 3.75 \cdot 10^5 \frac{e(h)}{T^2(h)} \longleftarrow n_{\text{retr}}(h) \longleftarrow$$

Data analysis (Overview)

Carrier phase & SNR
from GPS Ground &
Space observations

Calibration
(differencing)

Precise Orbit Data

Atm. Excess phase vs. time

Radio occultation measurement are based on phase measurements on L_1/L_2 GPS carrier frequencies onboard CHAMP. The carrier phase can be described by the expression :

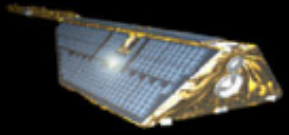
$$\Phi = \rho + c(dt - dT) - d_I + d_A + d_{MP} + dq + dQ + \lambda N + \varepsilon \text{ [m]}$$

- ρ true range between GPS satellite and receiver along ray path s
- c velocity of light
- dt satellite clock error
- dT receiver clock error
- d_I Ionospheric phase delay along s
- d_A Atmospheric phase delay along s
- d_{MP} error due to multipath
- dq instrumental bias of the satellite
- dQ instrumental bias of the receiver
- λ wave length of the radiowave
- N phase ambiguity number (integer)
- ε residual error on carrier phase

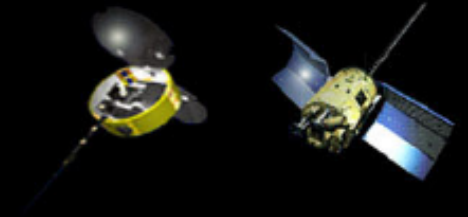
To calculate

Simplification mainly due to the fact, that bending angles will be derived from Doppler frequencies gives:

$$\Phi = \rho + c(dt - dT) - d_I + d_A + \varepsilon$$



Differencing



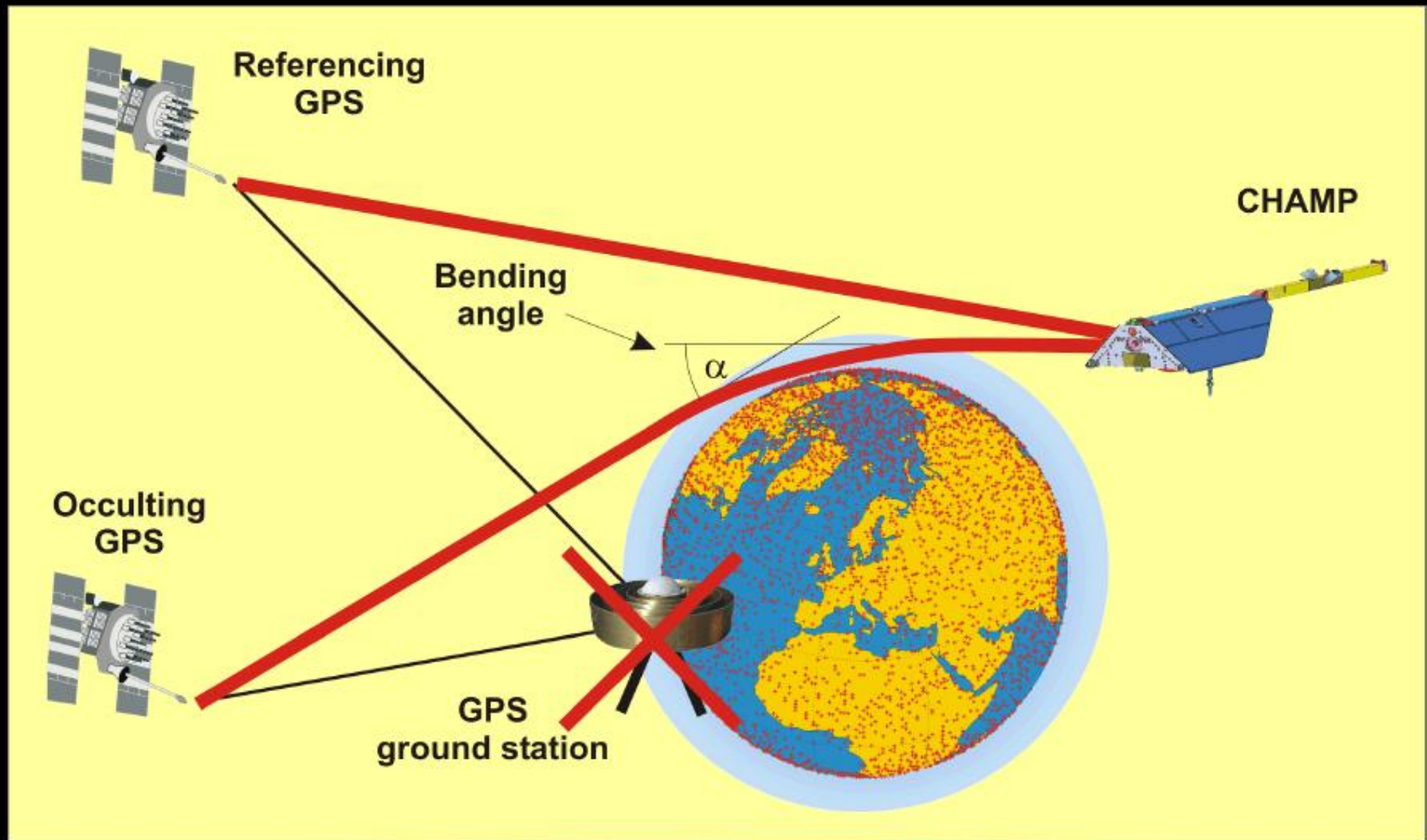
Double differencing (GPS/MET):

(„bad“ LEO oscillator, GPS oscillators with activated S/A)

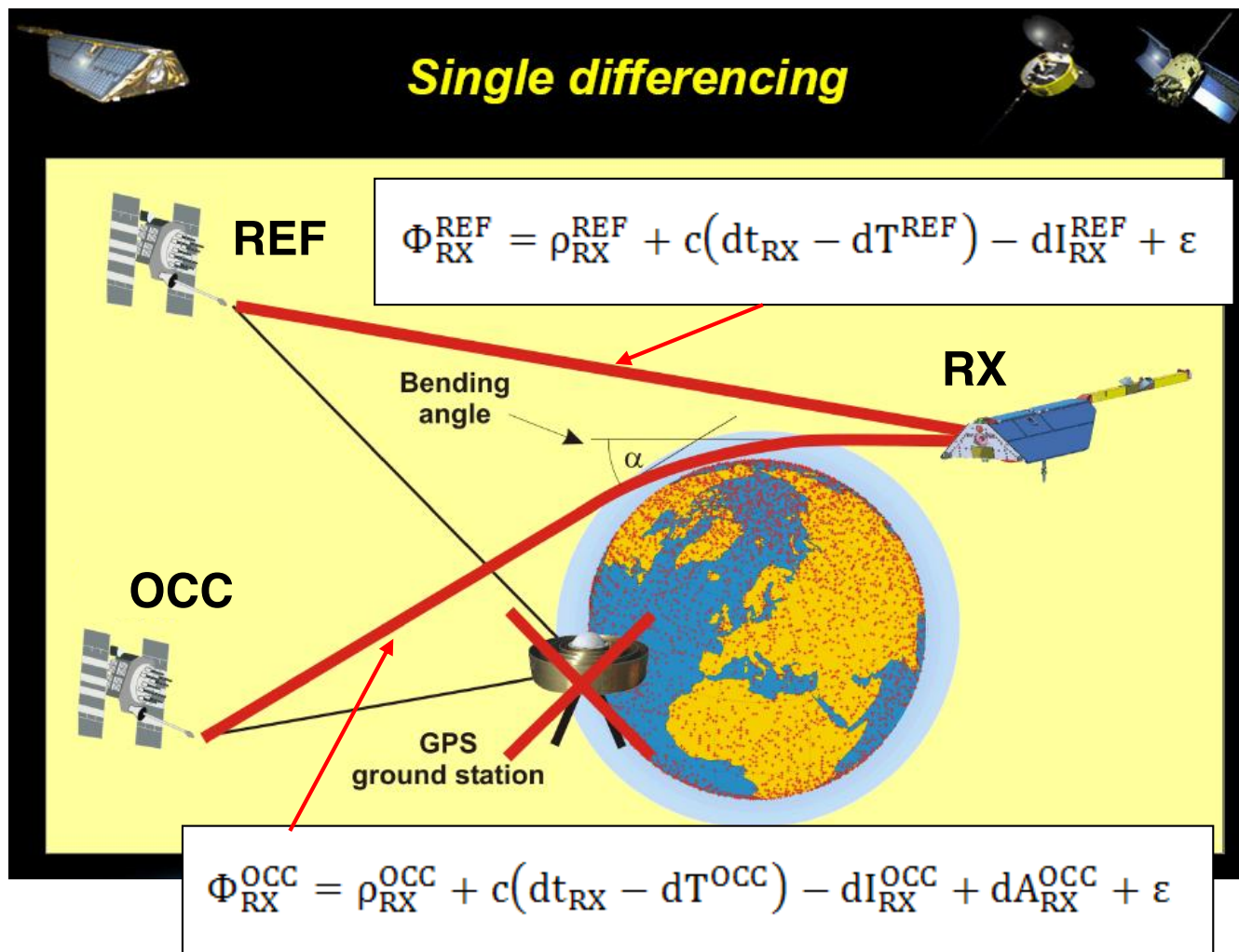
Single differencing (CHAMP):

(„bad“ LEO oscillators, GPS with deactivated S/A)

Single differencing



J. Wickert, presented at OPAC-2 Workshop, Graz, 2004



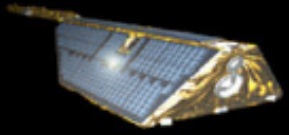
Single Differencing allows the removal of any receiver Clock "error" dt_{RX}

ρ_{RX}^{OCC} and ρ_{RX}^{REF} are estimated by Orbit Determination SW tools

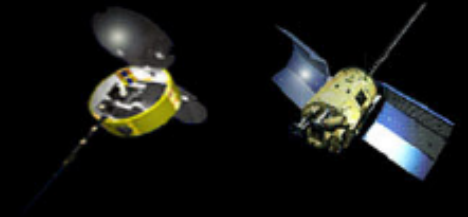
dT^{OCC} and dT^{REF} are normally taken by IGS or are estimated in the framework of Orbit Determination SW

dI_{RX}^{REF} has to be compensated for

After Single Differencing, the so-called Excess Phase ($-dI_{RX}^{OCC} + dA_{RX}^{OCC} + \varepsilon$) still remain



Differencing



Double differencing (GPS/MET):

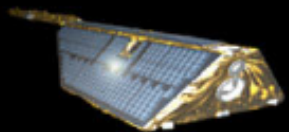
(„bad“ LEO oscillator, GPS oscillators with activated S/A)

Single differencing (CHAMP):

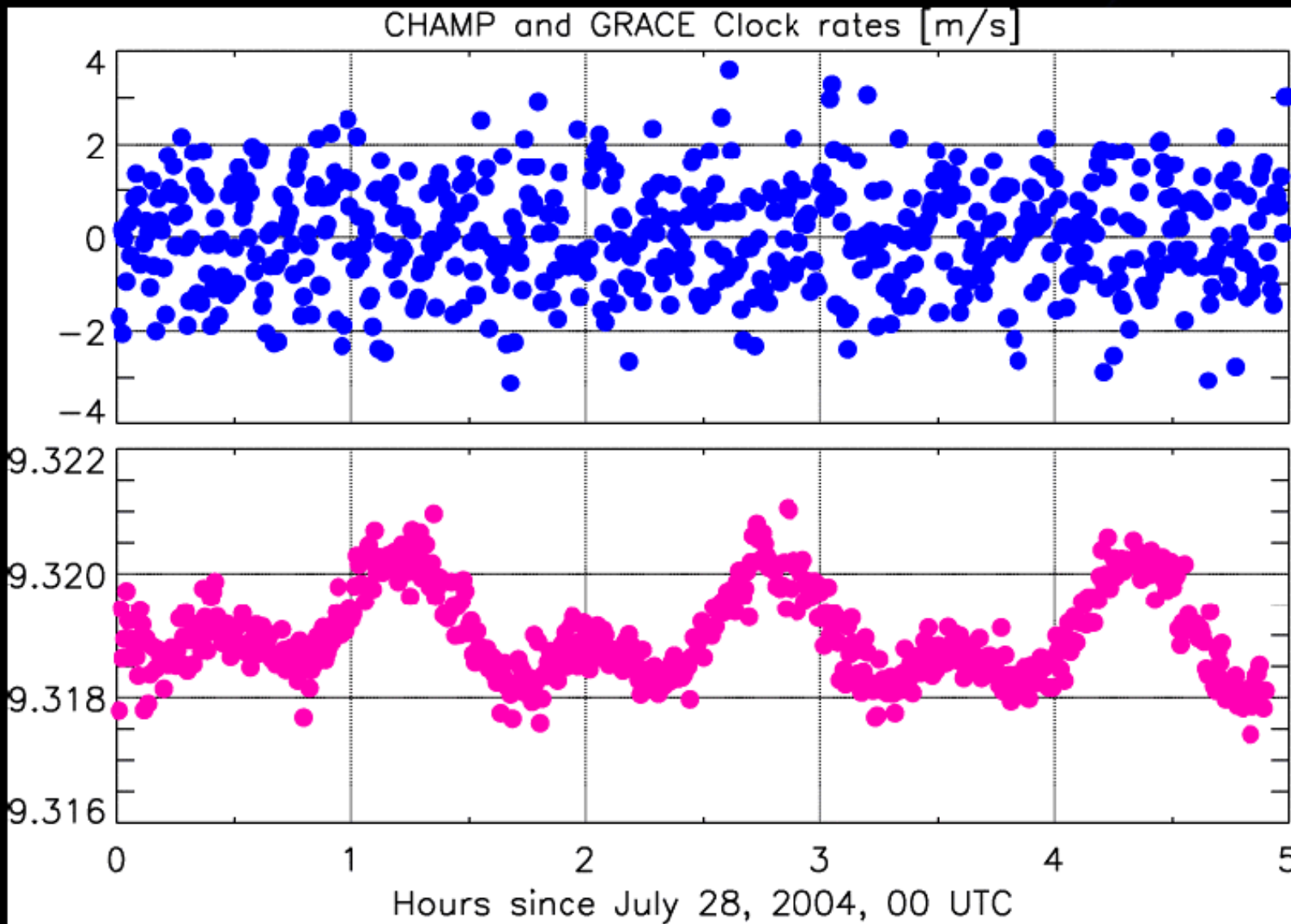
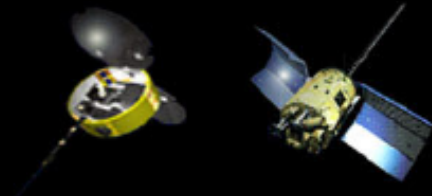
(„bad“ LEO oscillators, GPS with deactivated S/A)

Zero differencing (GRACE):

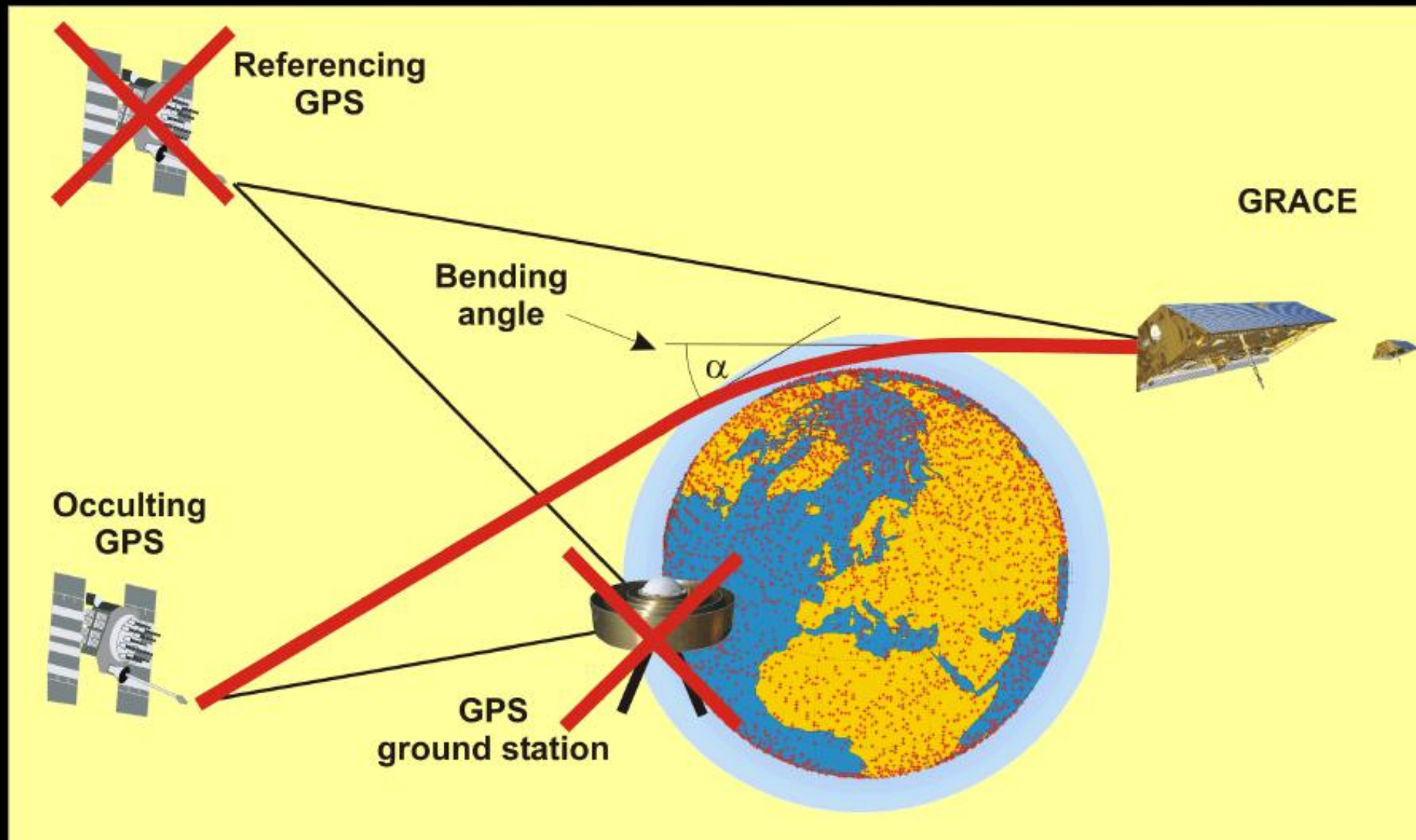
(stable LEO oscillator, GPS with deactivated S/A)



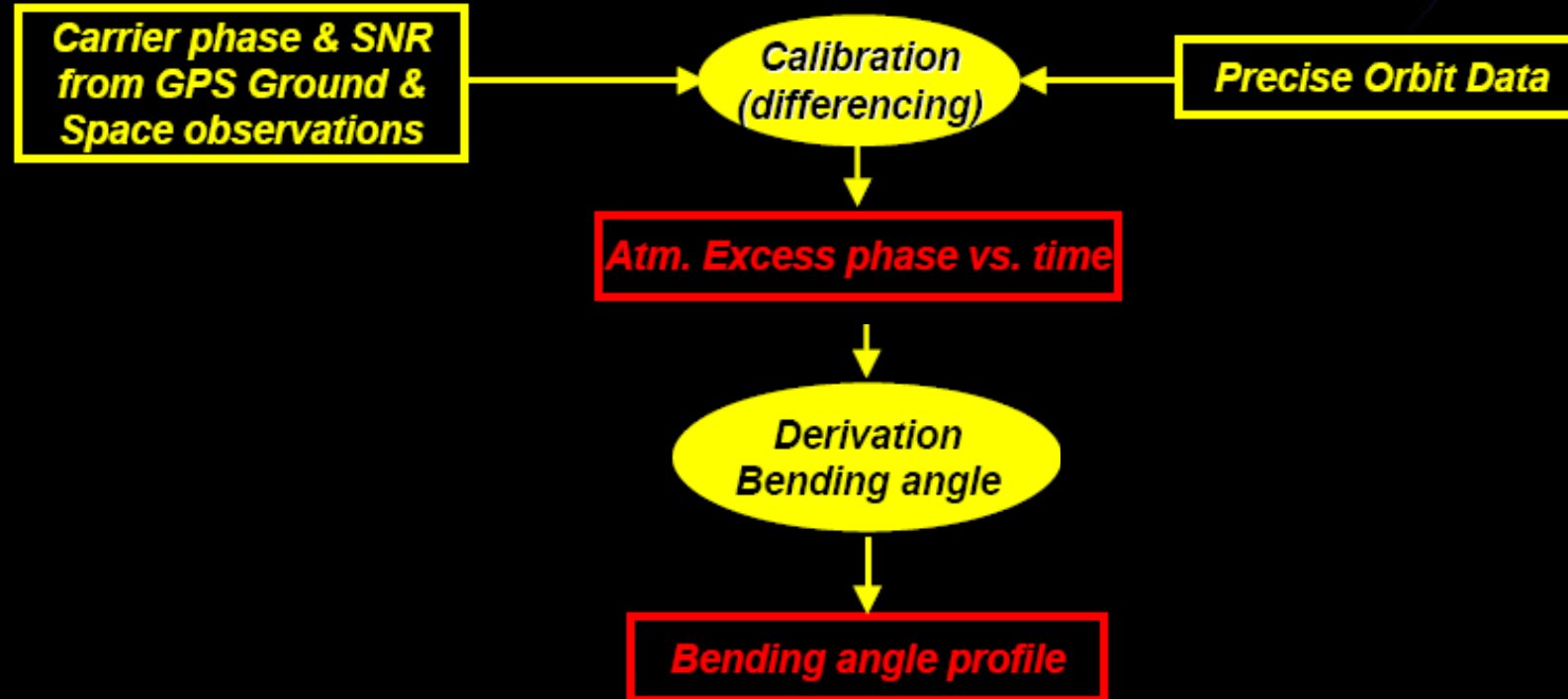
CHAMP and GRACE



Zero differencing



Data analysis (Overview)



- Excess Phases data filtering

- Refraction (symmetry) Centre computation

Since the formal expression between bending angle and refractivity is based on the hypothesis of atmospheric symmetry the refractivity centre is defined as the centre of the sphere which locally approximates the WGS-84 ellipsoid.

Excess Phases L1,L2

Positions LEO,GPS

Velocities LEO,GPS

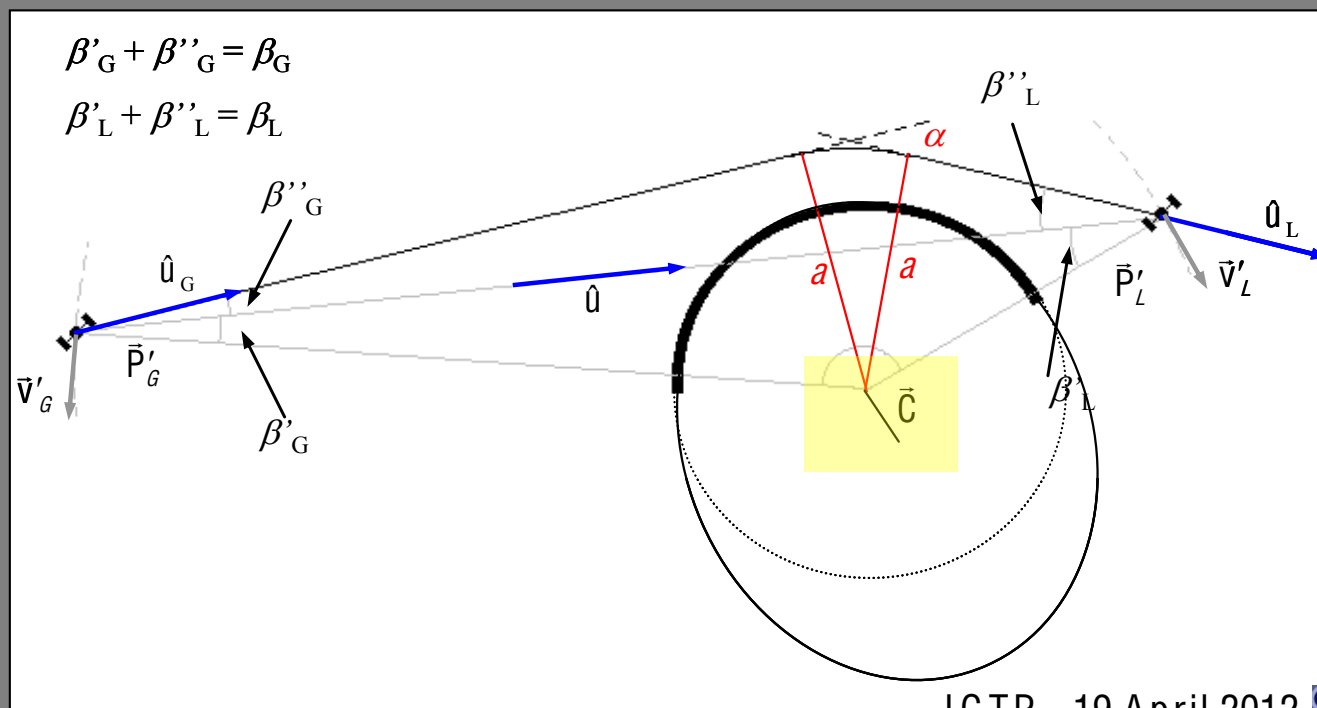
**BENDING
COMPUTATION**

Excess Doppler L1,L2

Bending angle L1,L2

Impact Parameters L1,L2

Lat,Long Tangent point

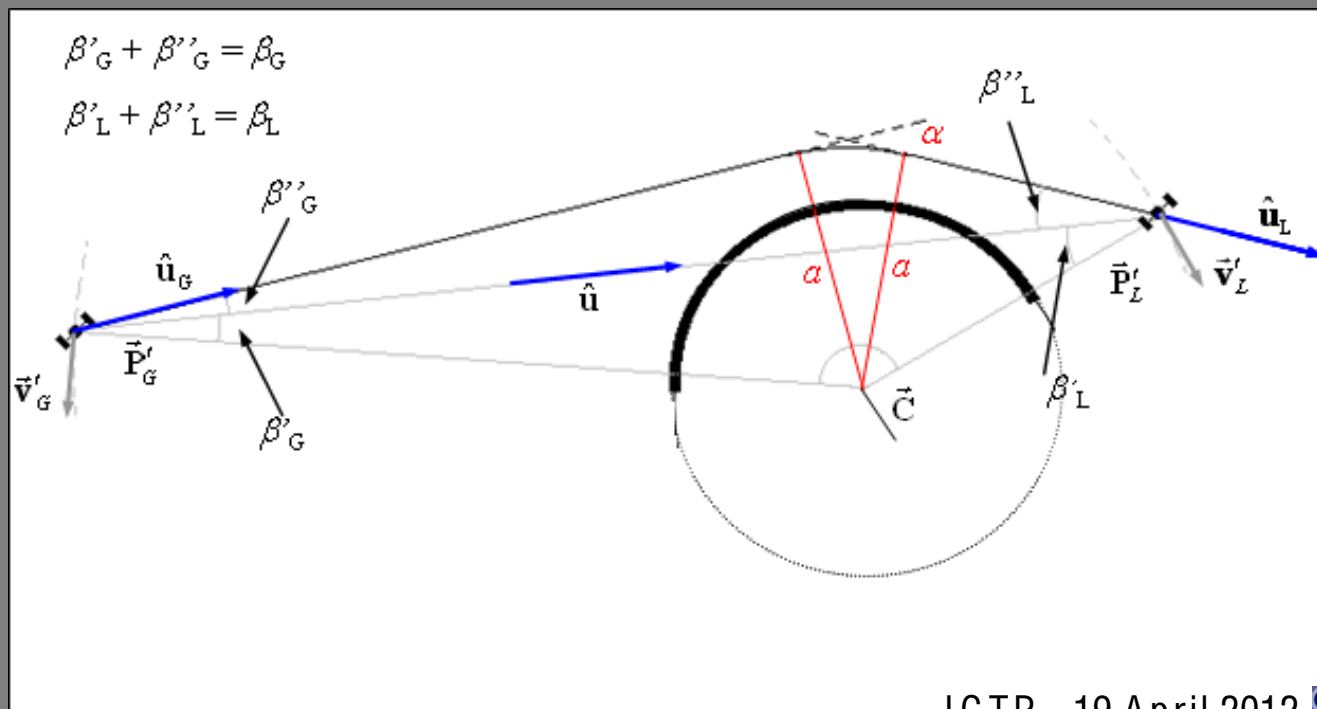
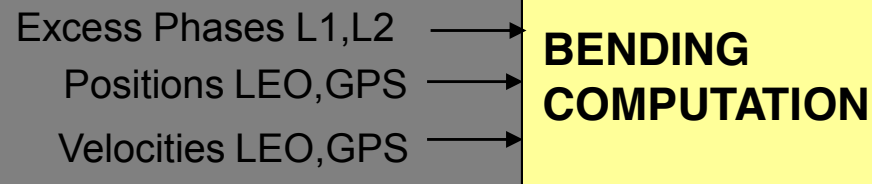


- Excess Phases data filtering

- Refraction (symmetry) Centre computation

Since the formal expression between bending angle and refractivity is based on the hypothesis of atmospheric symmetry the refractivity centre is defined as the centre of the sphere which locally approximates the WGS-84 ellipsoid.

- Bending angle vs impact parameter profile



Ionosphere correction

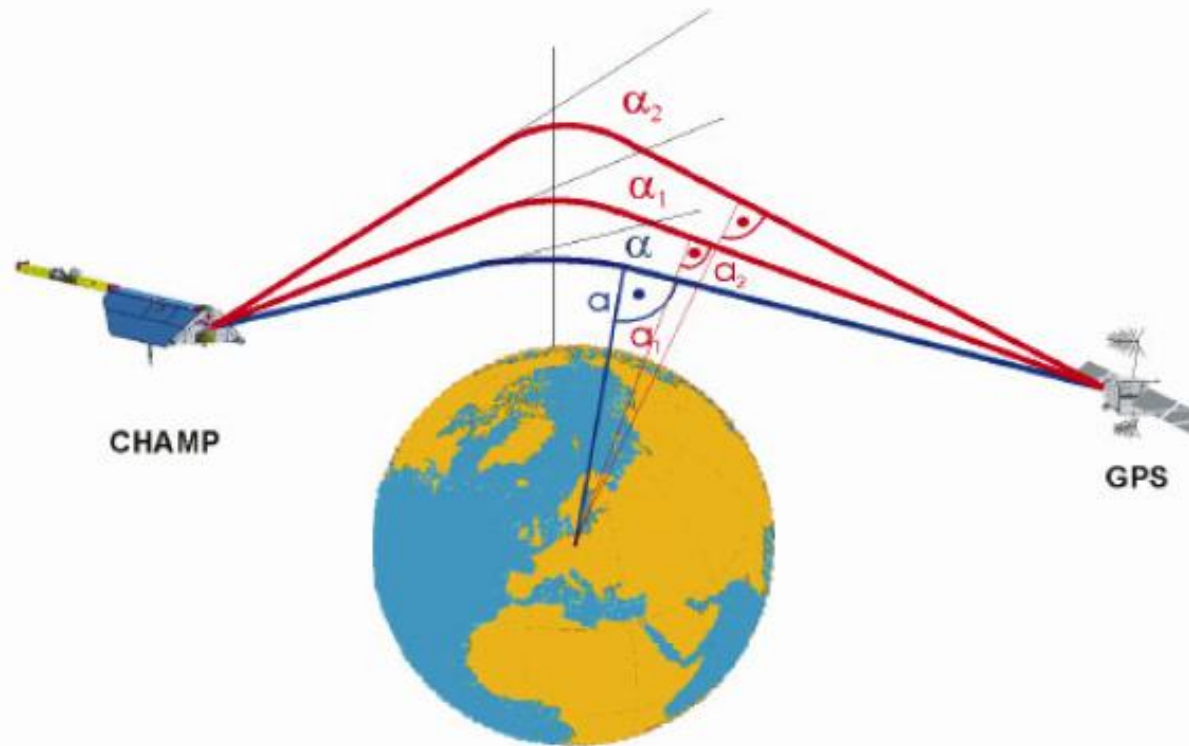
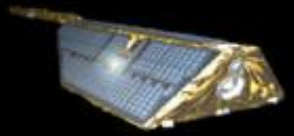
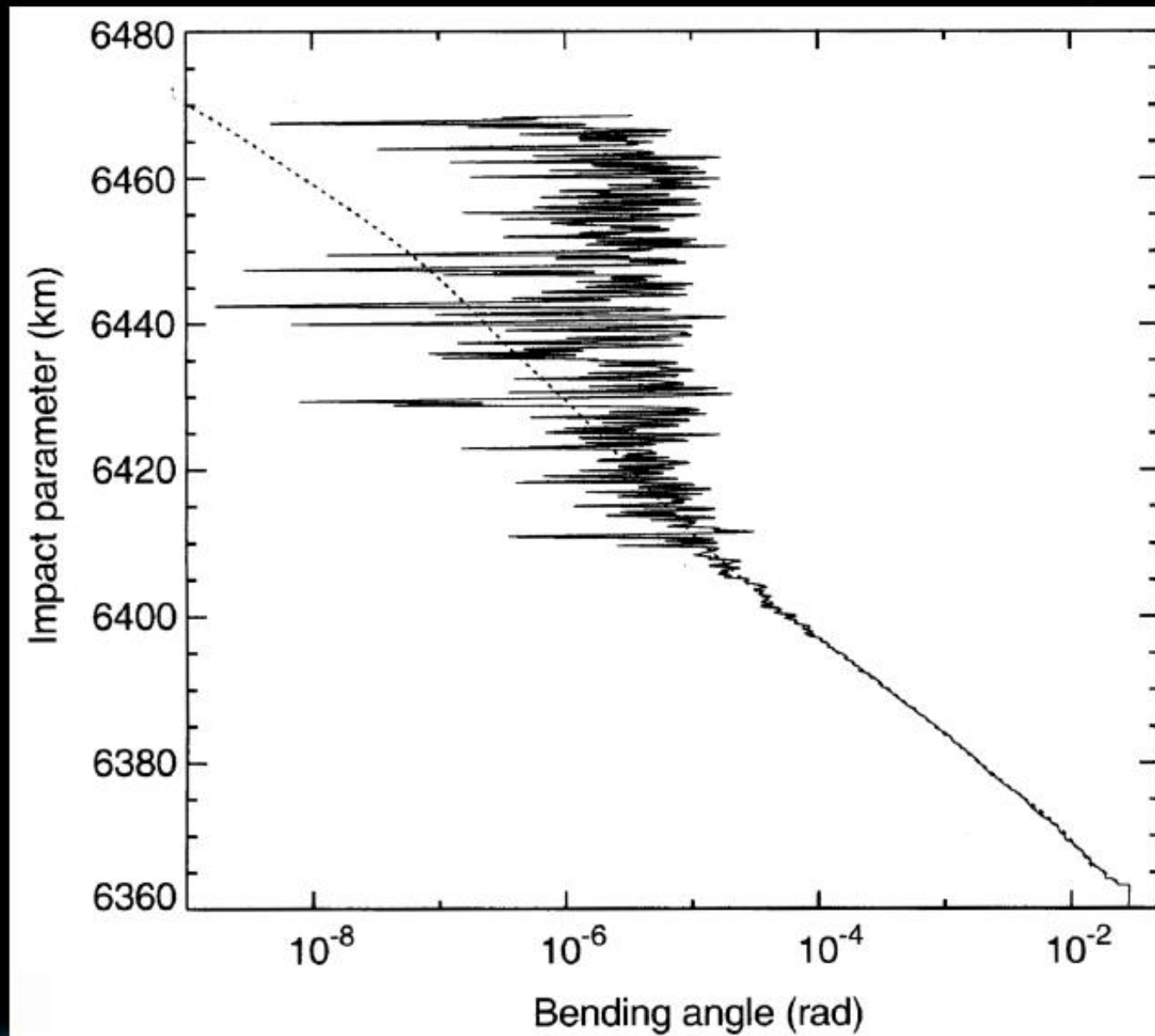
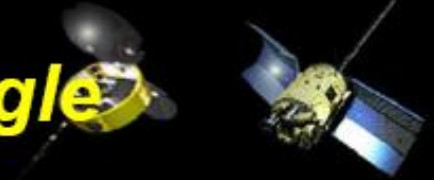


Abb. 3.15: Separierung der Strahlenwege der L1- und L2-Signale (rot) durch die dispersive Ionosphäre. Mit blau ist der fiktive Strahlenweg ohne Ionosphäreneinfluss gekennzeichnet.

$$\alpha(a) = \frac{f_1^2}{f_1^2 - f_2^2} \alpha_1(a) - \frac{f_2^2}{f_1^2 - f_2^2} \alpha_2(a). \quad (3.50)$$

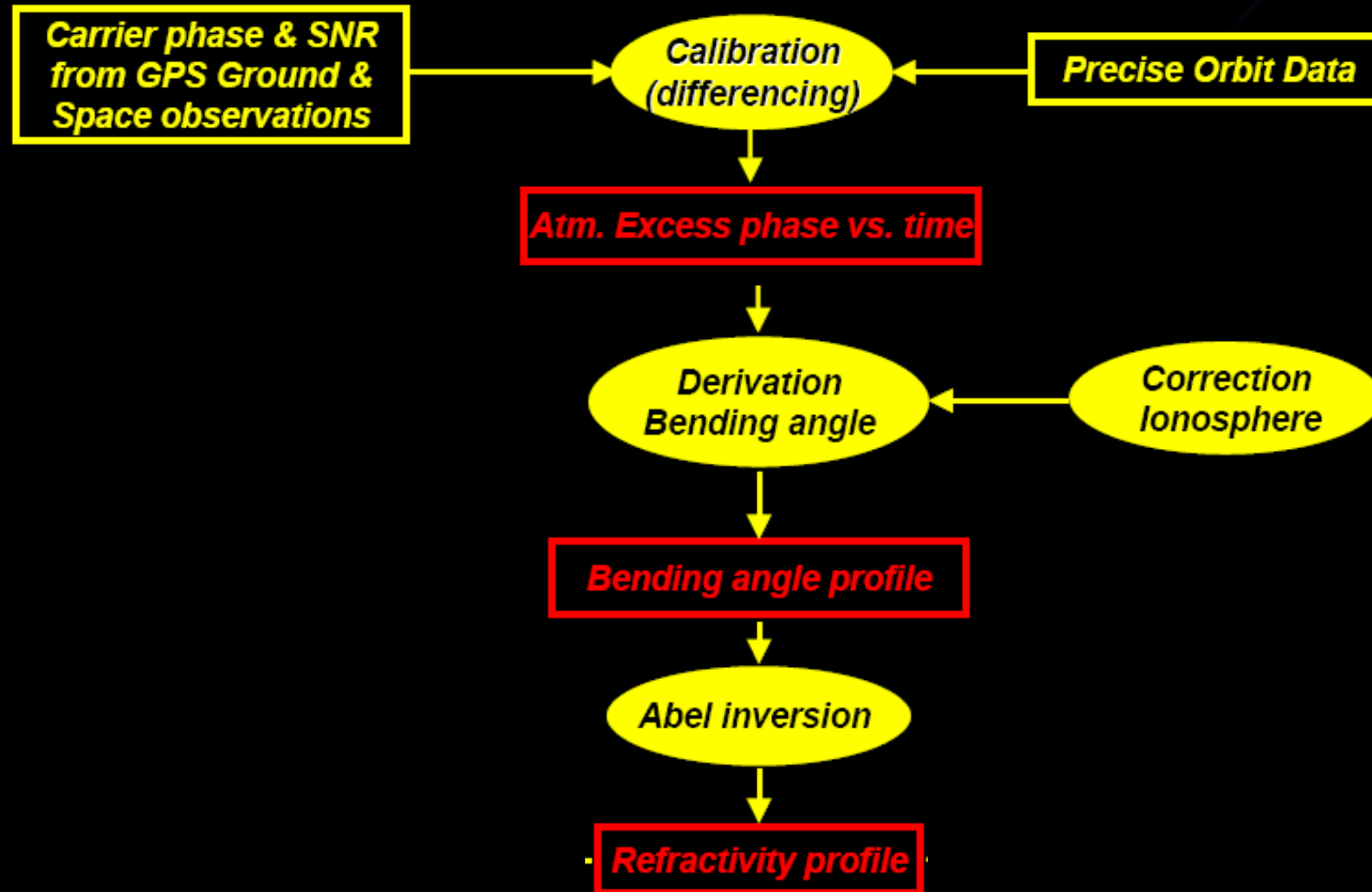


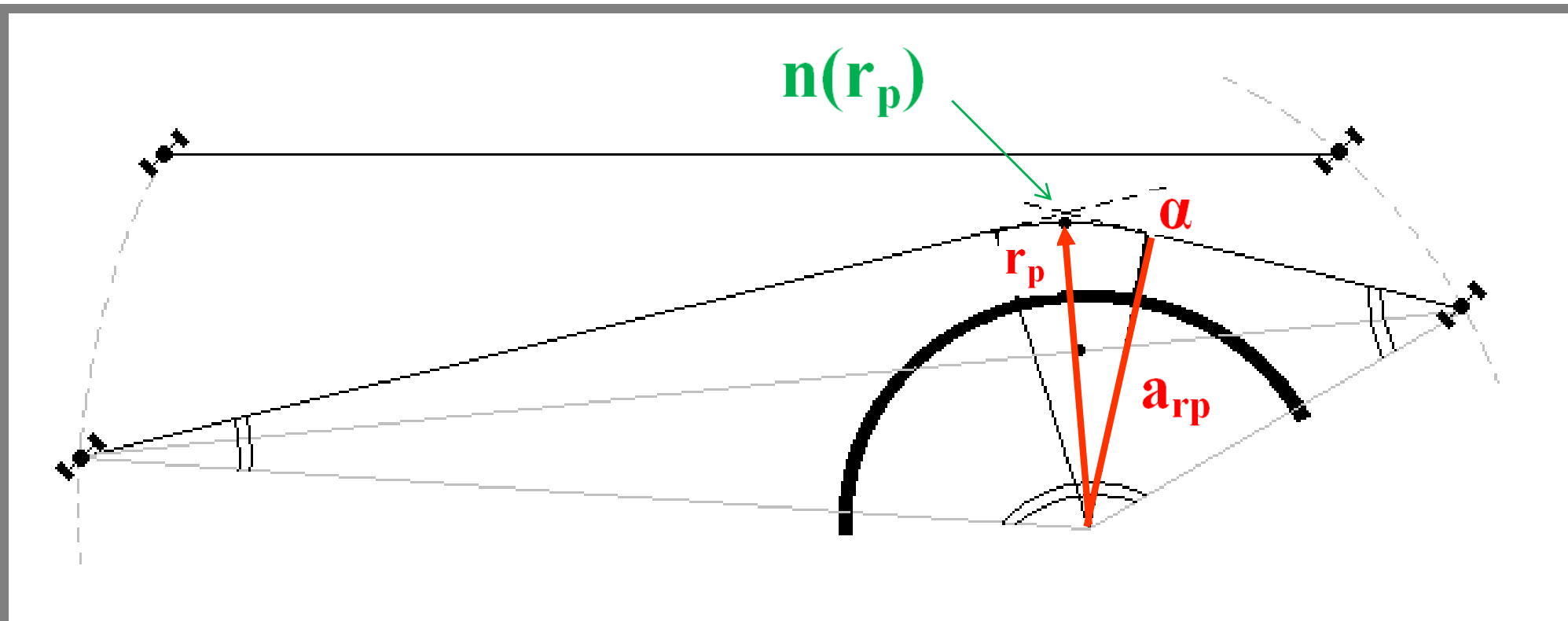
„Optimization“ of the bending angle



Hocke, 1997

Data analysis (Overview)





$$\alpha(a) = -2a \int_a^{\infty} \frac{1}{\sqrt{(R_t + h)^2 n^2(h) - a^2}} \frac{1}{n(h)} \frac{dn(h)}{dh} dh$$

For each Trajectory (i.e. Excess Doppler value)

REFRACTIVITY PROFILE

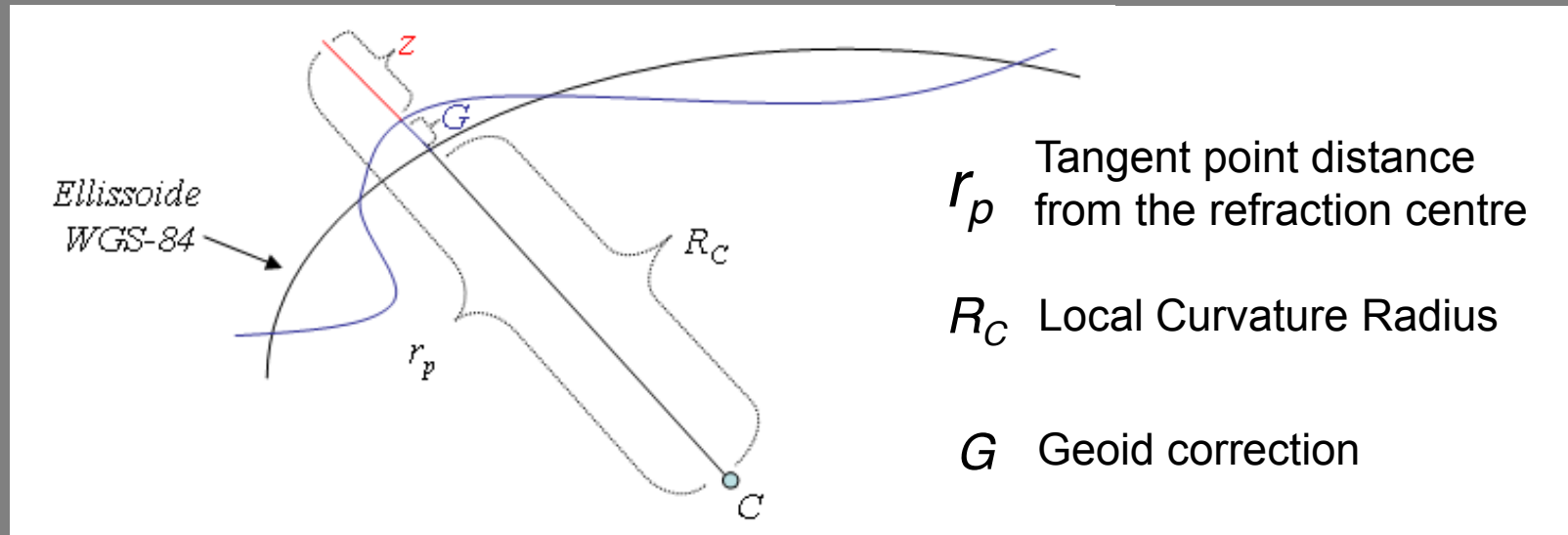
$$n(r_p) \begin{cases} n = e^{-\frac{1}{\pi a_{rp}} \int \ln \left[\frac{a}{a_{rp}} + \sqrt{\frac{a^2}{a_{rp}^2} - 1} \right] \frac{d\alpha}{da} da} \\ n(r) r \sin(\psi) = \text{const} = n(r_p) r_p = a_{rp} \end{cases} \rightarrow r_p = \frac{a_{rp}}{n(r_p)}$$

- Abel Inversion

- Heights from surface

Considering the Geoid undulations (hundred of meters with respect the Ellipsoid), Refractivity profile can be given with respect to the true height (the height above sea level) :

$$z = r_p - R_s = r_p - R_c - G$$



Statist. Optim. Bending angle

Lat, Long Tangent point

Impact parameter

REFRACTIVITY PROFILE

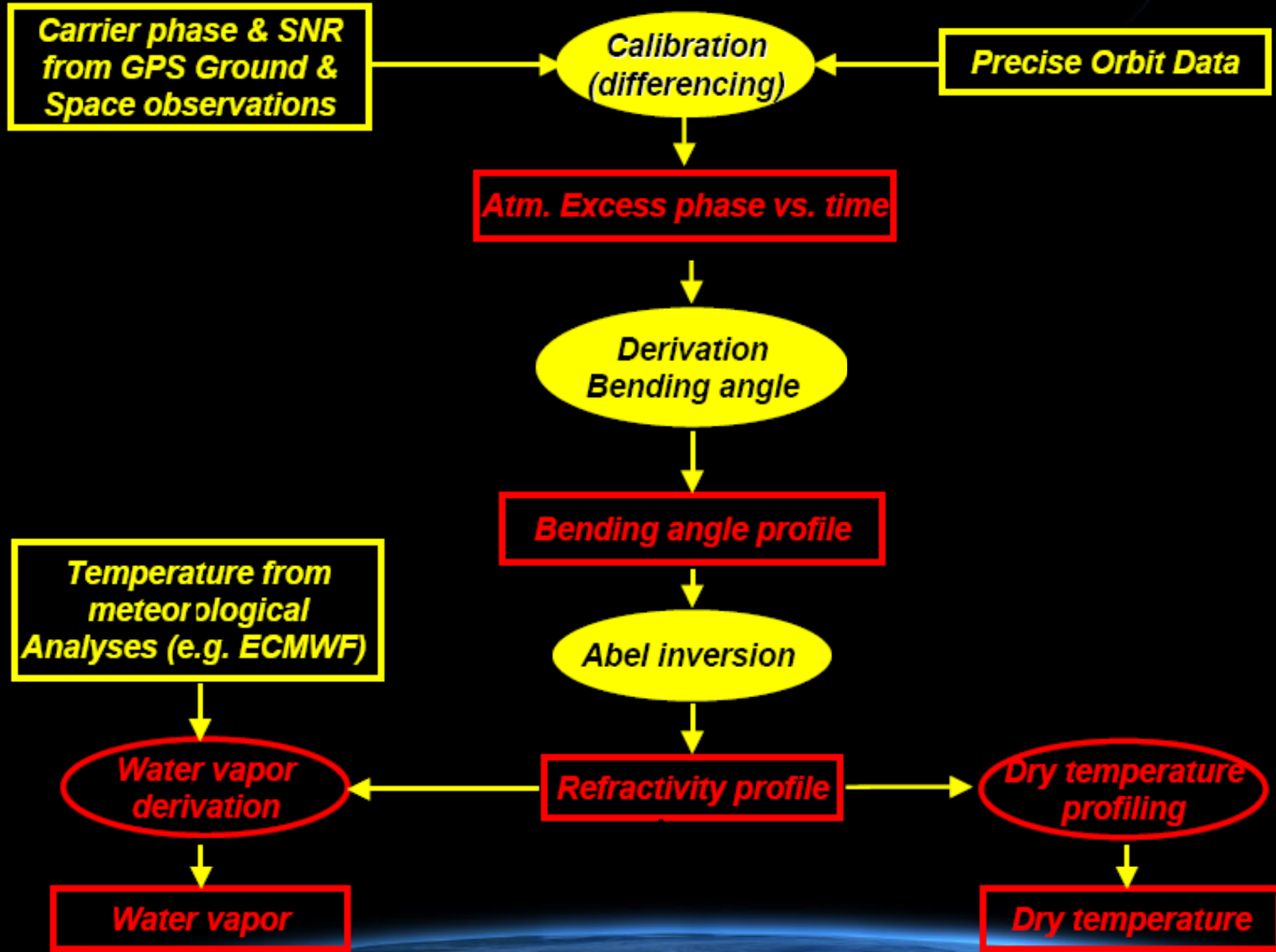
Refractivity

Dry Pressure

Dry Temperature

Tangent point Height

Data analysis (Overview)



- Abel Inversion

- Heights from surface

- Atmospheric profiles extraction

Statist. Optim. Bending angle

Lat, Long Tangent point

Impact parameter

REFRACTIVITY PROFILE

Refractivity

Dry Pressure

Dry Temperature

Tangent point Height

$$N = 77,6 \frac{p_D}{T} + 3,75 \cdot 10^5 \frac{e}{T^2} + \cancel{40,5 \cdot 10^7 \frac{n_e}{f^2}}$$

Dry contribution

Water Vapour contribution

Exploiting the Ionospheric Compensation, this term vanishes

- Abel Inversion

- Heights from surface

- Atmospheric profiles extraction

- Air Density profile evaluation

Where water vapour can be neglected:

$$N = 77,6 \frac{\rho_D}{T}$$

Considering the ideal gases state law:

AIR DENSITY $\rightarrow \rho = \frac{\rho_D}{T} \frac{M_0}{R_D}$

← DRY AIR MOLECULAR WEIGHT M_0

← DRY GASES UNIVERSAL CONSTANT R_D

Thus:

$$\rho(z) = \frac{N(z)}{77,6} \frac{M_0}{R_D}$$

Statist. Optim. Bending angle \rightarrow

Lat, Long Tangent point \rightarrow

Impact parameter \rightarrow

REFRACTIVITY PROFILE

Refractivity \downarrow

Dry Pressure \downarrow

Dry Temperature \downarrow

Tangent point Height \downarrow

- **Abel Inversion**

- **Heights from surface**

- **Atmospheric profiles extraction**

- **Air Density profile evaluation**

Where water vapour can be neglected:

- **Dry Pressure profile**

It can be evaluated through integration of Hydrostatic equation

Statist. Optim. Bending angle →

Lat, Long Tangent point →

Impact parameter →

**REFRACTIVITY
PROFILE**

Refractivity ↓

Dry Pressure ↓

Dry Temperature ↓

Tangent point Height ↓

$$dp_D(z) = -g\rho(z)dz$$

Gravity acceleration

The result is the following

$$p_D(z_{M-1}) = p_D(z_M) + g \int_{z_{M-1}}^{z_M} \rho(z) dz$$

$$p_D(z_{M-2}) = p_D(z_{M-1}) + g \int_{z_{M-2}}^{z_{M-1}} \rho(z) dz$$

z_M, z_{M-1}, \dots, z_0 are the heights of each atmospheric layer

$p_D(z_0)$ (from Climatology)

- **Abel Inversion**

- **Heights from surface**

- **Atmospheric profiles extraction**

- **Air Density profile evaluation**

Where water vapour can be neglected:

- **Dry Pressure profile**

It can be evaluated through integration of Hydrostatic equation

- **Dry Temperature profile**

$$T(z) = 77,6 \frac{\rho_D(z)}{N(z)}$$

Statist. Optim. Bending angle →

Lat, Long Tangent point →

Impact parameter →

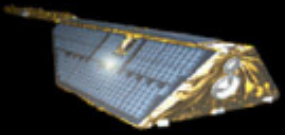
**REFRACTIVITY
PROFILE**

Refractivity ↓

Dry Pressure ↓

Dry Temperature ↓

Tangent point Height ↓



Water vapor retrieval



$$N = 77.6 \frac{p}{T} + 3.73 \times 10^5 \frac{p_w}{T^2}$$

N: atmospheric refractivity

T: atmospheric temperature [K]

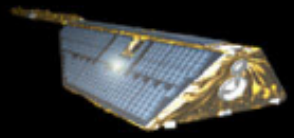
p: atmospheric pressure [hPa]

p_w: water vapor partial pressure [hPa]

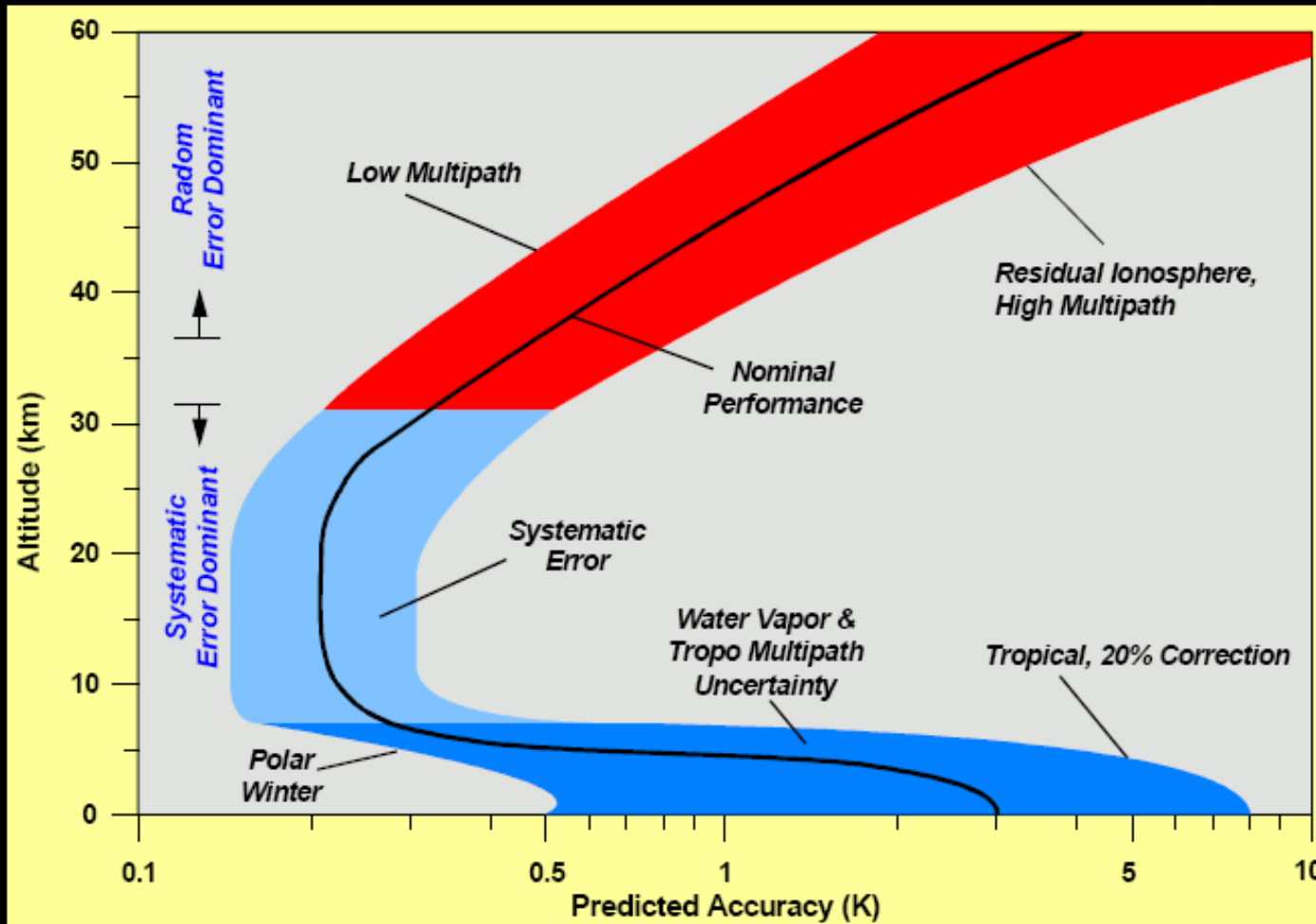
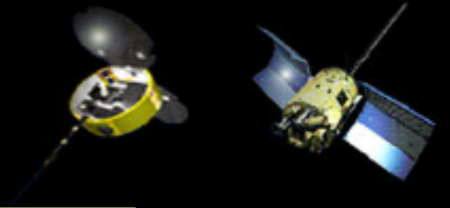
**background
information: *p*, *T*
e.g. from ECMWF**

**refractivity
profile**

humidity profile

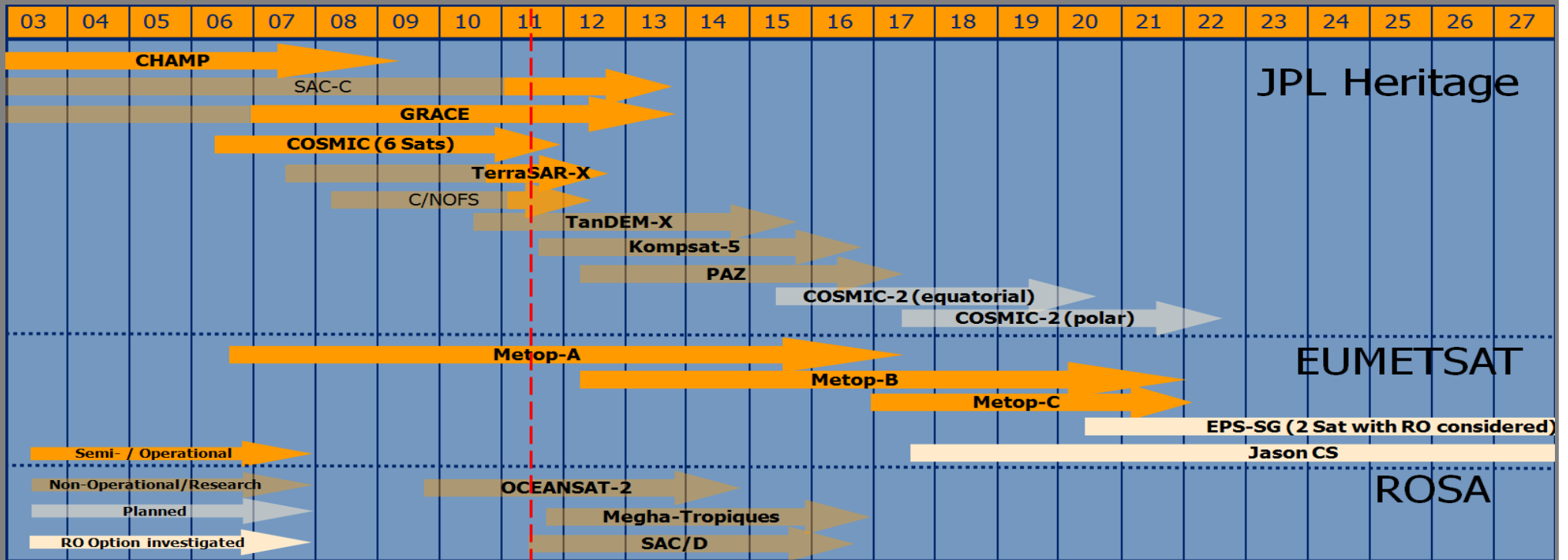


Error Estimation



Melbourne et al., 1994

Radio Occultation missions



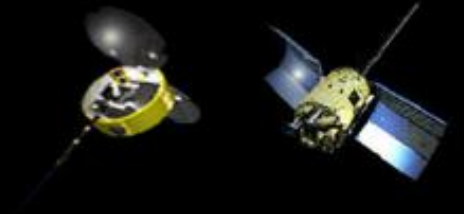
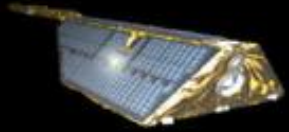
now

Recent EUMETSAT Activities

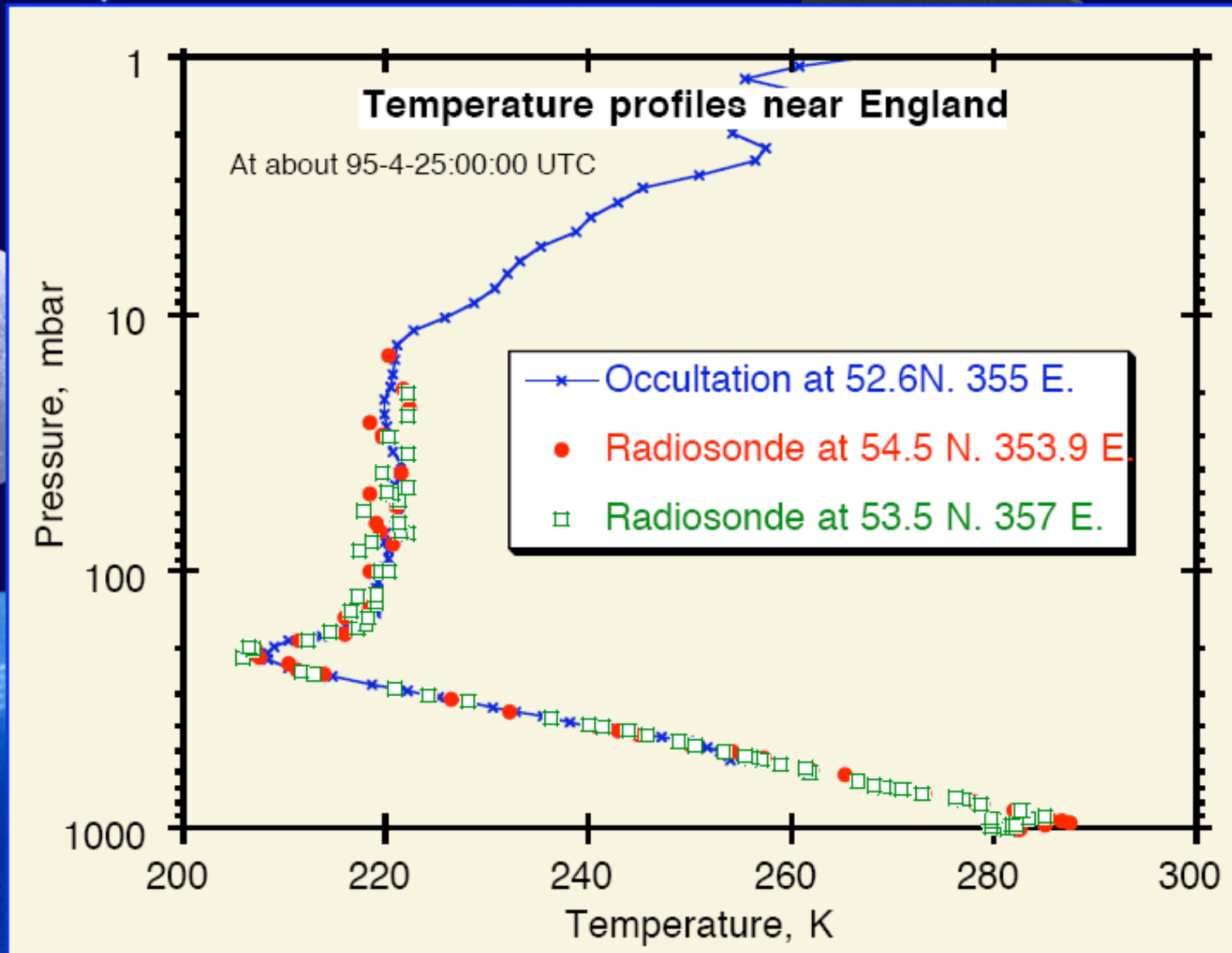
GRAS Team at EUMETSAT

GRAS SAG 26, EUMETSAT
22nd, 23rd of June 2011

EUMETSAT

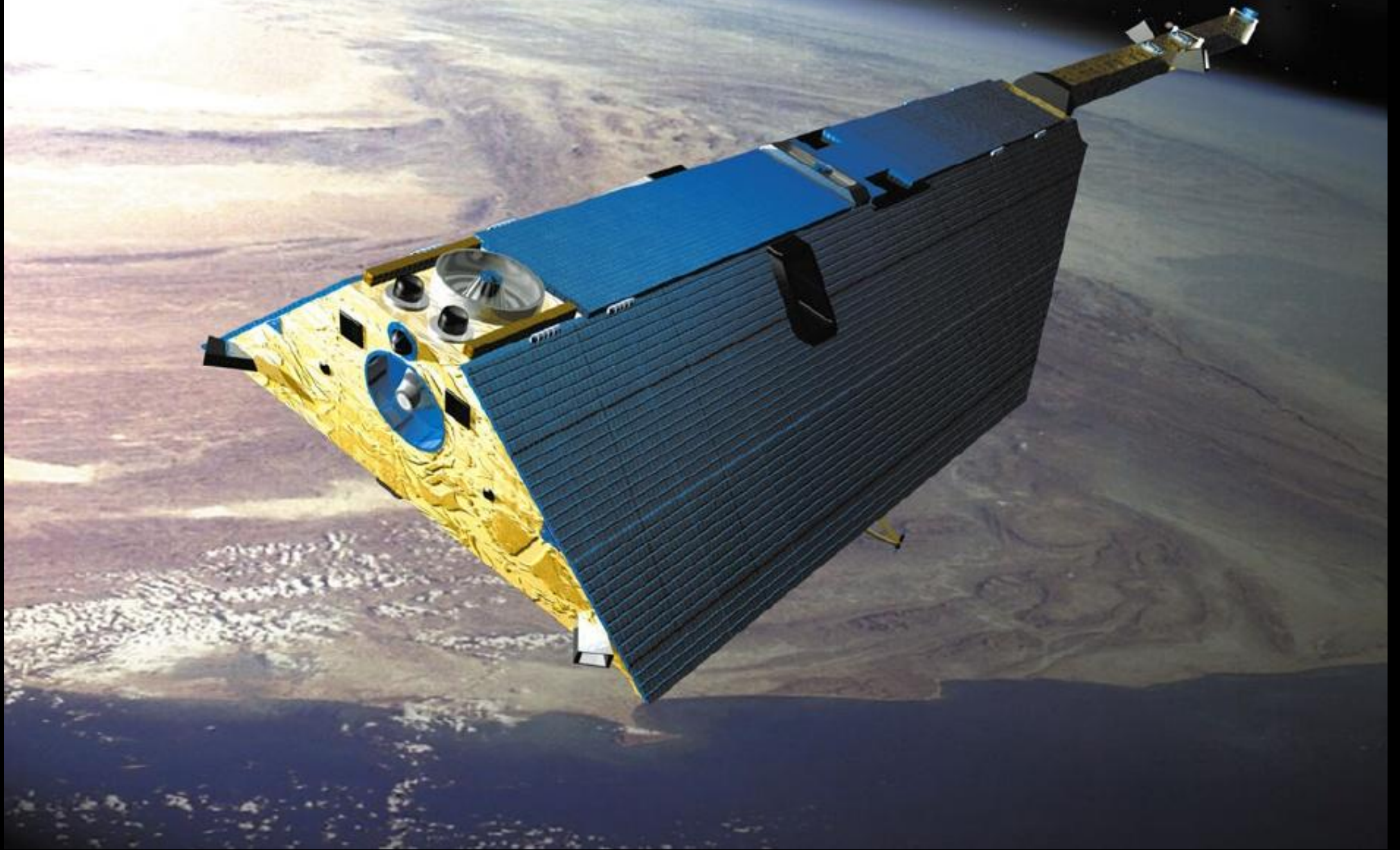


GPS/MET: The pioneer



T. P. Yunck, presented at Colloquium On Atmospheric Remote Sensing Using the GPS, Boulder, Colorado, 2004

CHAMP

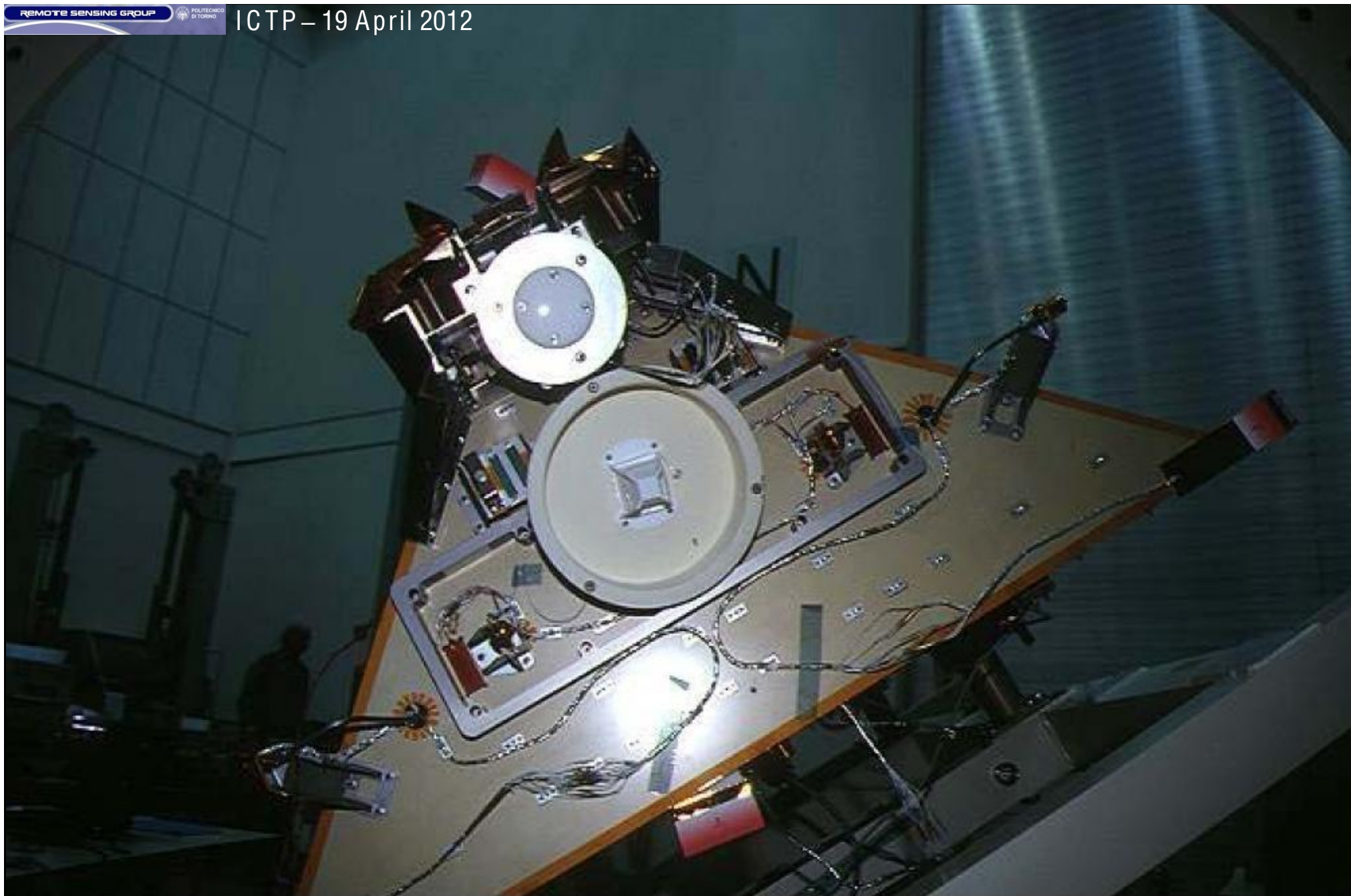


J. Wickert, presented at OPAC-2 Workshop, Graz, 2004

ICTP – 19 April 2012

REMOTE SENSING GROUP

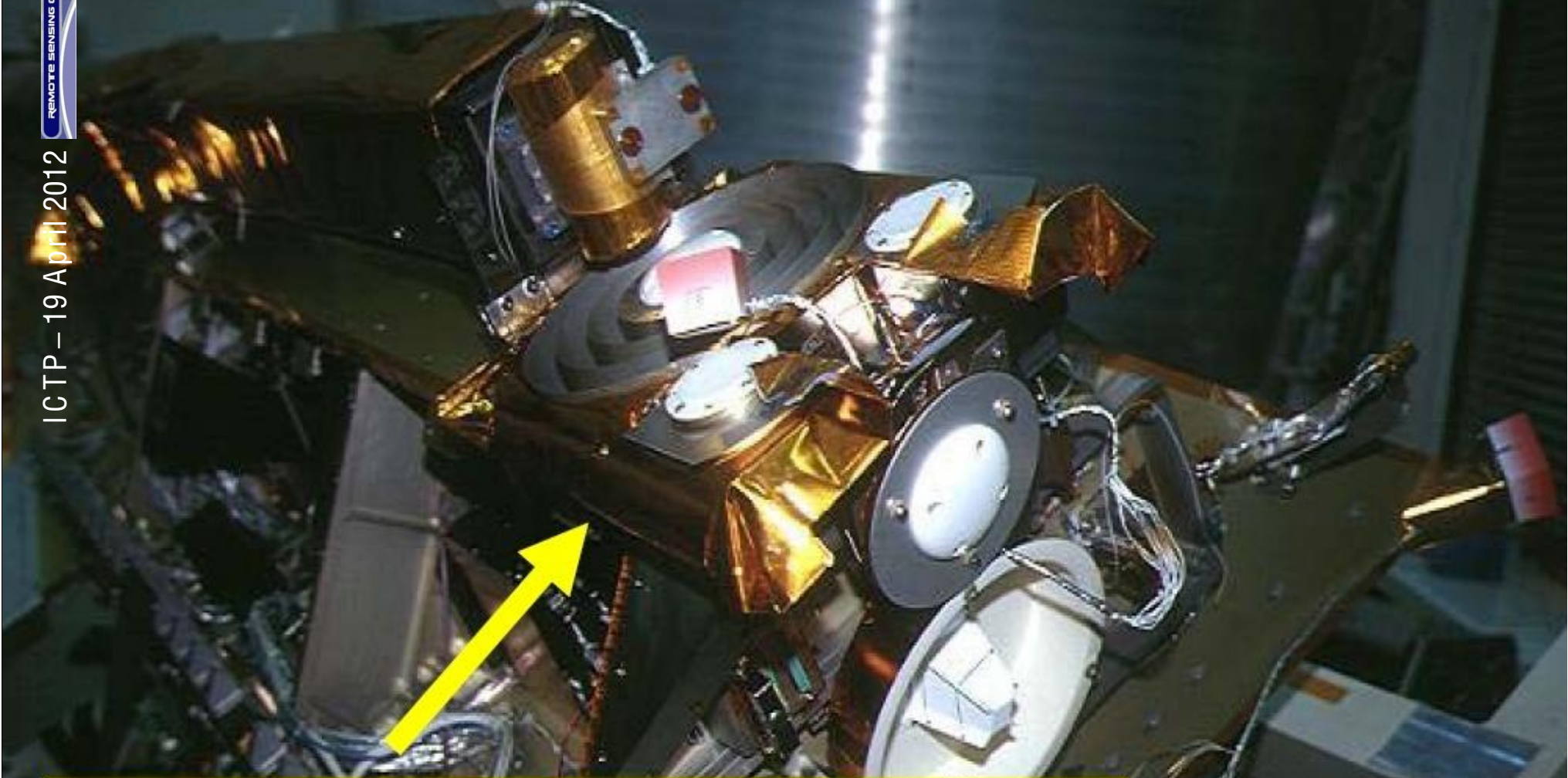
POLITECNICO DI TORINO



Occultation antenna

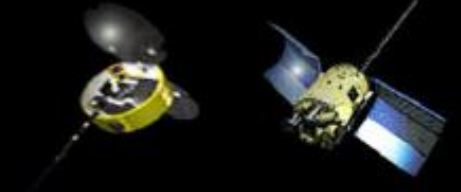
J. Wickert, presented at Colloquium On Atmospheric
Remote Sensing Using the GPS, Boulder, Colorado, 2004

„BlackJack“ and GPS antennas aboard CHAMP



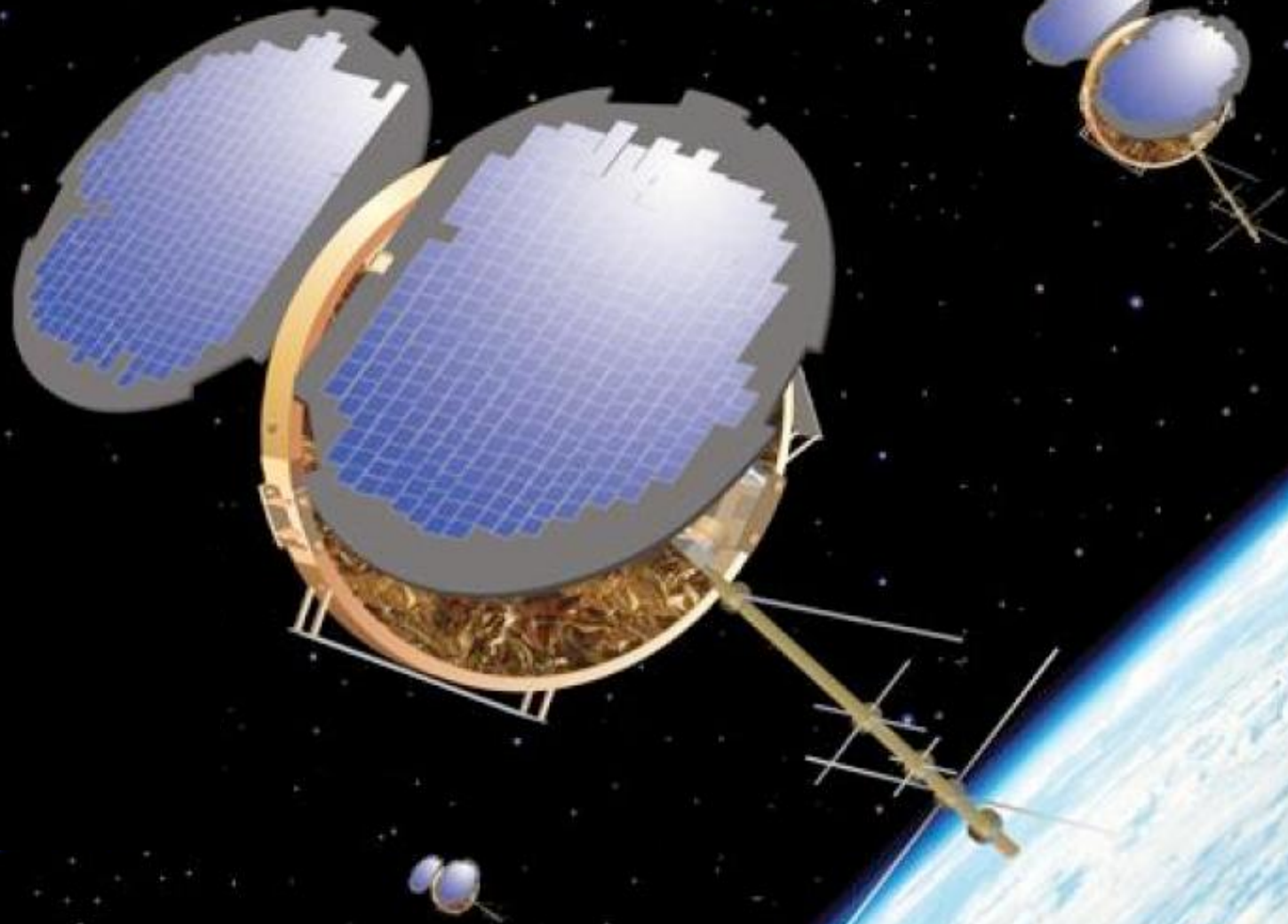
**GPS receiver
„BlackJack“ (JPL)**



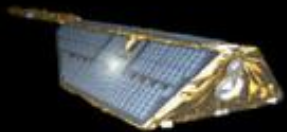


OTHER RO MISSIONS

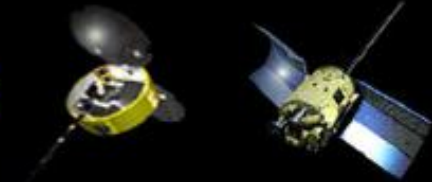
COSMIC/Rocsat3 (6)



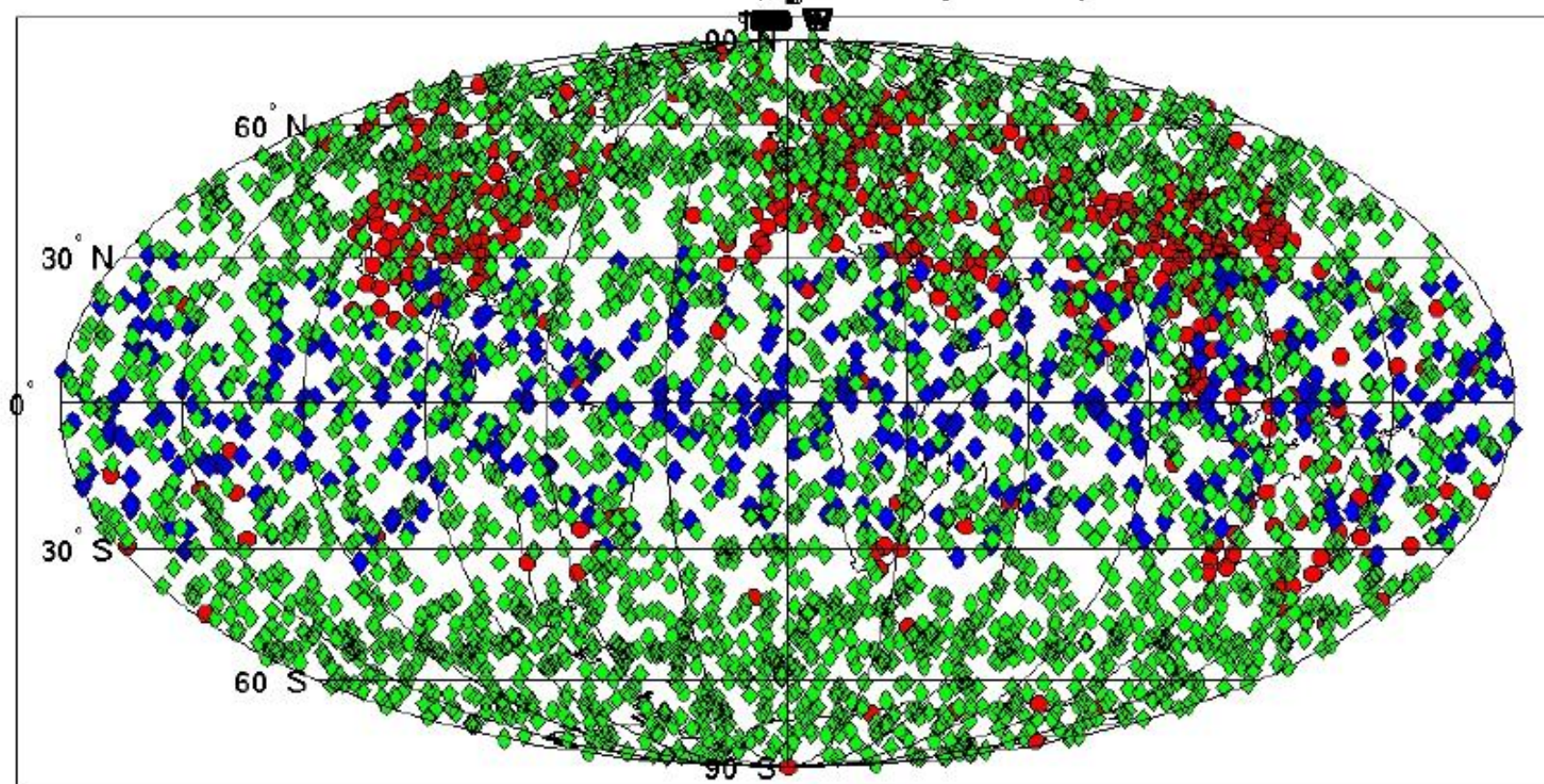
T. P. Yunck, presented at Colloquium On Atmospheric
Remote Sensing Using the GPS, Boulder, Colorado, 2004



COSMIC&EQUARS

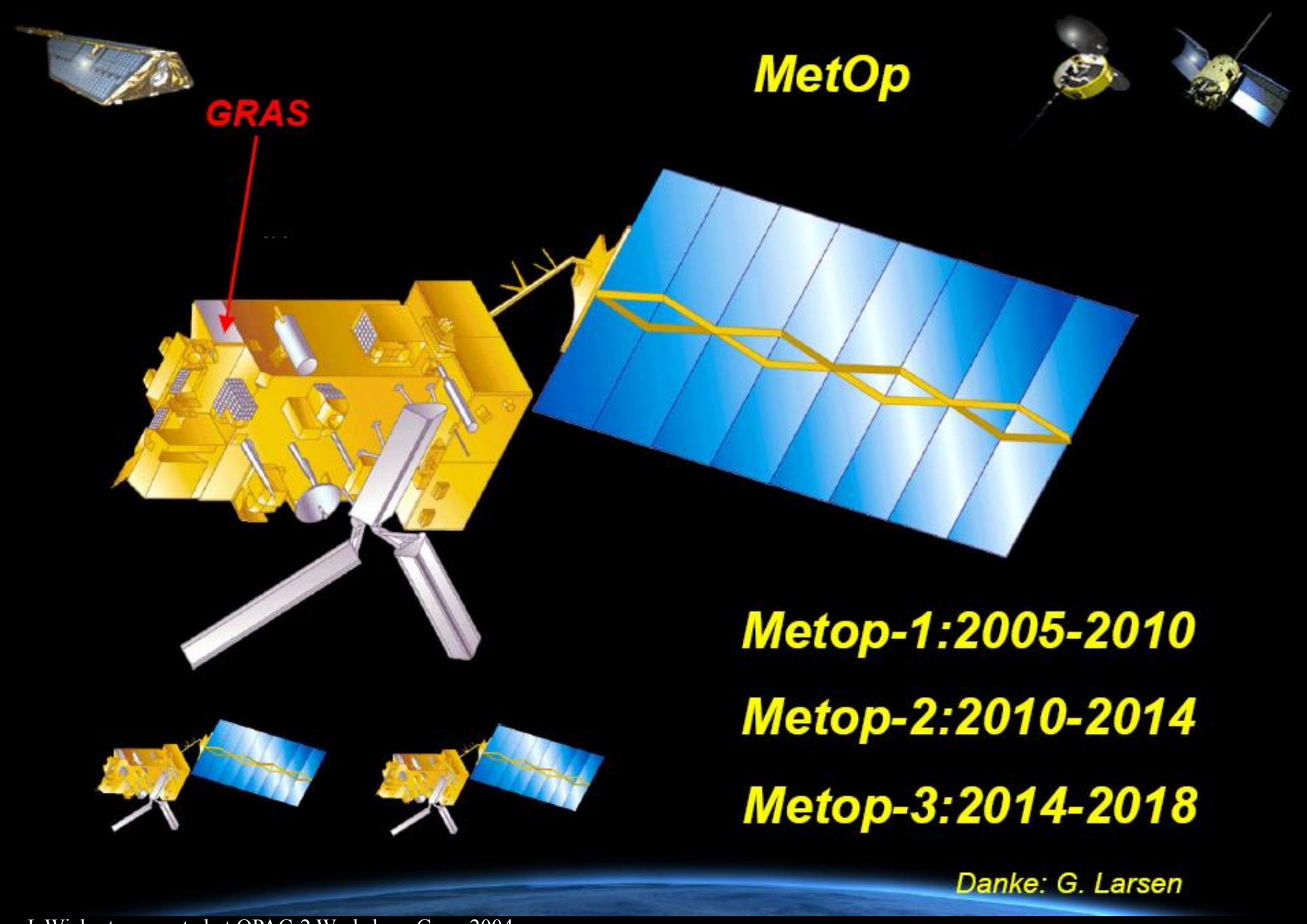


Occultation Locations for COSMIC (6 S/C, 3 planes) and EQUARS, 24 Hrs



Simulation: **COSMIC**, **EQUARS**, **Radiosondes**

Danke: C. Rocken, H. Takahashi

The image features a central 3D cutaway of a satellite with a large blue solar panel array. A red arrow labeled 'GRAS' points to a specific instrument on the satellite's surface. In the top left, a smaller satellite is shown. In the top right, two more satellites are depicted. At the bottom, two smaller cutaway diagrams of the satellite are shown. The background is a dark space with a blue horizon line at the bottom.

MetOp

GRAS

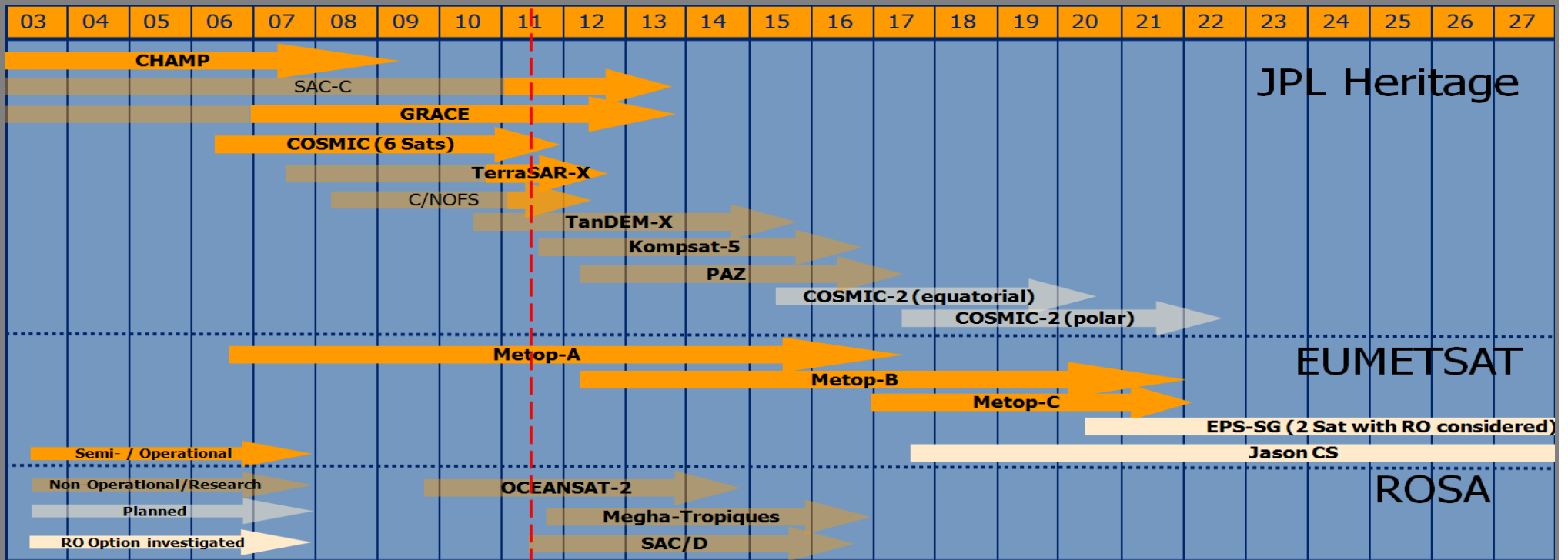
Metop-1:2005-2010

Metop-2:2010-2014

Metop-3:2014-2018

Danke: G. Larsen

Radio Occultation missions



now


Recent EUMETSAT Activities
 GRAS Team at EUMETSAT



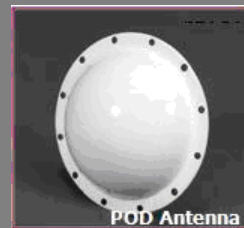
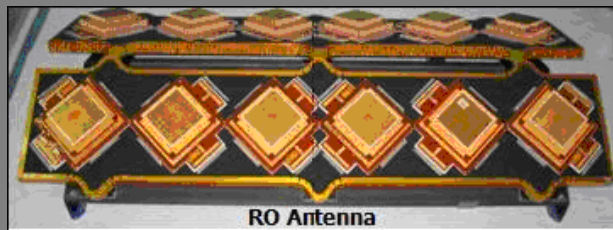
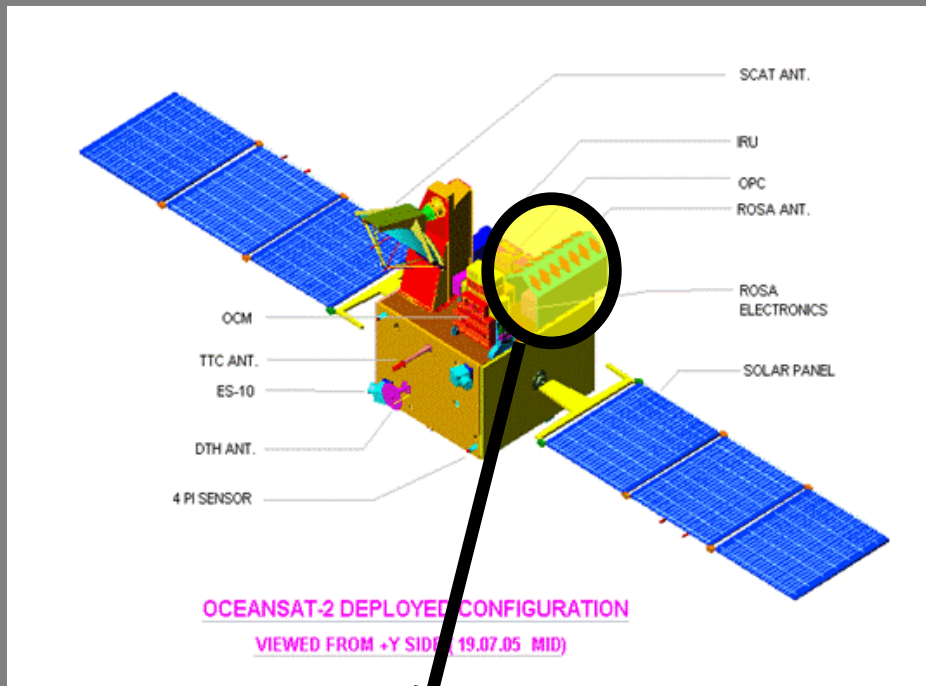
GRAS SAG 26, EUMETSAT
22nd, 23rd of June 2011



THE ITALIAN RO Receiver (ROSA)

Radio Occultation Sounder for Atmosphere (ROSA)

- Radio Occultation GPS receiver
- Developed for Italian Space Agency by Thales Alenia Space
- Open loop (raw sampling) tracking for low troposphere sounding, for **multi-tone low SNR signals** and for a **faster tracking in rising occultations**
- High Gain Radio Occultation antenna





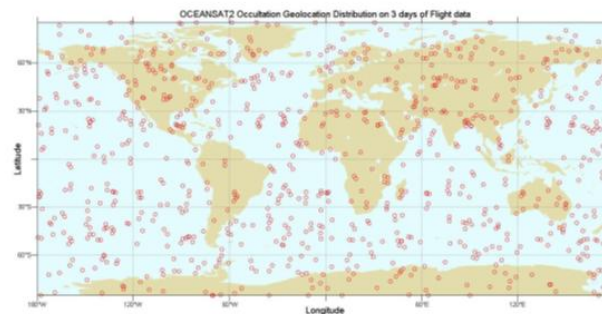
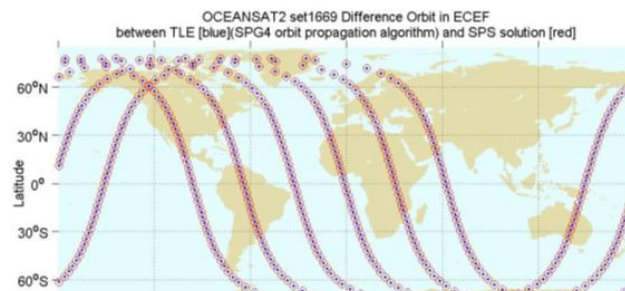
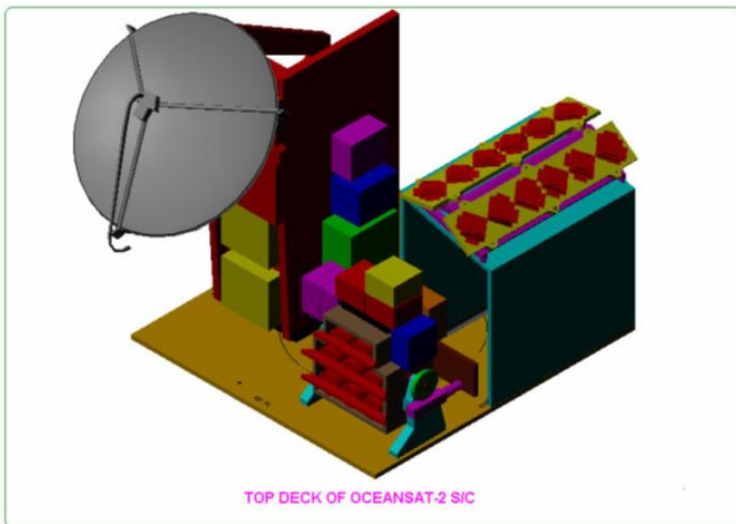
- Space-borne (LEO), Dual-Freq Receiver for Atmospheric Sounding
- 48 single frequency channels configured as 16 L1CA-L1P(Y)-L2P(Y)
- Raw Data (NAV / OCC):
 - L1 C/A, L1P(Y), L2P(Y) Code phase, Carrier phase
 - OL Raw sampling (I/Q) at high frequency (100 Hz)
 - SNR, Amplitude and Noise measurements
- Real-Time Navigation Solution, using GPS L1 C/A code phase (through SPS and EKF - Extended Kalman Filter)
- On-board atmospheric model for excess doppler prediction of occultations (Cira86aQ_UoG climatological Model)
- Rising and setting occultation capabilities (ROA Vel + ROA A-Vel)

© copyright kees waenenbos



ROSA on OCEANSAT-2

- ISRO OCS-2 mission launched Sept 23, 2009
- Ocean studies, meteorology and prediction of Monsoon
- **Opportunity Mission for in-flight Verification of ROSA**
- ROSA configuration limited to one directive Velocity antenna (rising only)
- RO +/- 45° azimuth, 0 to -30° elevation
- 15°+20° tilt wrt velocity direction



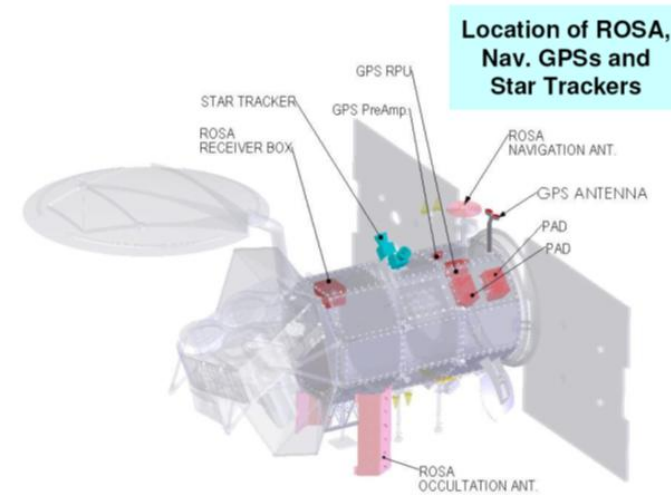


ROSA on SAC-D

ION 2010 International Technical Meeting Program
January 25-27, 2010 · Catamaran Resort Hotel · San Diego, CA



- CONAE / NASA Earth Science mission, to provide global meas of sea water salinity
- Sun-synchronous orbit, 657 km
- Strong pulsed interference from Aquarius required dedicated RF filter box
- Velocity + Anti-Velocity antennas allow Rising + Setting occultations
- SAC-D satellite has been launched on 10 June 2011
- ROSA instrument has been switched ON the 31 August 2011

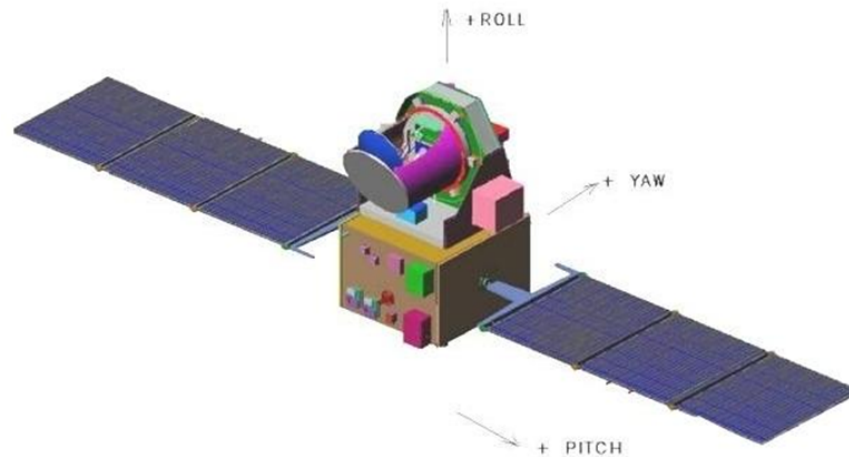


Kindly provided by A. Zin



ROSA on MeghaTropiques

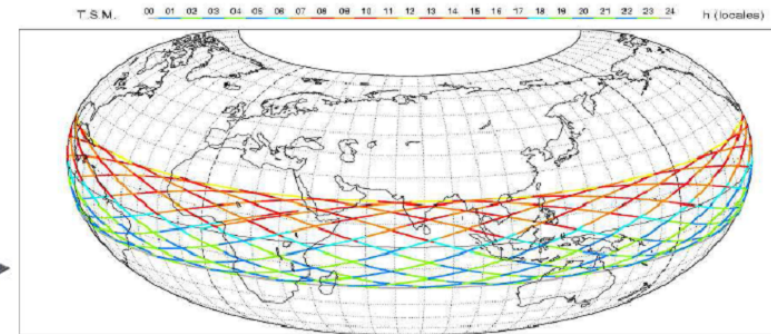
- ISRO mission dedicated to tropical atmosphere studies: 3 radiometric instruments to observe water vapour, condensed water and radiative fluxes
- Highly repetitive sampling of inter-tropical band: latitudes 10°-20°, 870Km
- MT periodically performs yaw axis rotation causing ROSA to exchange velocity ROA with anti-velocity ROA
- RO Antennas are one half 6-patch panel, azimuth FOV limited to ±35°
- MEGHA TROPIQUES satellite has been launched on 12 October 2011
- ROSA instrument has been switched ON 12 October 2011



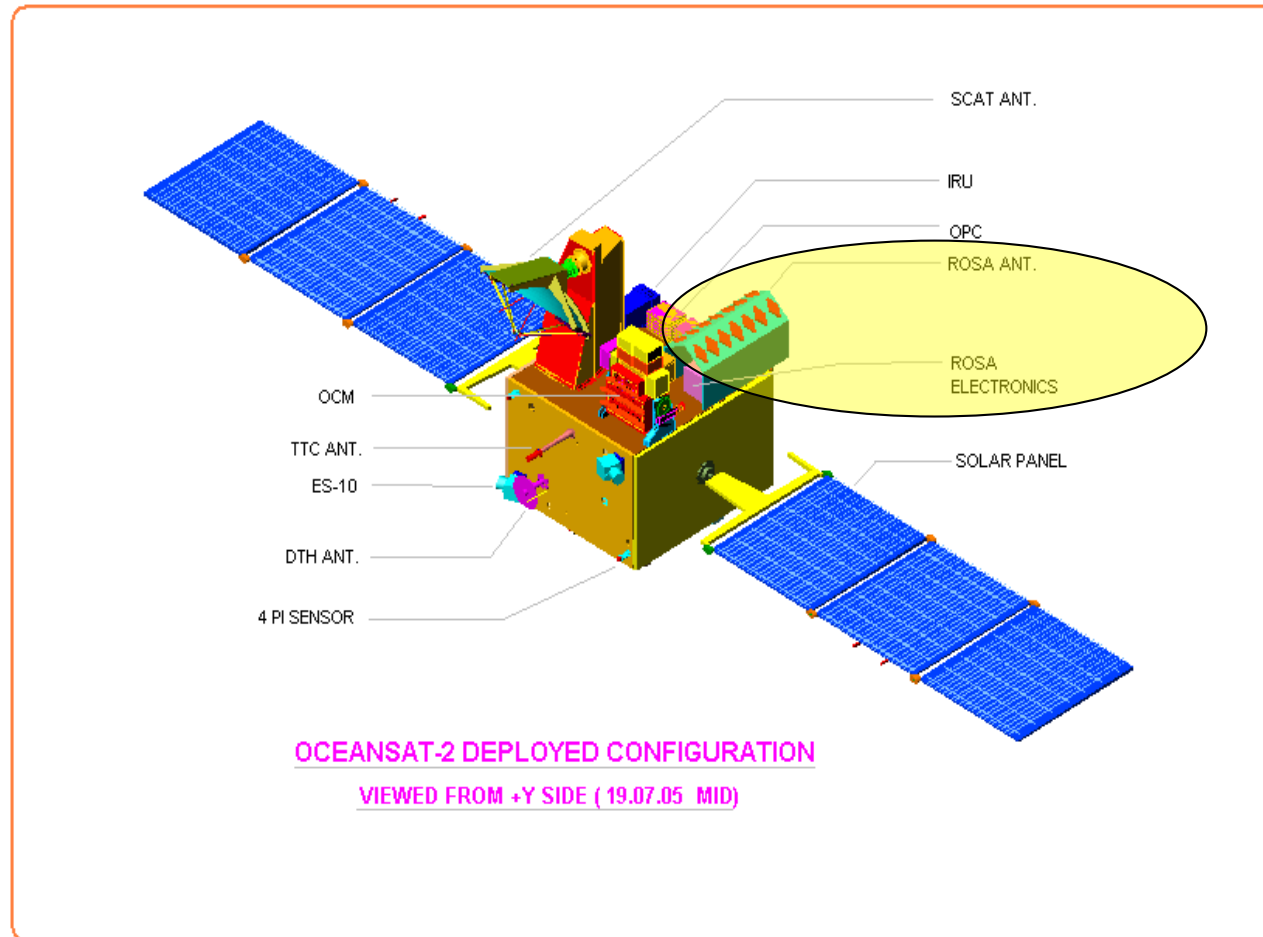
Megha-Tropiques
Trace de l'orbite

Phasage = [14; -1; 7] 97
>>> Durée représentée : 1440.0 mn = 1.00j

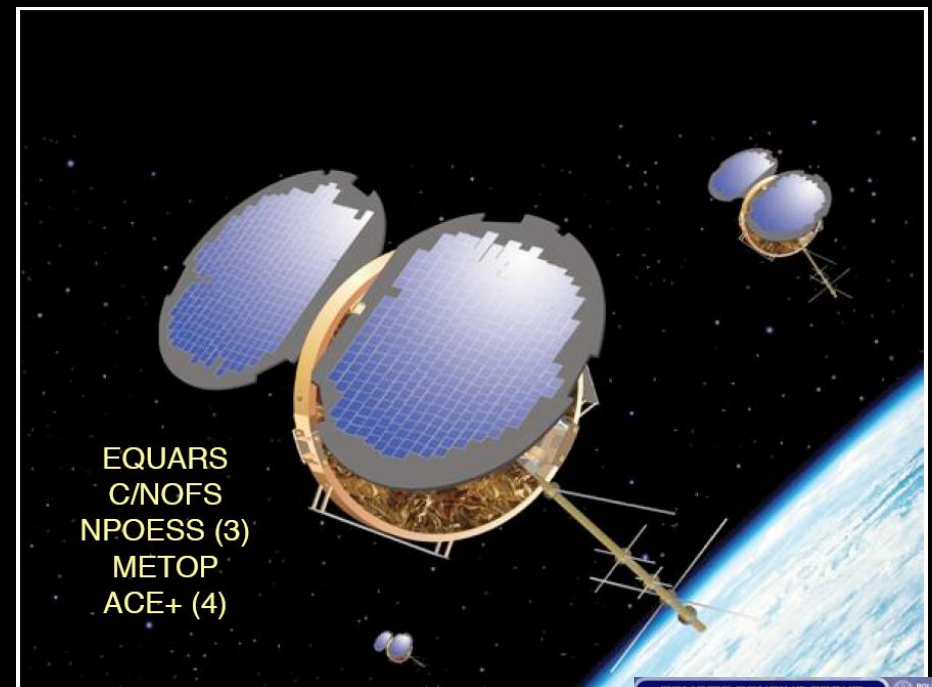
Altitude = 865.6 km a = 7243.700 km
Inclinaison = 20.00 °
Période = 101.93 mn * Tours/j = 14.13
Décalage à l'équateur = 2892.0 km (26.0 °)

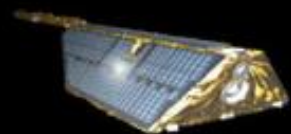


ROSA-ROSSA: Radio Occultation Software for ROSA on-board OCEANSAT-2 data processing

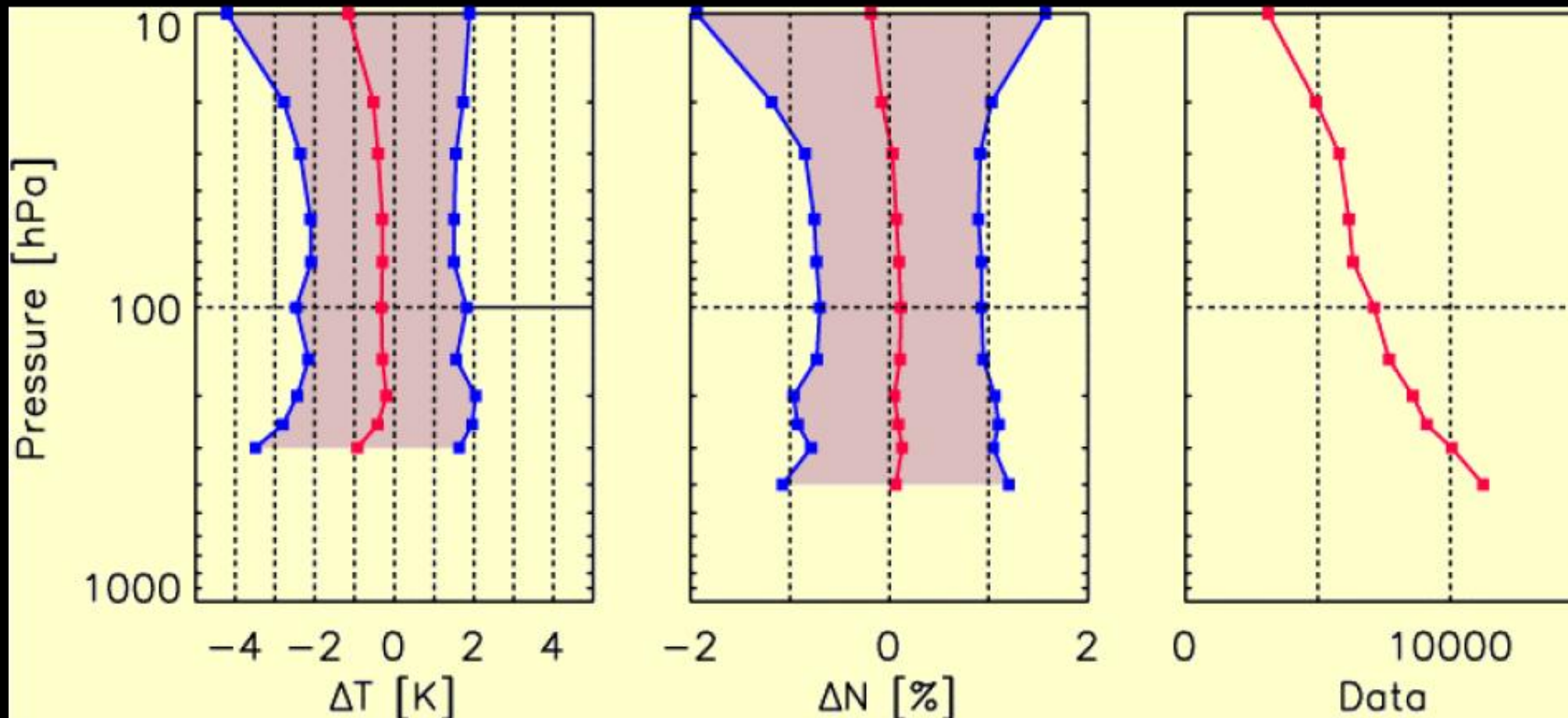
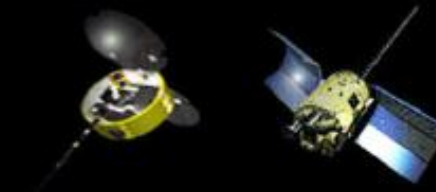


... SOME SUMMARIZING RESULTS



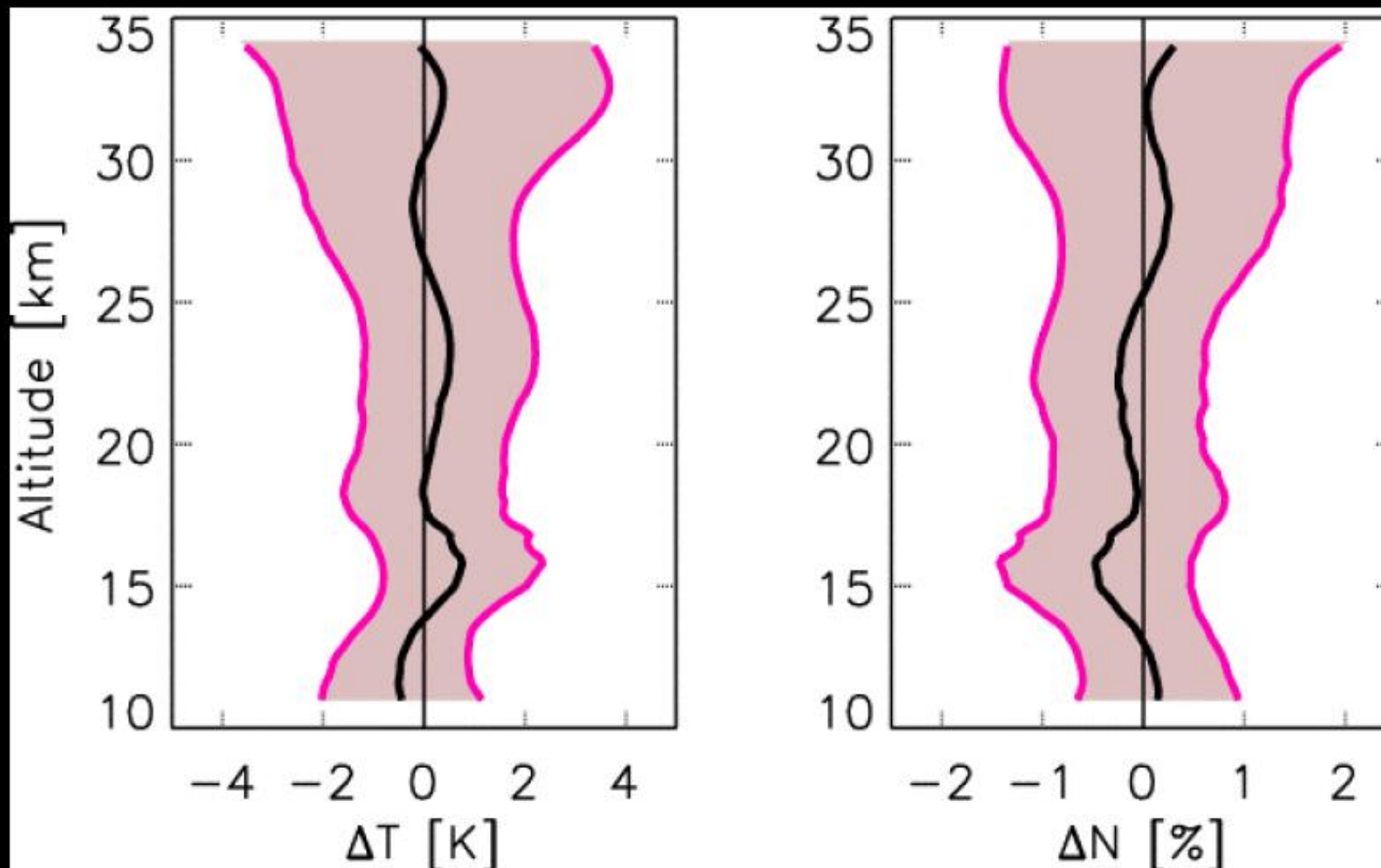
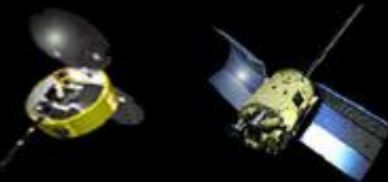


Comparison with RS (2003)

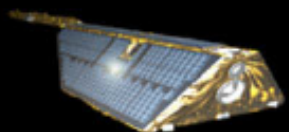




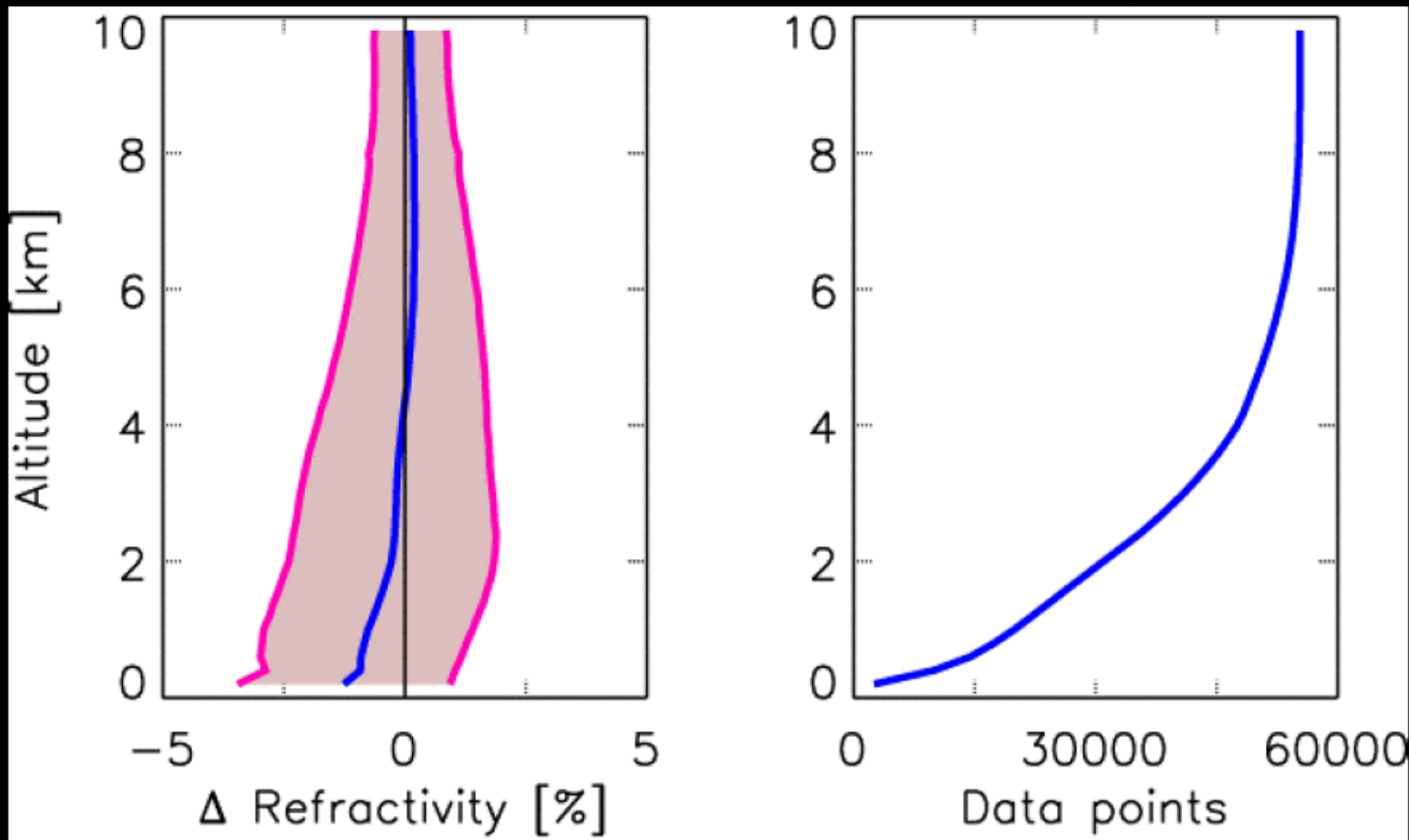
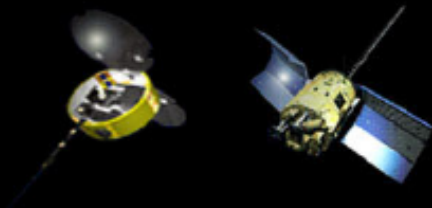
Comparison with ECMWF (2003)



~60,000 profiles



Comparison with ECMWF



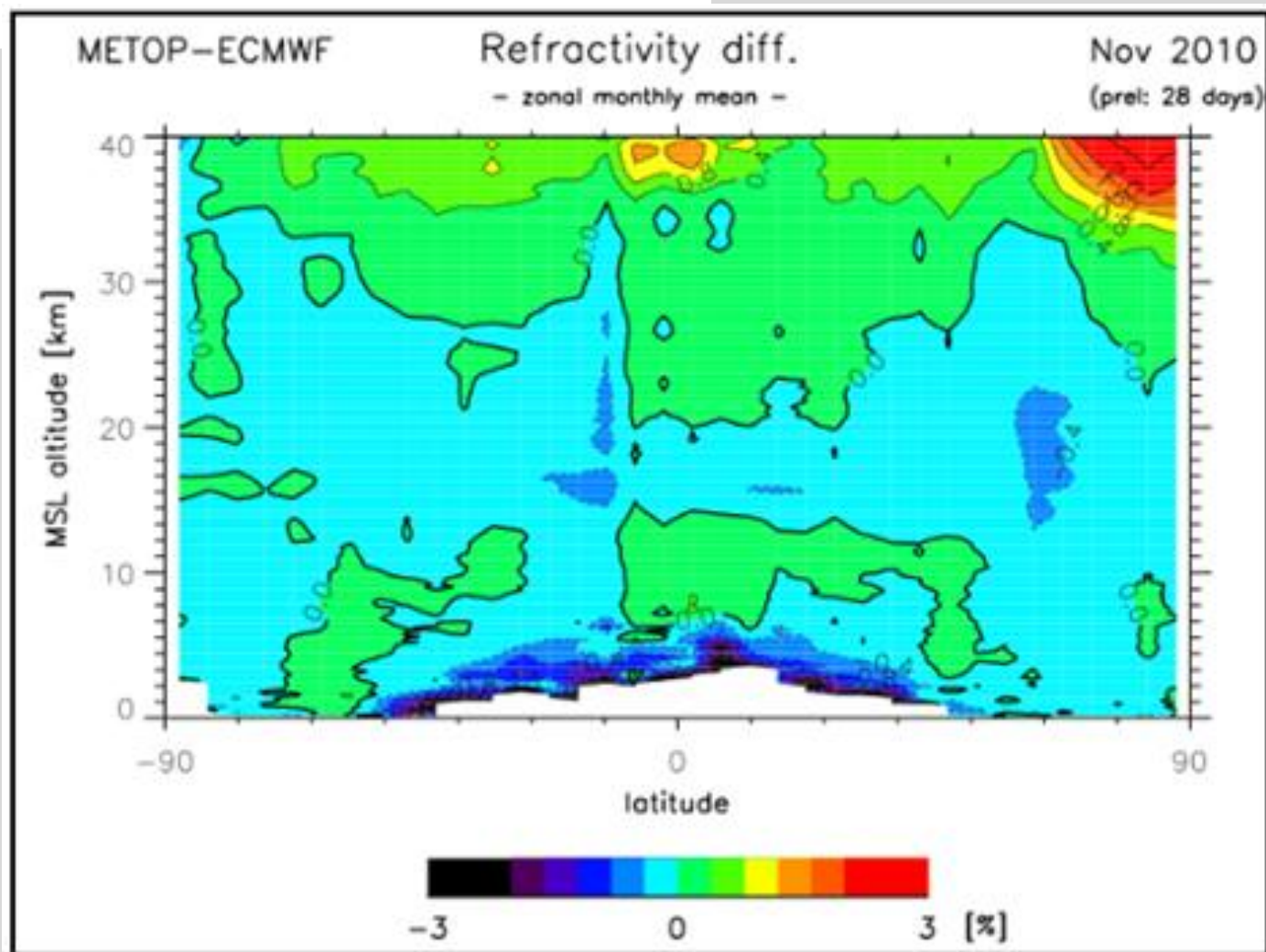
GRAS SAF Climate Products

SAG26, EUMETSAT, 22-23 June 2011

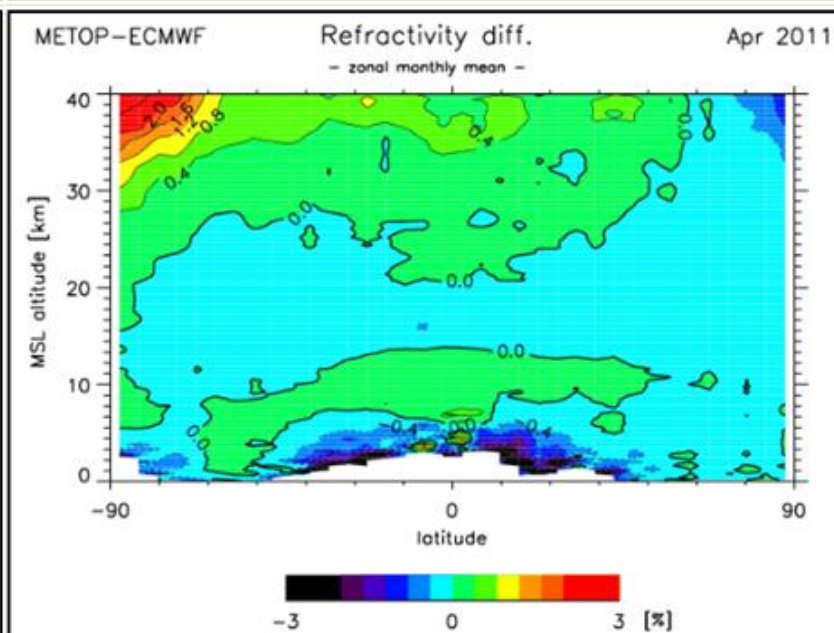
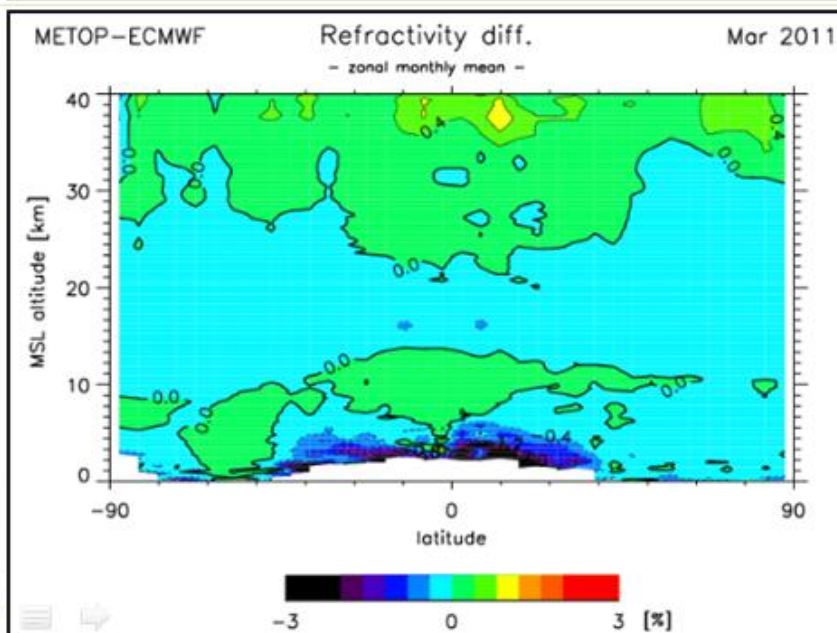
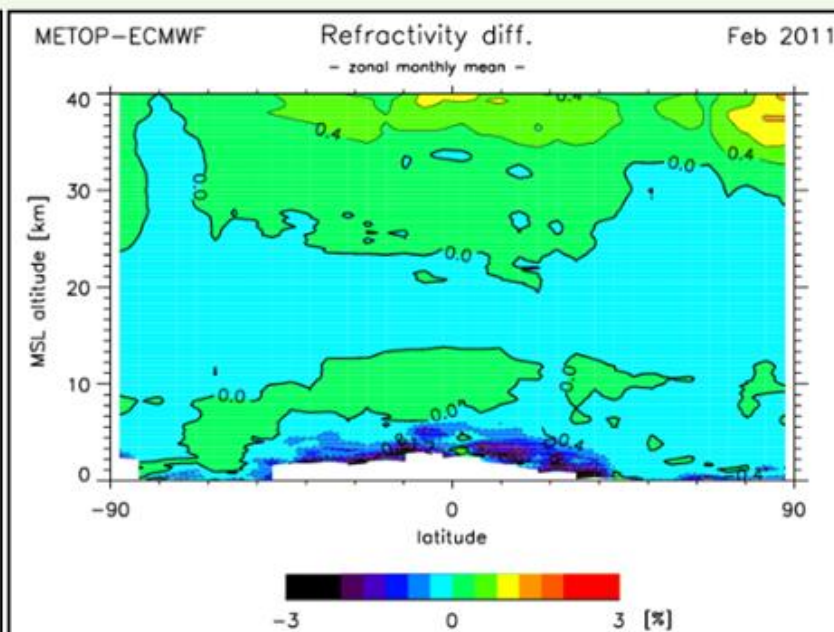
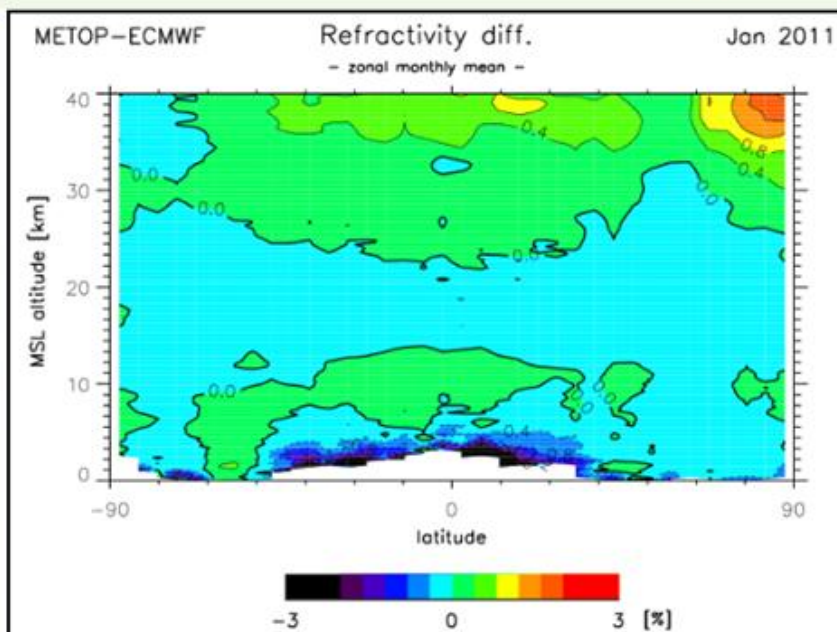
Hans Gleisner & Kent B. Lauritsen

Danish Meteorological Institute

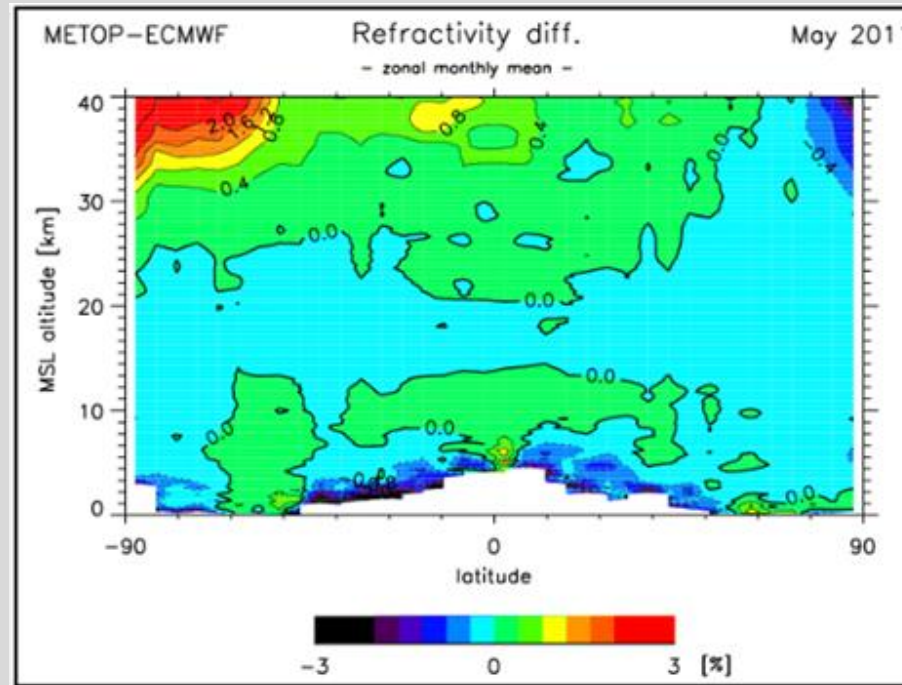
Metop REF O-B/B



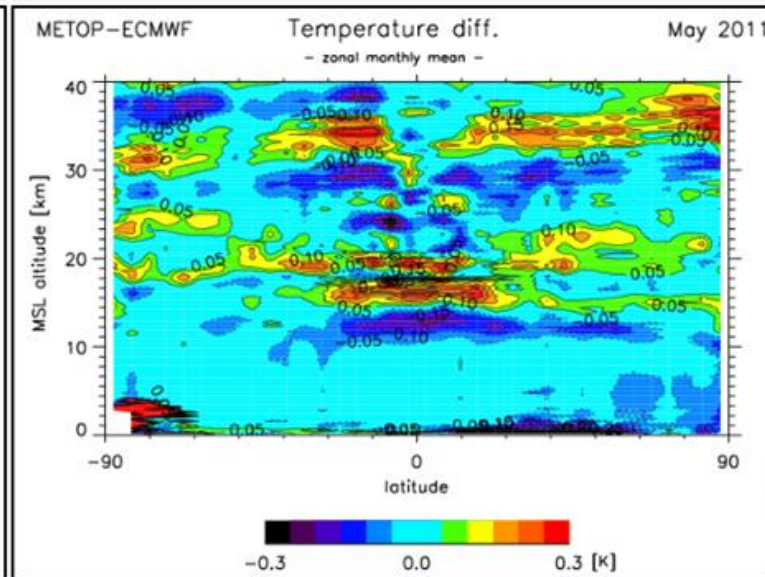
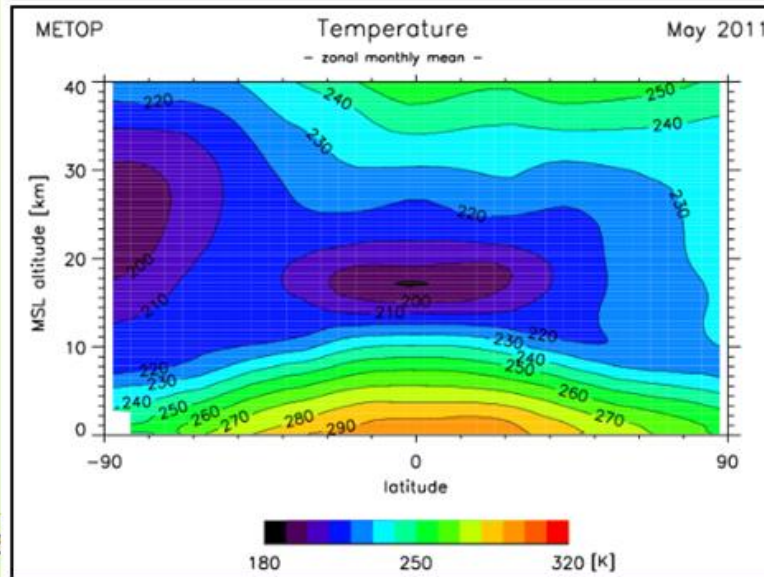
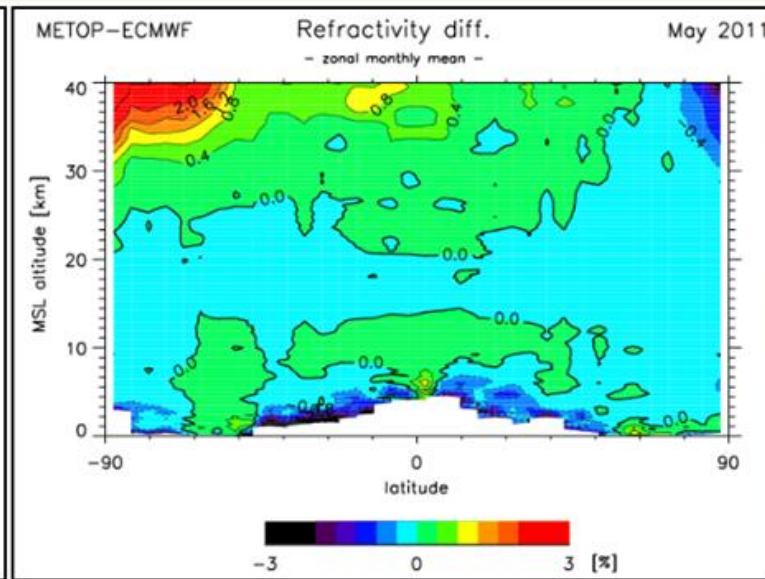
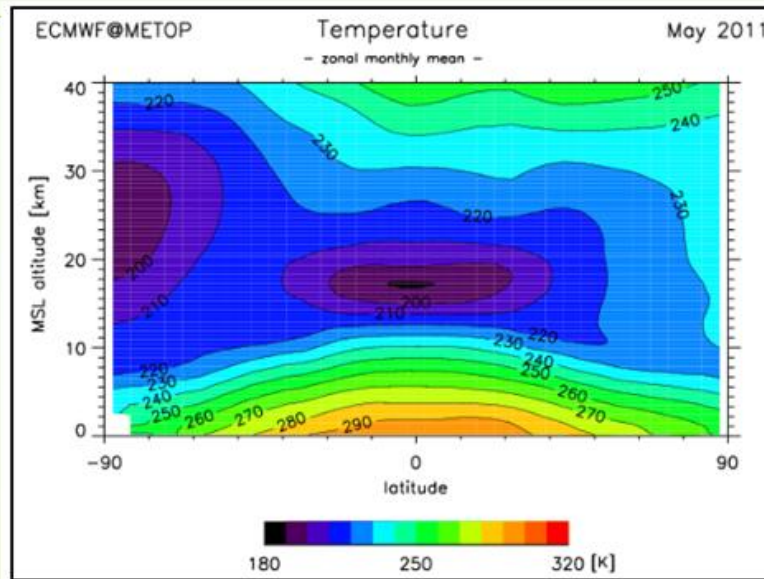
Metop REF O-B/B



Metop REF 0-B/B



Metop REF & T: Polar bias May 2011



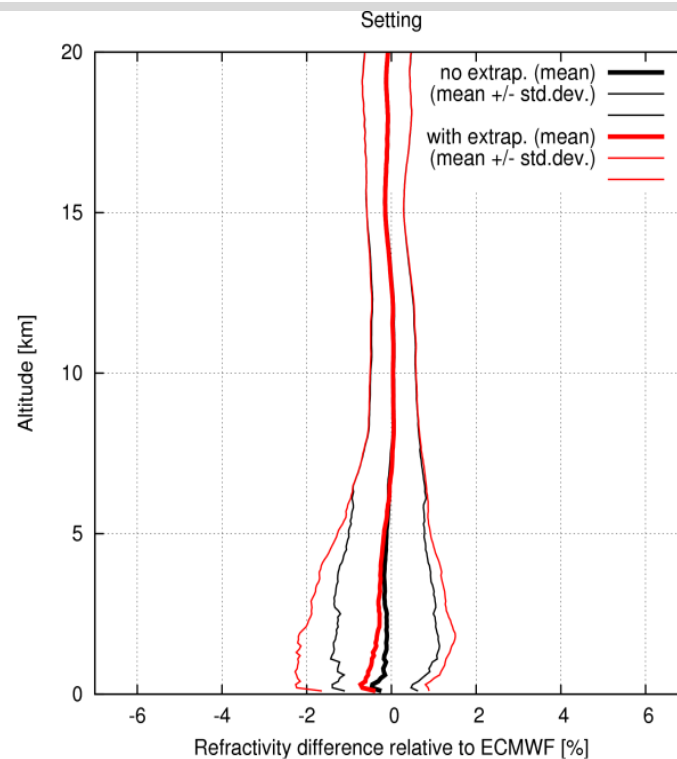
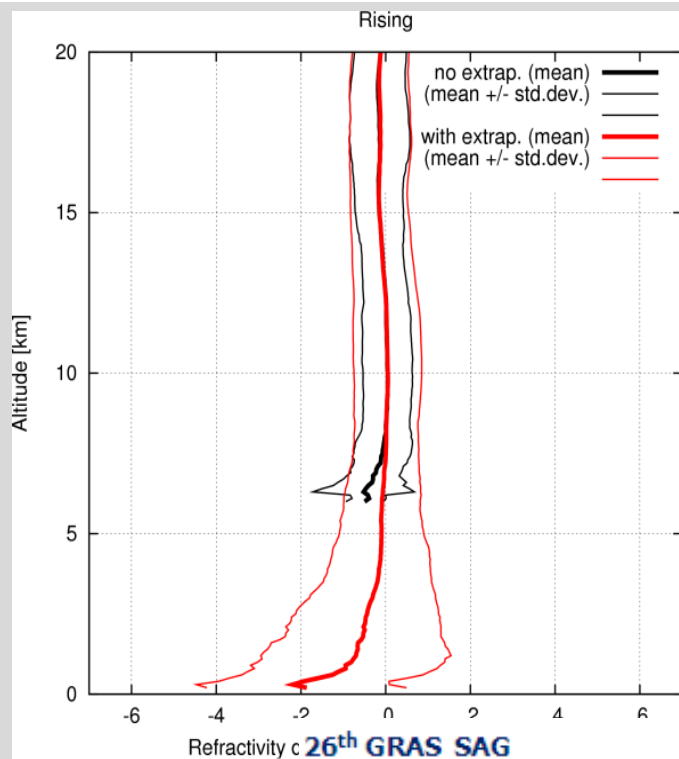
GRAS SAF Status & Next Steps

Kent B. Lauritsen

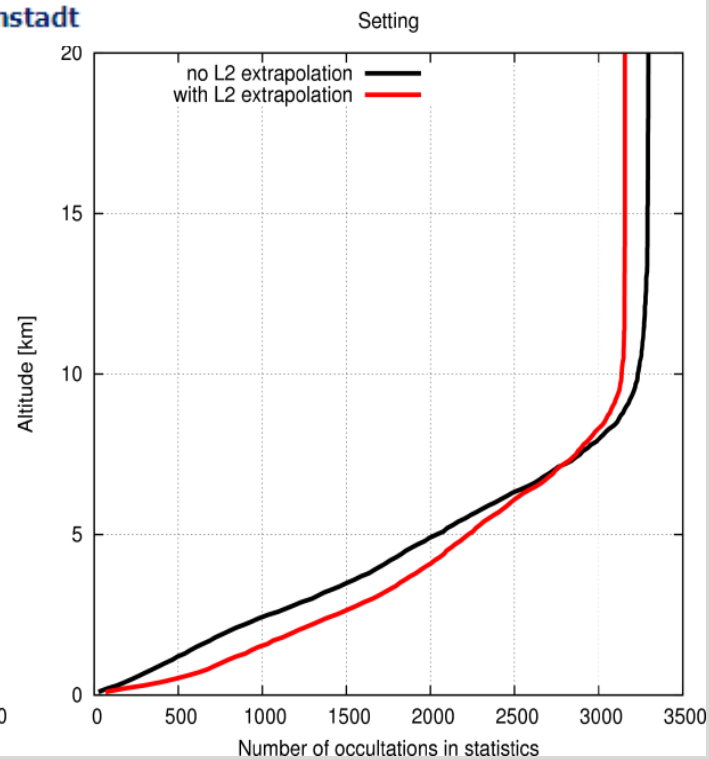
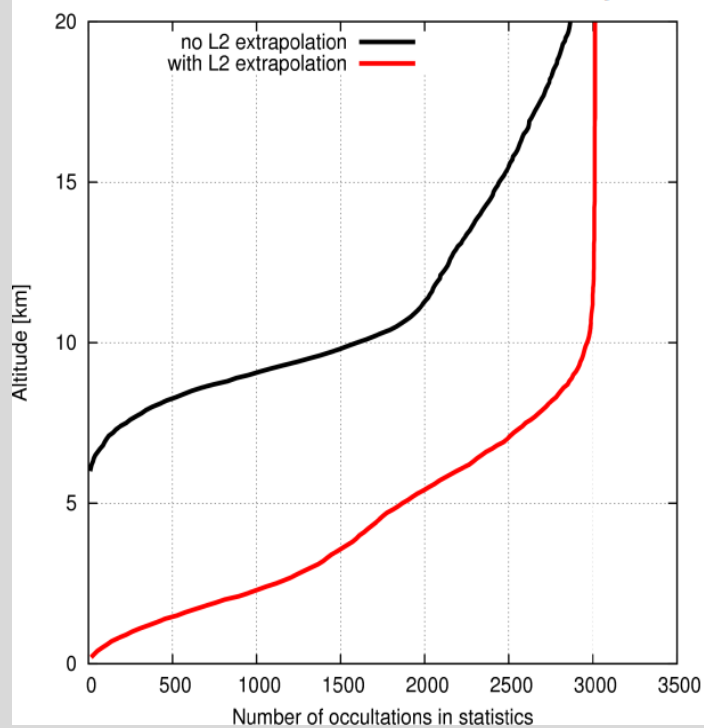
*Danish Meteorological Institute
Copenhagen, Denmark*

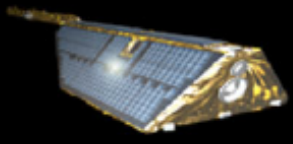
SAG26, EUMETSAT, 22-23 June 2011

Data
observed in
Dec 2010



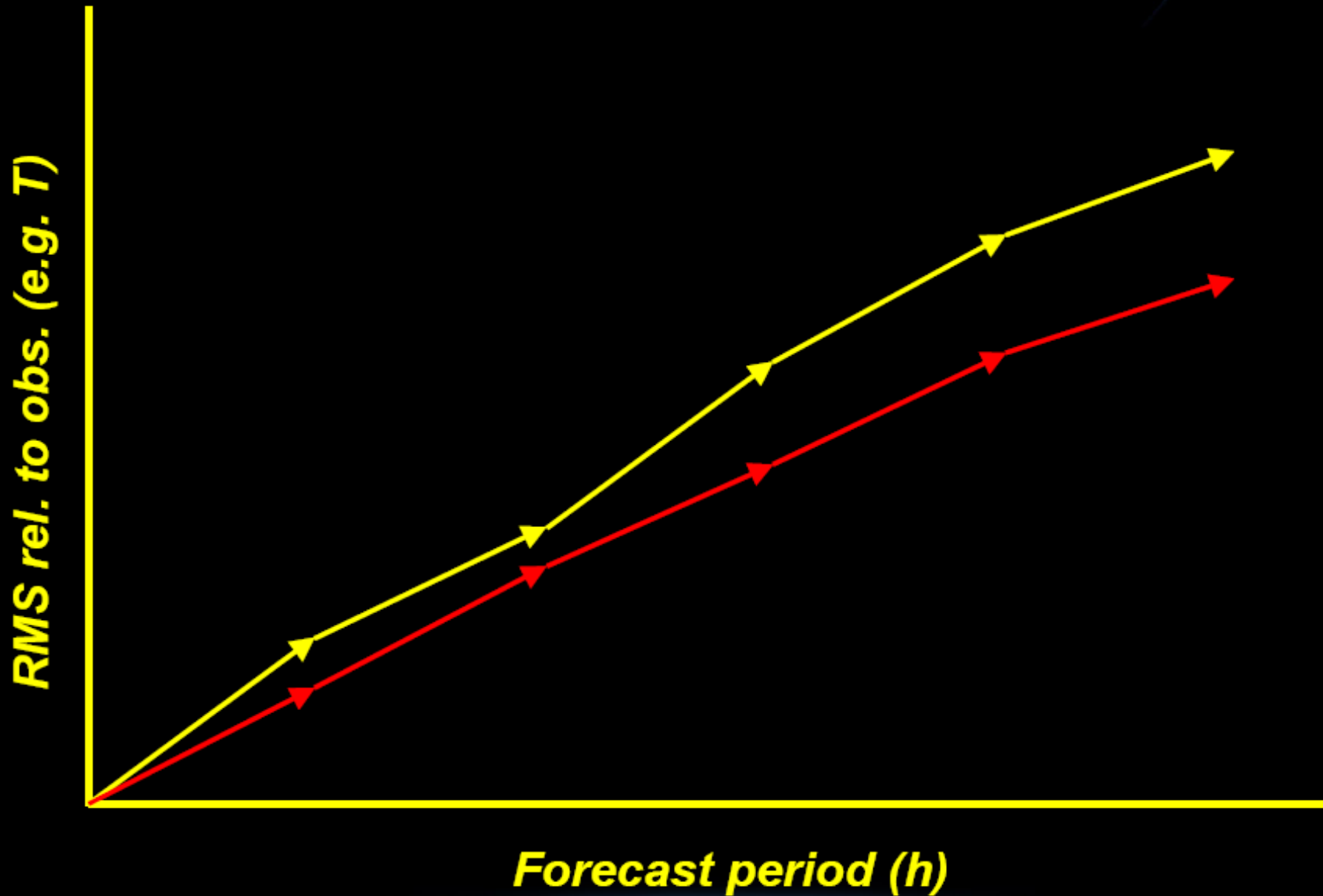
26th GRAS SAG
22nd – 23rd June 2011, Darmstadt





Application: Weather forecast (study by S. Healy et al.)

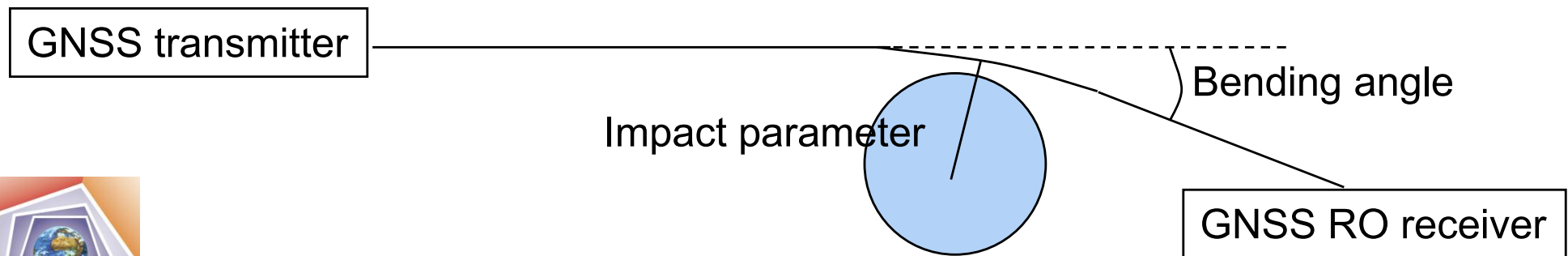
How to evaluate the impact of GPS RO ?



GNSS Radio Occultation Assimilation Methodology

Methodology developed by Healy and Thépaut (2006) for NWP

- Assimilation of bending angles as a function of impact parameters
- No bias correction (data assumed unbiased)
- Between the near-surface and 40 km altitude
- Observation errors assumed uncorrelated in the vertical



Poli et al., "Climate Applications of GNSS Radio Occultation in European Global Reanalysis", *2nd Galileo Colloquium*, Padua, 2009



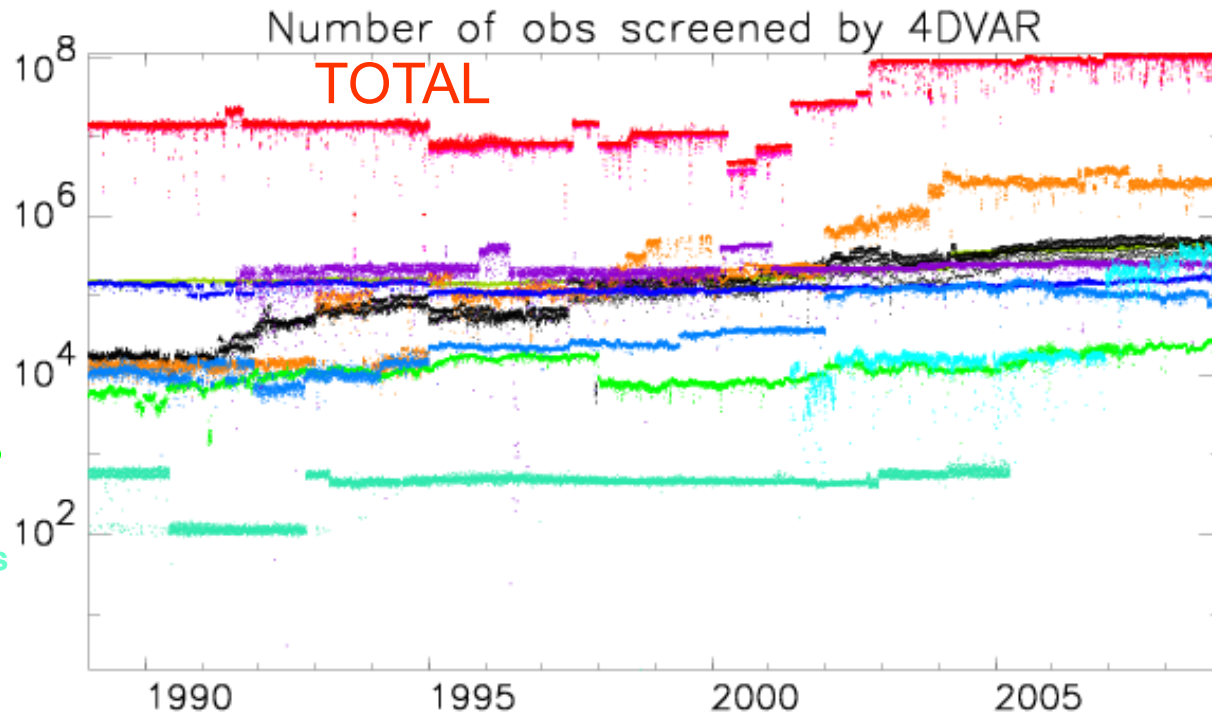
Observations available for ERA-Interim

“Conventional”

- Radiosondes
- Surface
- Aircraft
- Radiosondes (wind only)
- Drifting buoys
- Surface pressure pseudo-observations from Australian Bureau of Meteorology (PAOB)

“Satellite”

- Radiances
- Atmospheric motion vectors
- Scatterometers
- GNSS Radio Occultation



PAOB	DRIBU	LIMB	PILOT	TEMP	AIREP	SCATT	SYNOP	SATOB	SATEM	TOTAL
5,192,278	184,281,536	441,193,792	789,762,112	1,912,945,664	2,618,648,064	2,838,112,256	3,209,333,604	12,630,662,144	532,684,079,104	657,314,211,840

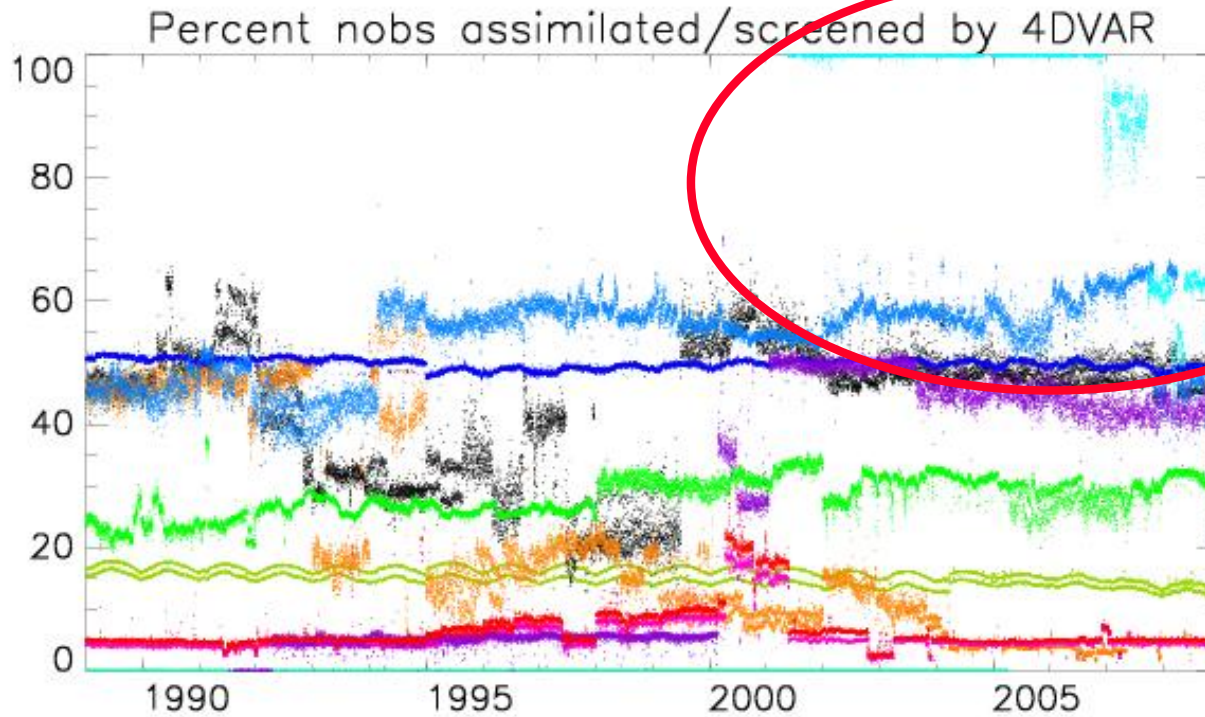


Reanalysis involves many observations and types of observations

Poli et al., “Climate Applications of GNSS Radio Occultation in European Global Reanalysis”, *2nd Galileo Colloquium*, Padua, 2009



Average daily usage rate, by data-type



Sat Conv Sat Conv Sat Conv Conv Conv Sat

PAOB 0 SATEM 5 TOTAL 6 SYNOP 16 SATOB 19 DRIBU 26 SCATT 32 AIREP 42 TEMP 49 PILOT 53 LIMB 61



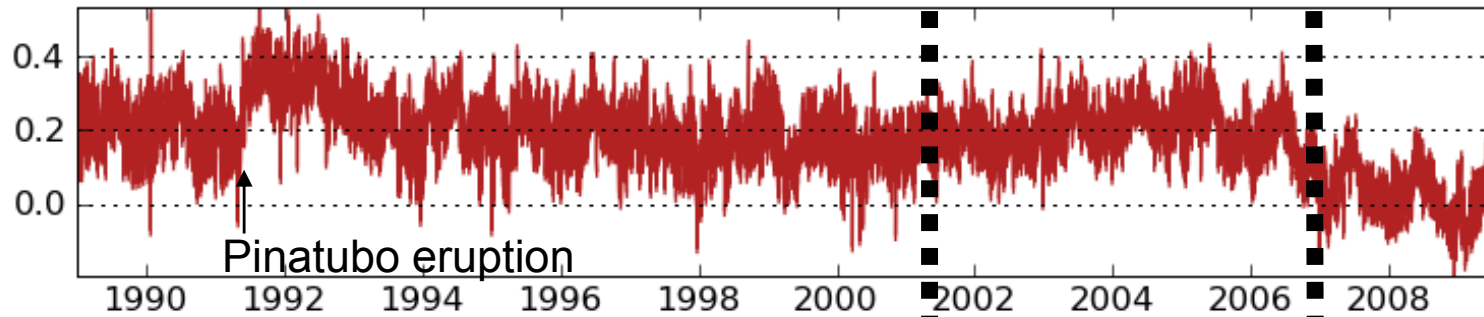
GNSS Radio Occultation are the most largely used (i.e., readily usable)

Poli et al., "Climate Applications of GNSS Radio Occultation in European Global Reanalysis", *2nd Galileo Colloquium*, Padua, 2009

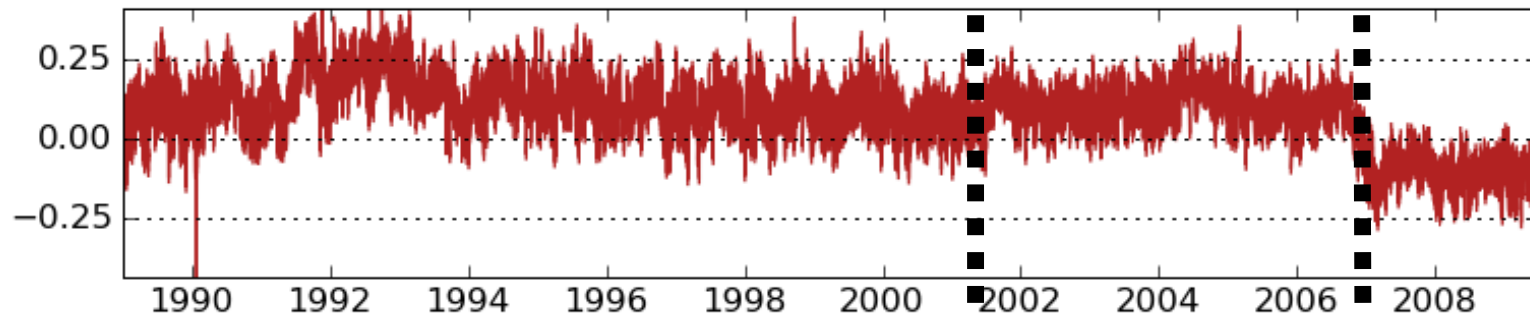


Radiosonde temperature validation, North Hemisph.

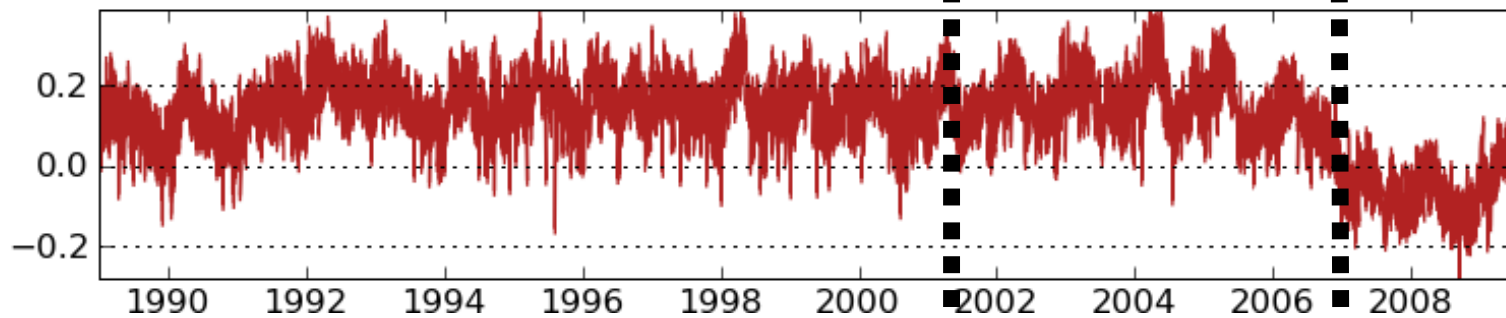
(a) Temper. diff. NH land RS minus ERA-Interim (in K), Pressure layer 60-40hPa



(b) Temper. diff. NH land RS minus ERA-Interim (in K), Pressure layer 85-60hPa



(c) Temper. diff. NH land RS minus ERA-Interim (in K), Pressure layer 125-85hPa



Introduction of CHAMP

Introduction of COSMIC

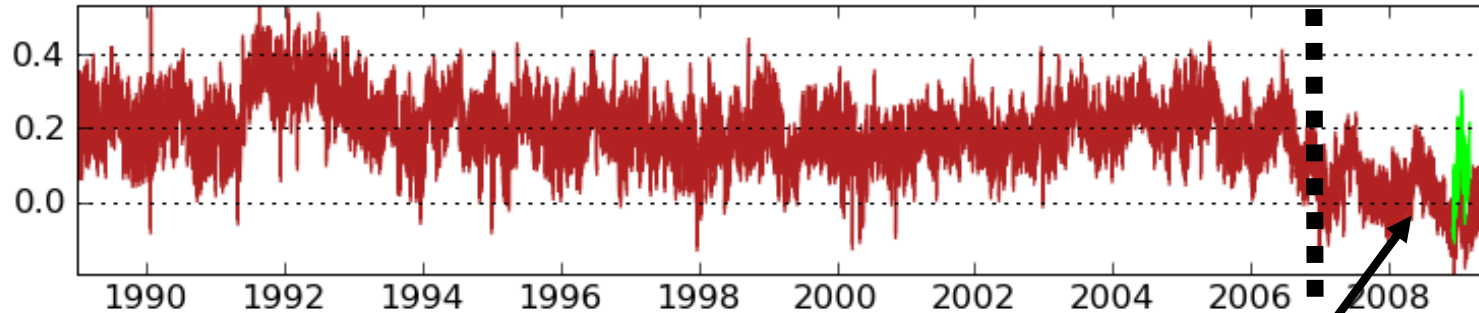


Poli et al., "Climate Applications of GNSS Radio Occultation in European Global Reanalysis", *2nd Galileo Colloquium*, Padua, 2009

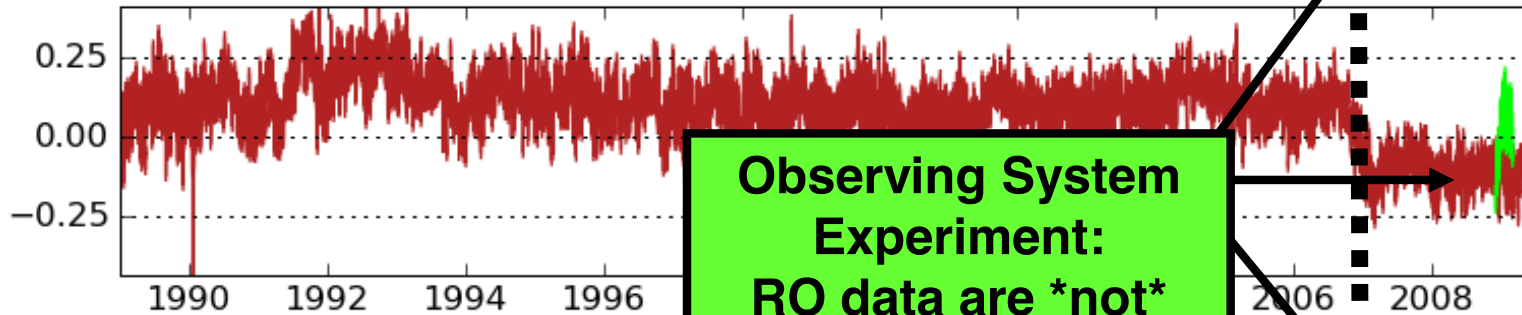


Radiosonde temperature validation, North Hemisph.

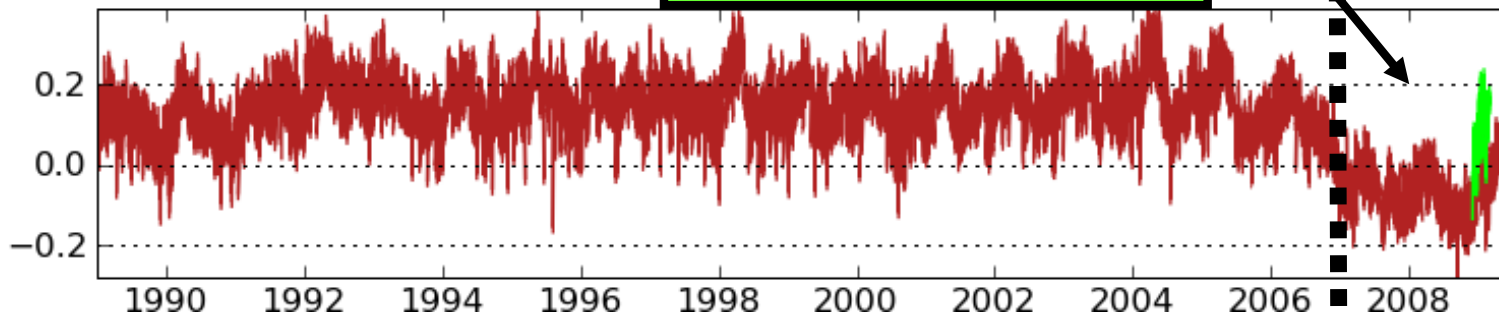
(a) Temper. diff. NH land RS minus ERA-Interim (in K), Pressure layer 60-40hPa



(b) Temper. diff. NH land RS minus ERA-Interim (in K), Pressure layer 85-60hPa



(c) Temper. diff. NH land RS minus ERA-Interim (in K), Pressure layer 125-85hPa



**Observing System Experiment:
RO data are not assimilated**

Introduction of COSMIC



Poli et al., "Climate Applications of GNSS Radio Occultation in European Global Reanalysis", *2nd Galileo Colloquium*, Padua, 2009

Applications:

Climate, Tropopause, ABL detection,
Impacts on Tropical Cyclones
Forecast

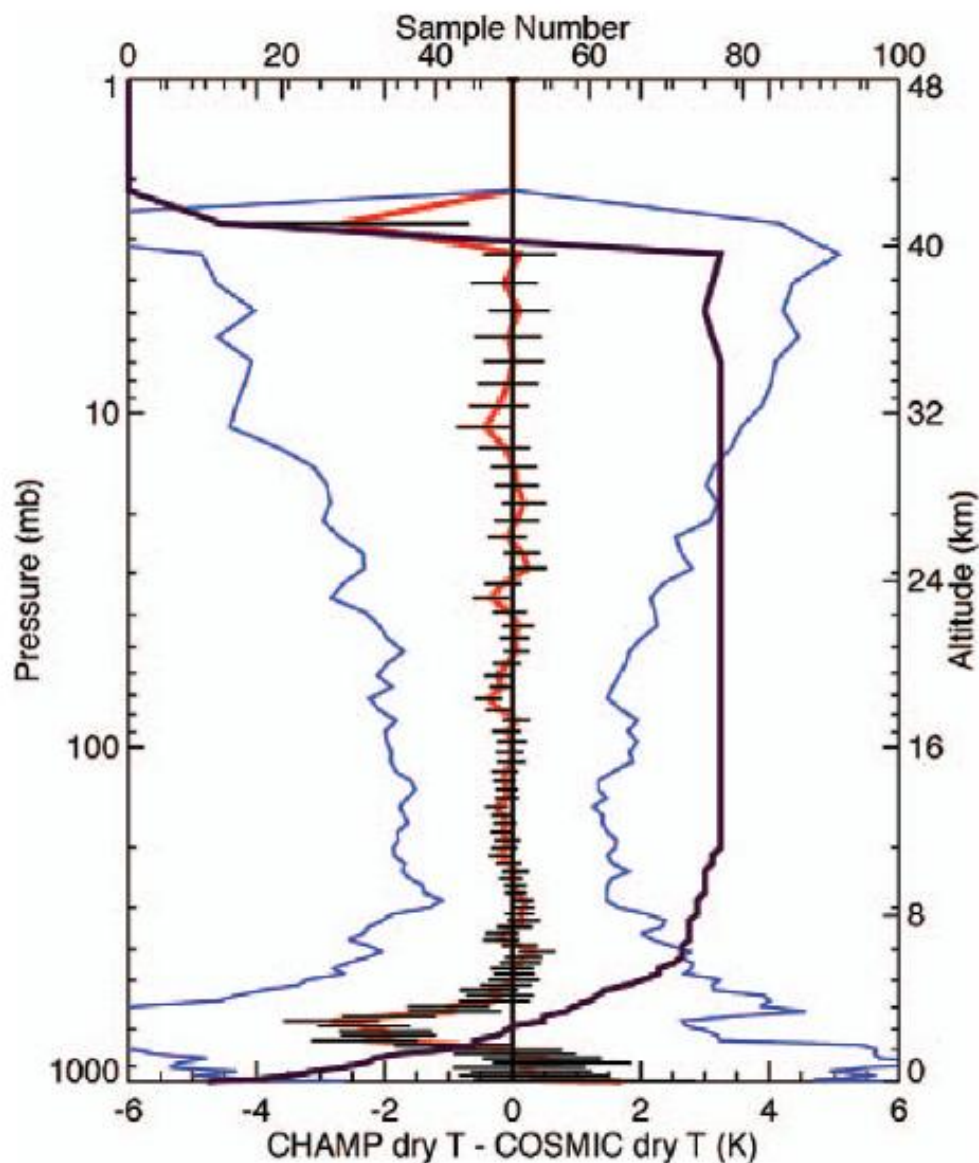
CLIMATE APPLICATIONS

- WMO climate monitoring requirements: **0.5 K** accuracy and **0.04 K/dec** stability
- RO observations are thus well suited for establishing a stable, long-term record required for climate monitoring
- Remember that the fundamental observations is a **measurement of time!** Given the long-term stability assured by the GPS system, an accurate measurement of time of flight and time of flight variations with long-term stability can be achieved.
- Consequently, RO products are theoretically expected to have the accuracy and stability required for climate applications
- Finally RO products are also expected to be **mission independent** (results from actual RO missions can be directly compared [using the same processing software] directly to results from RO missions that will be launched many decades from now

As an example: ...

CLIMATE APPLICATIONS

RO results are mission independent!



Comparison statistics (mean: red; standard error of the mean: horizontal black lines superimposed on the mean; std dev: blue; sample number of compared soundings: solid black line) of 80 CHAMP and COSMIC profiles that were collocated within 200 km and 90 min from 1 Sep to 31 Oct 2006, within 60°S-60°N.

Ho et al., "A comparison of lower stratosphere temperature from microwave measurements with CHAMP GPS RO data", *Geophys. Res. Lett.*, 34, 2007.



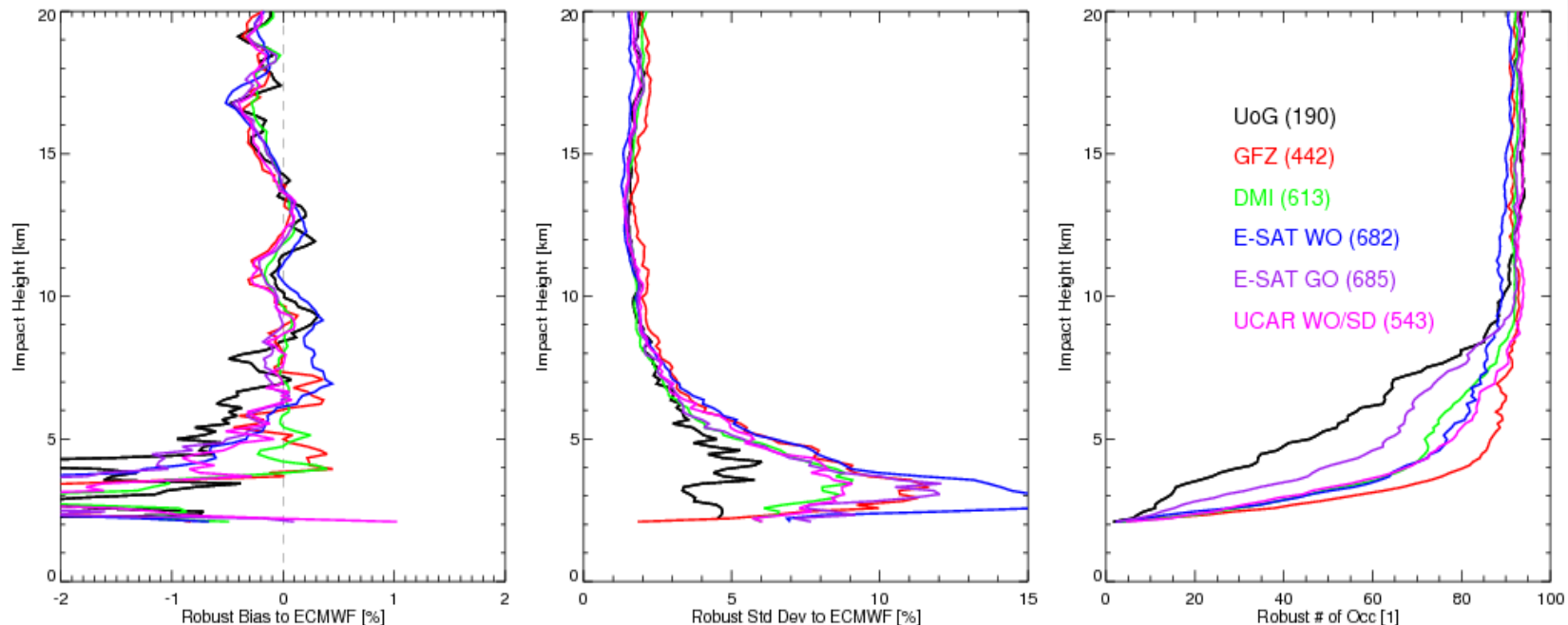
Tropospheric Intercomparison

Studies on GRAS Data Quality

C. Marquardt & Study team

- GRAS raw sampling measurements extensively studied within ESA study
- First systematic cross-comparison of advanced tropospheric retrievals (ever!)
- Statistics includes UCAR retrievals of GRAS data from EUMETSAT's Structural Uncertainty study

26th GRAS SAG
22nd – 23rd June 2011, Darmstadt

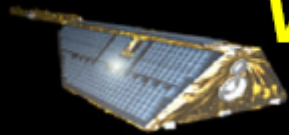


Bending angle bias (left), standard deviations (middle), and penetration depth (right) of GRAS raw sampling data processed by different centres. Statistics are against ECMWF forecasts. Number of occultations processed on sample day (30/09/2007) in brackets.

26th GRAS SAG
22nd – 23rd June 2011, Darmstadt

ICTP – 19 April 2012





Vertical structure atmospheric structure e.g. Tropopause



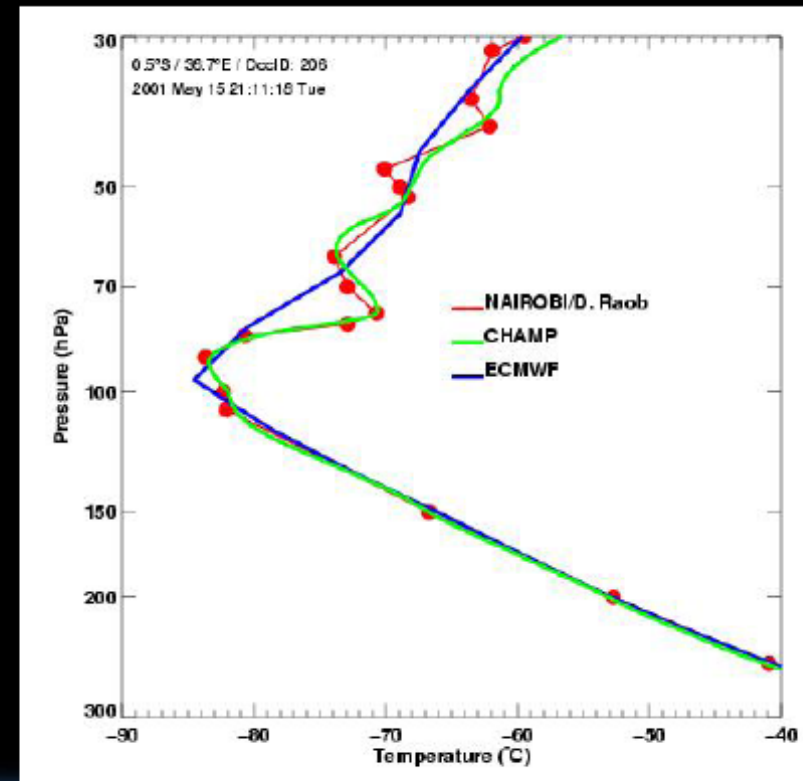
Perfect for climate monitoring, E.g. Tropopause:



Precise monitoring of vertical atmospheric structure with high vertical resolution on global scale



Temperature and altitude is indicator for climate change (Warming of the troposphere, cooling in the stratosphäre)



DETECTING THE ATMOSPHERIC BOUNDARY LAYER

- ABL is the lowermost atmosph layer (affected by Earth's surface interaction)
- It is the boundary between turbulent mixed layer (below) and stably stratified layer (above)
- It is characterized by temperature inversion phenomena and decrease of humidity
- The Top of ABL is sharper (its detection is possible only with High Resol measurements)
- It's depth is an important parameter for Numerical Weather Prediction and Climate models

DETECTING THE ATMOSPHERIC BOUNDARY LAYER

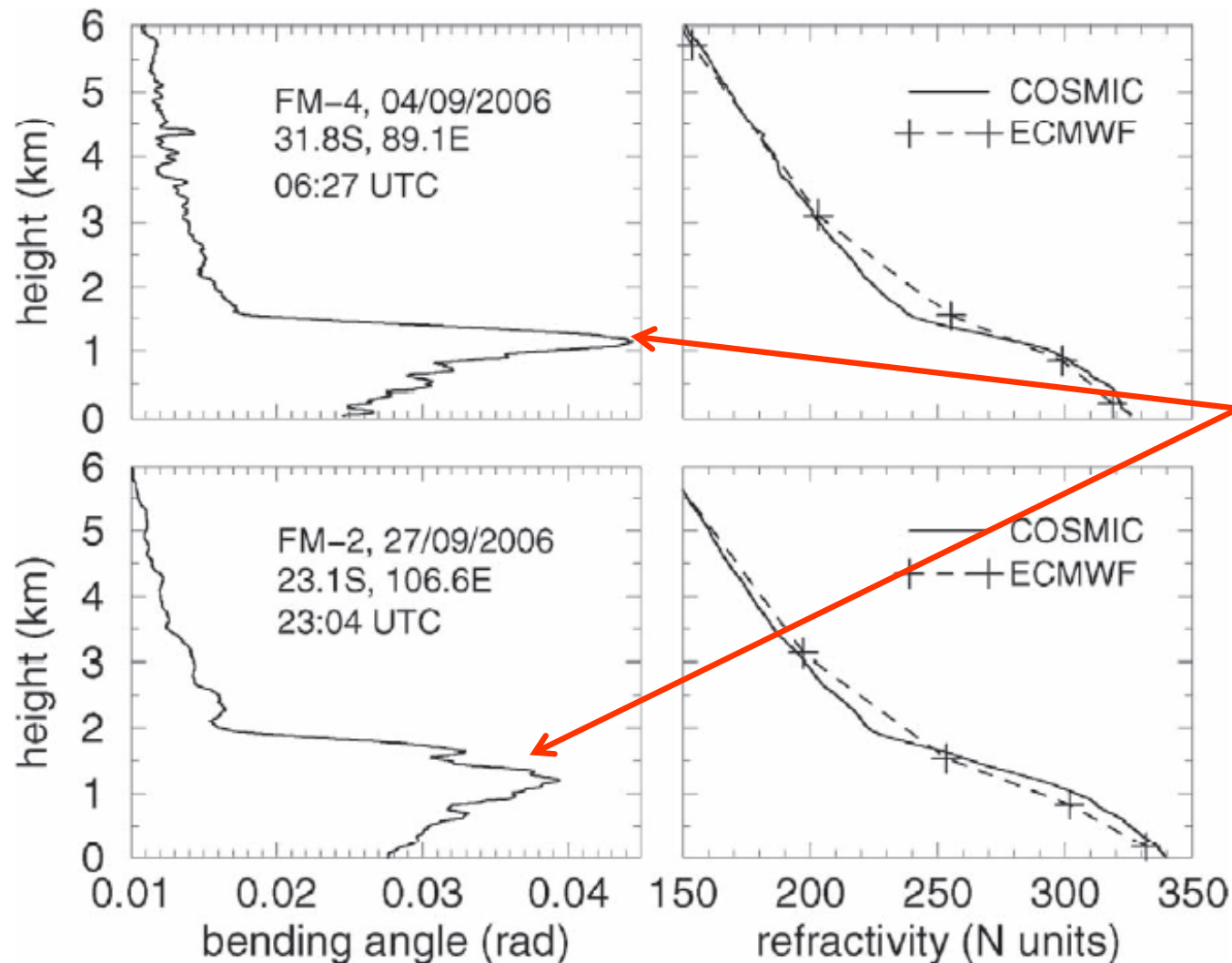
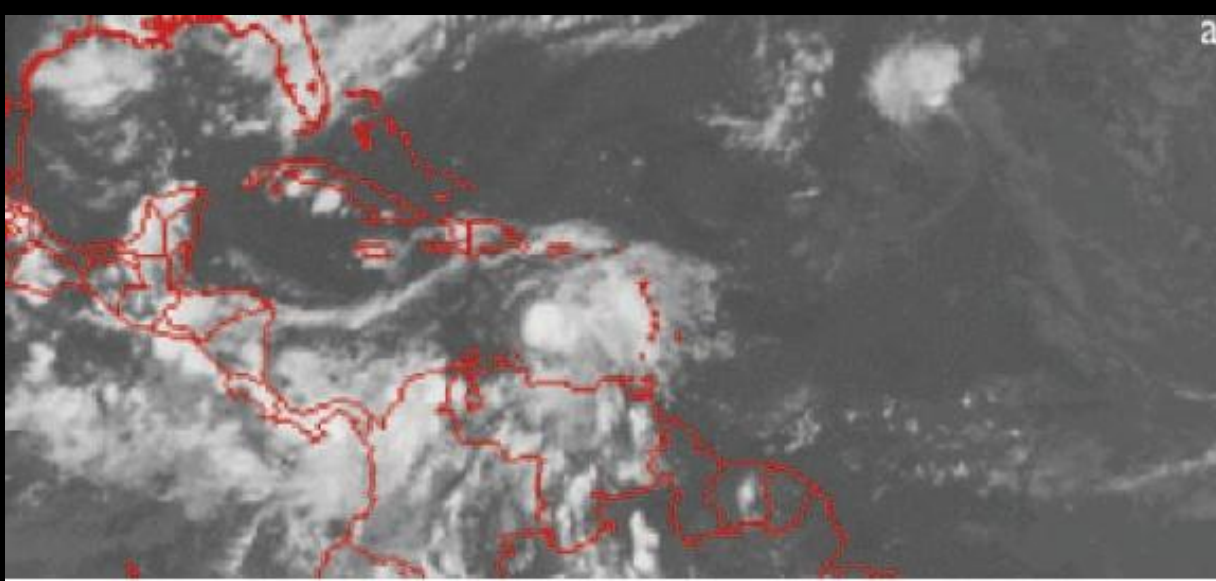


FIG. 5. Examples of COSMIC RO-retrieved bending angle and refractivity profiles in the subtropics, showing the sharp ABL top compared to ECMWF analyses.

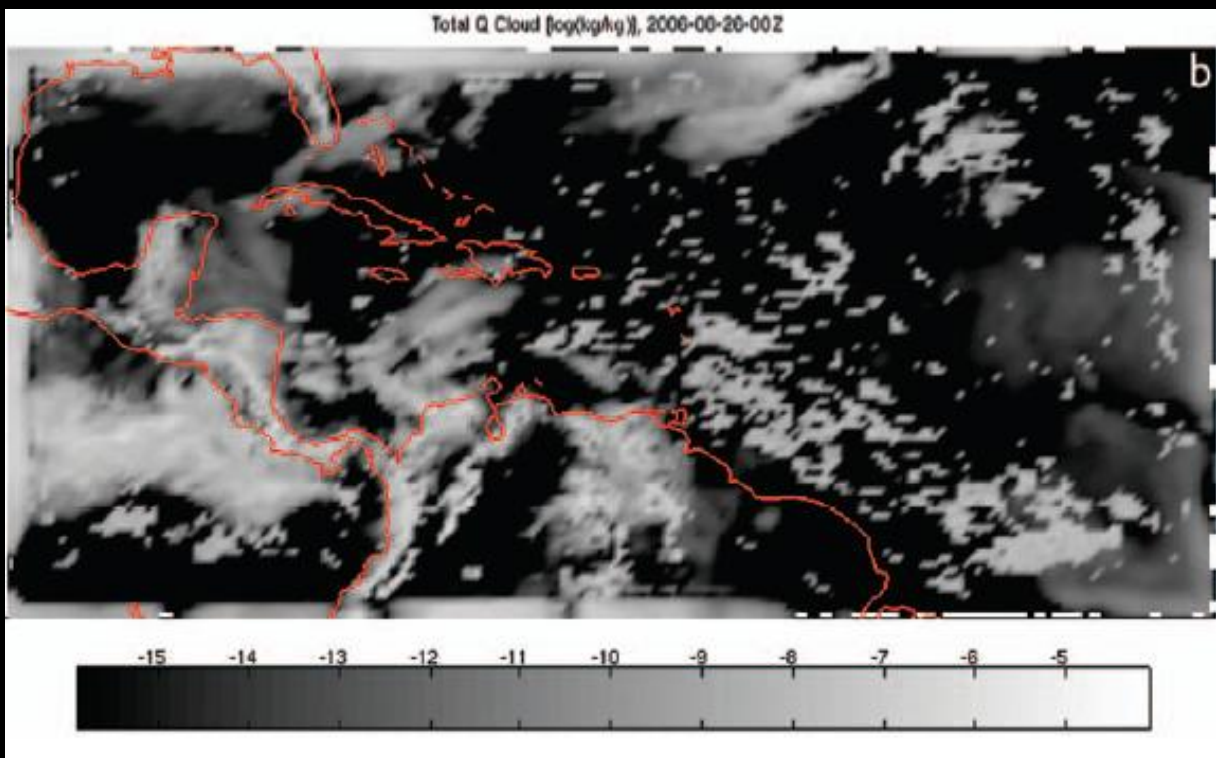
Thanks to high resolution and Open Loop capabilities, ABL can be detected by RO observations and its parameters can be accurately measured

IMPACT ON TROPICAL STORM FORECAST

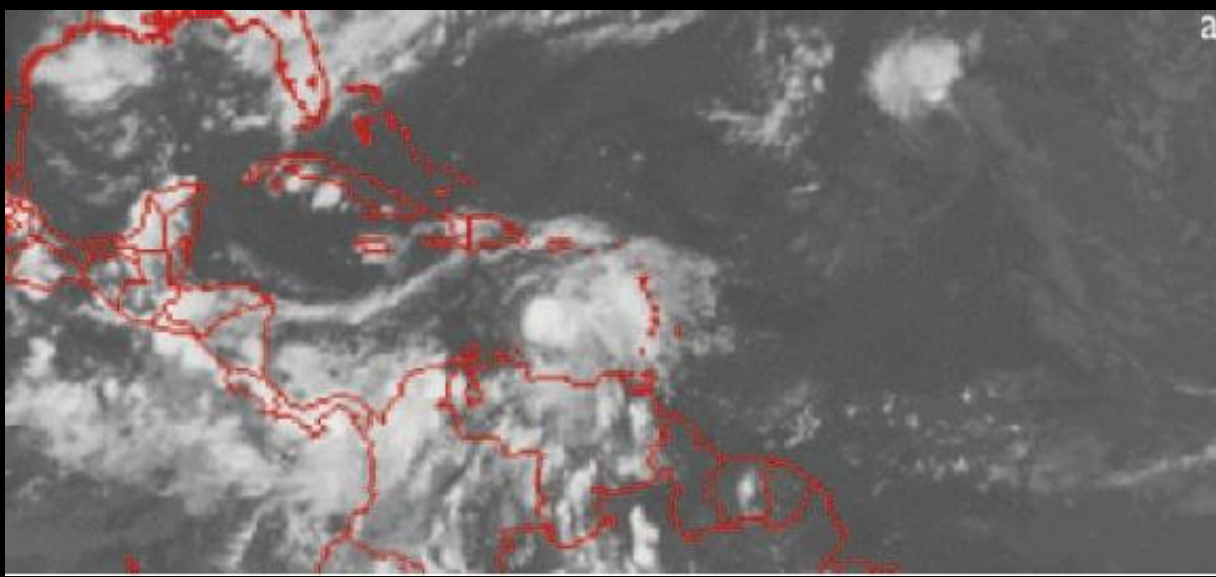
- Observations of moisture fields over oceans (where tropical storms/cyclones form and spend most of their life) is critical. Consequently, the numerical forecast of their development (cyclone genesis) often fails.
- RO observations provide accurate and valuable informations on tropospheric moisture and temperature. Thus they have great potential to improve tropical cyclone predictions.
- As an example, Tropical Storm Ernesto, originated from East Africa on 18 August 2006, crossed the Atlantic Ocean.



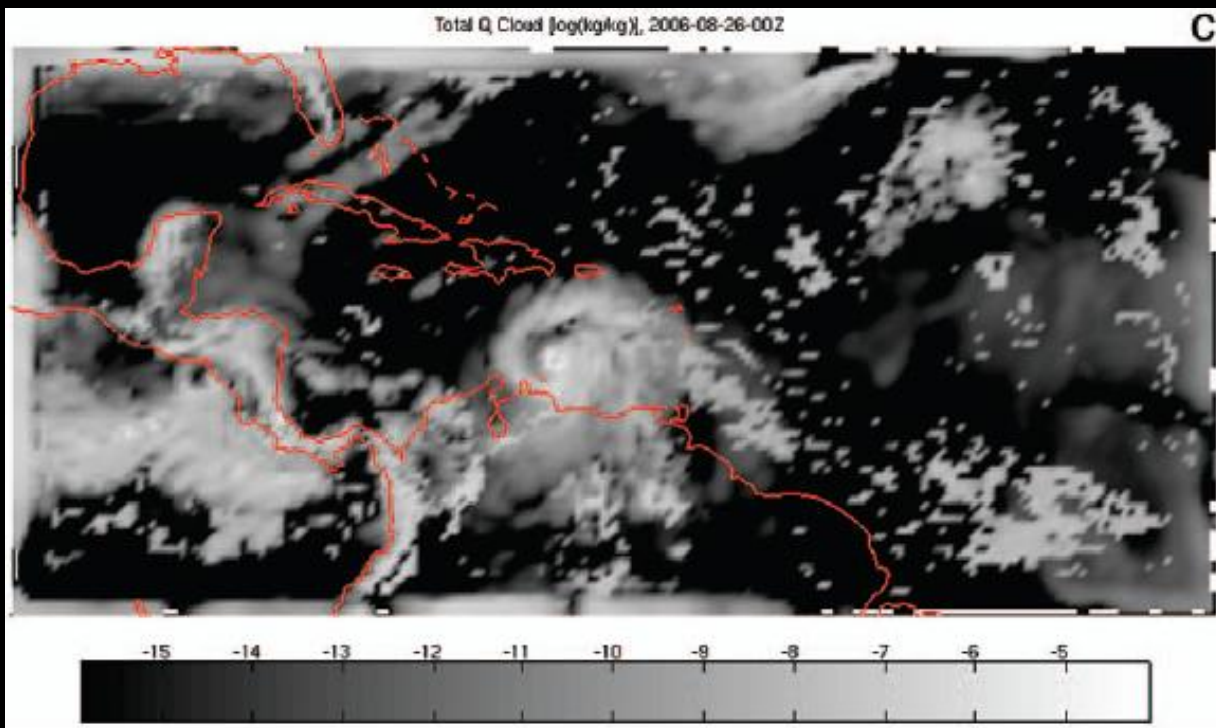
IR satellite photo of Tropical Storm Ernesto for 00:00 UTC, 26 Aug 2006



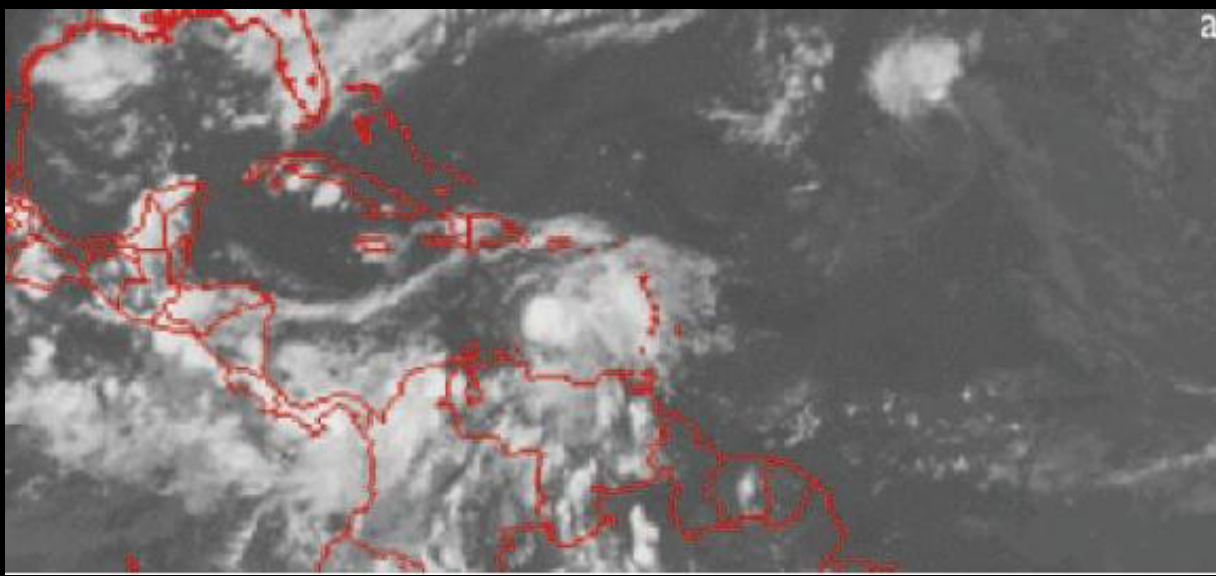
66 h forecast of vertically integrated cloud water mixing ratio generated by WRF NWP Mdl (initialized using NCEP analysis at 06:00 UTC, 23 Aug, 2006) **without RO observations assimilation**



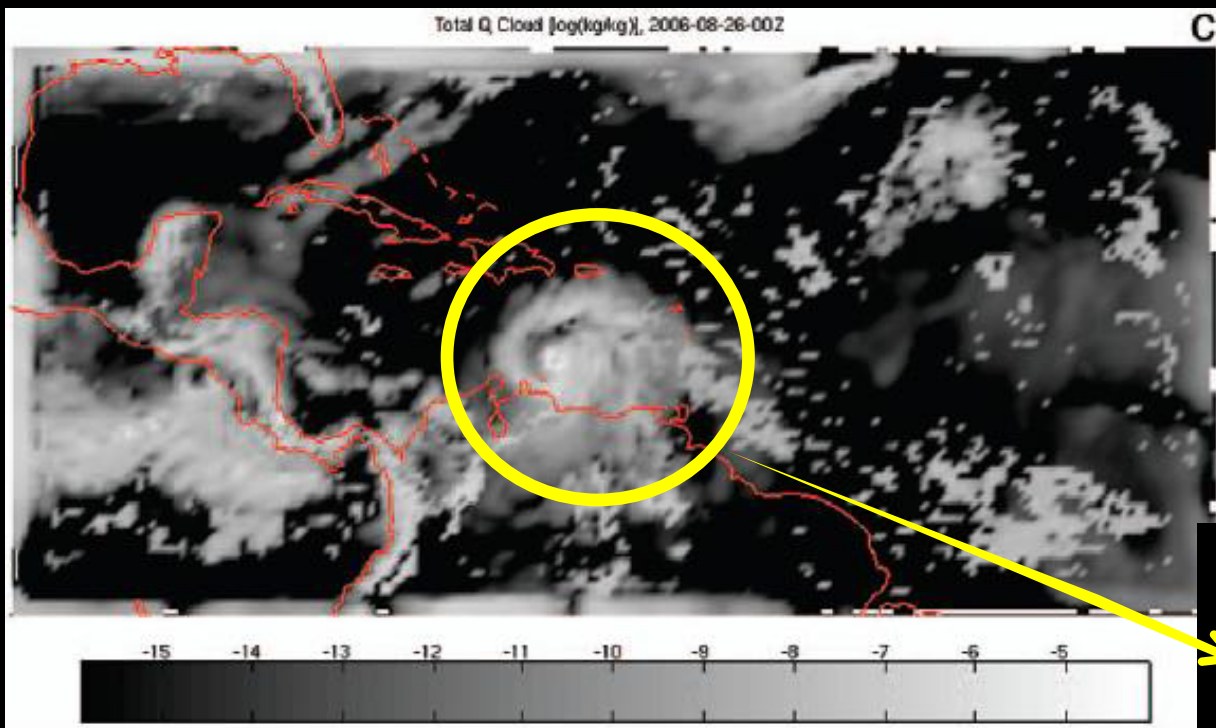
IR satellite photo of Tropical Storm Ernesto for 00:00 UTC, 26 Aug 2006



66 h forecast of vertically integrated cloud water mixing ratio generated by WRF NWP Mdl (initialized using NCEP analysis at 06:00 UTC, 23 Aug, 2006) with the assimilation of 15 COSMIC RO observations performed between 03:00 and 09:00 UTC, 23 Aug, 2006



IR satellite photo of Tropical Storm Ernesto for 00:00 UTC, 26 Aug 2006



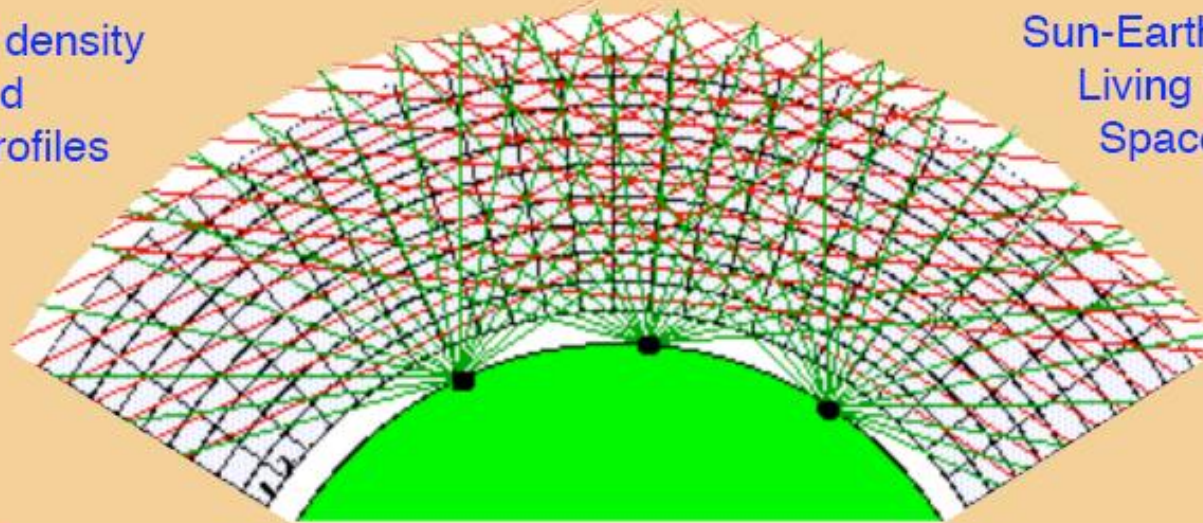
GPS RO data may be useful in improving numerical forecasts of tropical cyclone genesis

Applications:

IONOSPHERE PROFILING
IMAGING AND SPACE WEATHER

Snapshot 3D Ionospheric Imaging

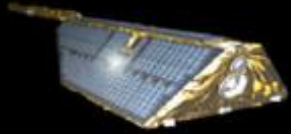
Electron density
and
TEC profiles



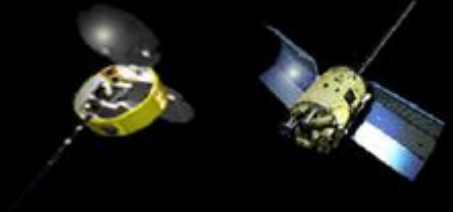
Sun-Earth Connections
Living With a Star
Space Weather

Applications

- Observe ionospheric dynamics and refine models
- Chart the course and evolution of space storms
- Provide near term prediction of space weather
- Study TIDs and global energy transport
- Probe iono-thermo-atmosphere interactions



Ionospheric profiling



... DETAILS ABOUT THIS VERY EFFECTIVE APPLICATION WILL BE GIVEN IN THE FRAMEWORK OF THE NEXT TALKS. In particular, for the RO point of view...

B. Nava: “GNSS Remote Sensing: Electron Density Profiling through Radio Occultation”

**Workshop on Science Applications of GNSS in Developing
Countries**

11-27 April, 2012



The Abdus Salam
International Centre for Theoretical Physics

THANK YOU FOR YOUR ATTENTION!

ANY QUESTION ???

**GNSS REMOTE SENSING: TROPOSPHERE
PROFILING THROUGH RADIO OCCULTATION**

RICCARDO NOTARPIETRO

POLITECNICO di TORINO

riccardo.notarpietro@polito.it +39.011.5644623



REMOTE SENSING GROUP

POLITECNICO
DI TORINO